

STRUCTURAL AND MOLECULAR BASIS OF INTERACTION OF CURCUMIN WITH PROTEINS

A thesis submitted to the
UNIVERSITY OF MYSORE
for the degree of
DOCTOR OF PHILOSOPHY in BIOCHEMISTRY

by
SNEHA RANI A. H.

Department of Protein Chemistry and Technology
Central Food Technological Research Institute
Mysore - 570020
India

December 2010

ABSTRACT

Curcumin (diferuloylmethane), a natural lipid-soluble yellow compound from the plant *Curcuma longa* L., is a potent antioxidant, antitumorigenic and anti-inflammatory molecule. Very limited solubility and stability in aqueous medium and poor bioavailability limits the use of curcumin as an efficient therapeutic agent. The present study was focused, towards exploring possible medium/carrier to increase the solubility and stability of curcumin. Further, studies were carried out to understand the basis of interaction.

β -Lactoglobulin (β LG), the major whey protein, can solubilize and bind many small hydrophobic molecules. The stability of curcumin bound to β LG in solution was enhanced 6.7 times, in comparison to curcumin alone, in aqueous solution. The complex formation of curcumin with β LG has been investigated employing spectroscopic techniques. β LG interacts with curcumin at pH 7.0, with an association constant of $1.04 \pm 0.1 \times 10^5 \text{ M}^{-1}$, to form a 1:1 complex, at 25 °C. Entropy and free energy changes for the interaction, derived from the van't Hoff plot, were $18.7 \text{ cal mol}^{-1}$ and $-6.8 \text{ kcal mol}^{-1}$, respectively; the interaction is hydrophobic in nature. Interaction of β LG with curcumin does not affect either the conformation or the state of association of β LG. Binding studies with denatured β LG, effect of pH on curcumin- β LG interaction, Förster energy transfer measurements and molecular docking studies suggested that curcumin binds to the central calyx of β LG. Nanoparticles of β LG, prepared by desolvation, are found to encapsulate curcumin with $> 96\%$ efficiency. The solubility of

curcumin in β LG nanoparticle, significantly enhanced to $\sim 625 \mu\text{M}$ in comparison with its aqueous solubility (30 nM).

The stability of curcumin in the presence of α_{S1} -casein was enhanced by ~ 39 folds at pH 7.2, in comparison of the stability of curcumin in aqueous medium. Curcumin binds to α_{S1} -casein at two different binding sites, one with high affinity and another with low affinity characterized by association constants of $2.01 \pm 0.6 \times 10^6$ and $6.3 \pm 0.4 \times 10^4 \text{ M}^{-1}$, respectively. The carboxyl-terminal of α_{S1} -casein (100-199 residues) and the residues 14-24 in α_{S1} -casein are hydrophobic in nature. The free energy change for the binding of curcumin to α_{S1} -casein, ΔG° at 27 °C, was $-8.65 \text{ kcal mol}^{-1}$. The ΔH° and ΔS° for the binding reaction were estimated to be $-1.28 \text{ kcal mol}^{-1}$ and $24.7 \text{ cal mol}^{-1}$, respectively. Hydrophobic force was the main contributing factor for the interaction of curcumin to α_{S1} -casein. Chaperone activity of α_{S1} -casein was enhanced when bound to curcumin. The biological activity of curcumin, like its protection against hemolysis was unchanged on interaction with α_{S1} -casein. Average size of curcumin encapsulated α_{S1} -casein nanoparticles was $\sim 166 \pm 5 \text{ nm}$. Encapsulation efficiency of curcumin was $> 94\%$ and 38% curcumin release was observed from nanoparticles in 24 h. The solubility of curcumin in α_{S1} -casein nanoparticle was enhanced to $\sim 620 \mu\text{M}$ in comparison with its aqueous solubility (30 nM).

The ability of curcumin to measure the surface hydrophobicity of proteins was analyzed and compared with a standard fluorescent probe - *cis*-parinaric acid.

Surface hydrophobicity of - BSA, β LG, soy LOX-1, ovalbumin and lysozyme are in the order BSA > β LG > soy LOX-1 > ovalbumin > lysozyme. The binding affinities of curcumin decreased with the decrease in surface hydrophobicity of proteins. Surface hydrophobicity index value (S_0), determined using curcumin correlated with the S_0 values of protein calculated using CPA. The S_0 value of proteins determined using curcumin decreased in the presence of urea, suggesting the possible use of curcumin as a probe to determine the surface hydrophobicity of proteins. Because of low quantum yield of curcumin compared to ANS and CPA, it may not be an appropriate fluorescent probe for measuring the S_0 of proteins.

The structural similarities between CPA and linoleic acid, the substrate for soy LOX-1, instigated to study the inhibition of soy LOX-1 with CPA. CPA, a C₁₈ fatty acid inhibits soy LOX-1 activity with the IC_{50} value of 18.8 μ M. The mechanism of inhibition of soy LOX-1 by CPA was competitive with the K_i value of 9.8 μ M. CPA binds close to iron cofactor with the distance of carboxylate group of CPA to the iron being 3.3 Å. The binding constant for the binding of CPA to soy LOX-1 is $2.1 \pm 0.5 \times 10^4 \text{ M}^{-1}$.

Tetrahydrocurcumin (THC; 1,7- bis(4-hydroxy-3-methoxyphenyl)heptane-3,5-dione) – the reduced form of curcumin, is the major metabolite *in vivo*. Inhibition of soy LOX-1 by THC was studied and the kinetics and mechanism of inhibition was evaluated. THC inhibited soy LOX-1 activity with an IC_{50} value of 59.4 μ M for THC in aqueous solution and 44.6 μ M for PC micelles encapsulated THC. The

lag phase for enzyme activation from its resting state increased with increasing concentrations of THC. A mixed linear type of inhibition of LOX-1 was observed with a K_i value of 39 μM . Molecular docking simulations suggested the binding of THC near the iron cofactor. Spectroscopic and CD studies revealed that, THC could prevent the conversion of the resting inactive ferrous form of the enzyme to its active ferric form thus inhibiting the enzyme. From these studies, it can be concluded that THC is less powerful in inhibiting the LOX-1 in comparison to curcumin however, the higher solubility and stability of THC, compared to curcumin, provides valuable leads for the use of this compound as an alternative to curcumin in anti-inflammatory drugs. These observations indicate the importance of methylene bridge at carbon seven in curcumin, in inhibiting the soy LOX-1 enzyme.

Carbonic anhydrase is a family of metalloenzymes that catalyze the rapid conversion of carbon dioxide to bicarbonate and protons, and is involved in biomineralization process. It catalyzes the reversible hydration of CO_2 to HCO_3^- and H^+ . It is a zinc containing enzyme with the molecular weight of 29000 Da and in red blood cells, it facilitates the transportation of CO_2 out of the body. The effect of curcumin on the activity of carbonic anhydrase was studied. No change in the activity of carbonic anhydrase, *in vitro* in the presence of curcumin was observed. Though, curcumin is a known chelator of metal ions, it had no effect on redox inactive metal - zinc containing enzyme.

ACKNOWLEDGEMENTS

I am sincerely grateful and my hearty thanks to...

My mentor and guide, Dr. A. G. Appu Rao, Head, Department of Protein Chemistry and Technology, for his inspiring guidance throughout the course of investigation and enabling me to grow, giving me the freedom to think and for providing a stimulating research atmosphere during my stay in his laboratory,

Dr. V. Prakash, Director, CFTRI, Mysore for providing facilities to work,

Dr. Sridevi Annapurna Singh for her support and encouragement during the course of investigation,

Dr. Lalitha R. Gowda, Head, FSAQCL, for helping in molecular docking studies,

Dr. P. Srinivas, Head, PPSFT, for providing tetrahydrocurcumin,

Dr. M. Eswaremoorthy, INCASR, Bangalore, for helping in analysis of particle size,

Dr. Kousthubha M. S., for editing the thesis,

Staff and colleagues of Protein Chemistry & Technology for their help,

FOSTIS and Central Instrumentation Facility & Services for their technical assistance rendered during the entire course of investigation,

Kiran, my husband and to my family for their support & favorably shifting their priorities to help me,

Harshal, my beloved son for pouring in joy,

University Grants Commission, New Delhi, India, for the financial support in the form of a research fellowship.

Sneha Rani AH

CONTENTS

List of Abbreviations

List of Tables

List of Figures

1. Introduction 1-63

Turmeric 2

Curcuminoids 2

Curcumin 3

Structure Activity Relationship of Curcumin with its Analogues 18

Hydrogenated derivative of curcumin: Tetrahydrocurcumin 23

Strategy for use of carrier molecule for ligand 25

Binding of ligands to macromolecule 29

Milk proteins 45

β -Lactoglobulin 46

Casein 51

Lipoxygenases 56

Surface hydrophobicity of proteins 61

cis-Parinaric acid 61

CFTRI Work on Curcumin 64-66

Aim and Scope of Present Investigation 67-69

2. Materials and Methods 70-89

3. Results and Discussion 90-174

3.1. Interaction of Curcumin with β -Lactoglobulin and α_{s1} -Casein and its Encapsulation in Nanoparticle

- 3.1.1. Interaction Studies of Curcumin with β -Lactoglobulin and its Nanoparticle Preparation 90-119**
- 3.1.2. Interaction Studies of Curcumin with α_{S1} -Casein and its Nanoparticle Preparation 120-143**
- 3.1.3. Curcumin as a Tool to Assess the Surface Hydrophobicity of Proteins 144-161**
- 3.2. Molecular basis of interaction of curcumin with proteins-Inhibition of soy LOX-1 by tetrahydrocurcumin 162-172**
- 3.3. Activity Modulation of Carbonic Anhydrase by Curcumin 173-174**
- 4. Summary and Conclusions 175-182**
- Bibliography 183-217**
- Appendices 218-233**

LIST OF ABBREVIATIONS

Å	Angstrom unit
λ	Wavelength
°C	Degree centigrade
ε	Molar extinction coefficient
μg	Microgram
μL	Microliter
ΔH°	Change in enthalpy
ΔG°	Change in free energy
ΔS°	Change in entropy
βLG	Beta-lactoglobulin
AAPH	2,2'-azo-bis(2-amidinopropane hydrochloride)
ANS	8-Anilino-1-naphthalene-sulfonic acid
BSA	Bovine serum albumin
CD	Circular dichroism
CPA	<i>cis</i> -Parinaric acid
cm	Centimeter
Da	Daltons
DEAE	Diethylaminoethyl
eq.	Equation
g	Grams
HEPES	4-(2-hydroxyethyl)-1-piperazine ethane sulfonic acid
HPLC	High performance liquid chromatography
HSA	Human serum albumin
h	Hour
IC ₅₀	Midpoint inhibitor concentration
K _a	Association constant
K _d	Dissociation constant
K _i	Inhibition constant

K_m	Michaelis-Menten constant
kcal	Kilo calories
L	Liter
LOX	Lipoxygenase
M	Molar concentration
min	Minute
mL	Milliliter
mM	Millimolar
mrw	Mean residue weight
nm	Nanometer
PAGE	Polyacrylamide gel electrophoresis
PC	Phosphotidyl Choline
R	Gas constant
RFI	Relative fluorescence intensity
rpm	Rotations per minute
S_0	Surface hydrophobicity index
SDS	Sodium dodecyl sulfate
TFA	Trifluoroacetic acid
THC	Tetrahydrocurcumin
Tris	Tris (hydroxymethyl) amino methane
UV	Ultraviolet
V_{max}	Maximum velocity
vs	Versus

LIST OF FIGURES

Figure No.	Title	Page No.
1.1	<i>Curcuma longa</i> , plant with inflorescence and rhizome	5
1.2	Structure of curcuminoids	7
1.3	Ball and stick model of curcumin, keto and enol form	8
1.4	Physiological and biochemical action of curcumin	11
1.5	Molecular targets of curcumin	12
1.6	Structure of Tetrahydrocurcumin	23
1.7	Schematic representation of nanoparticle preparation	28
1.8	Graphical representation of ligand binding curves	32
1.9	Forces involved in protein-ligand interaction	35
1.10	Structure of β LG	50
1.11	Structure of bovine α_{S1} -casein	55
1.12	Representation of soy LOX-1 structure	60
1.13	Structure of <i>cis</i> -parinaric acid	62
3.1	RP-HPLC profile to show the purity of curcumin	90
3.2	Absorption spectrum of curcumin in the presence of β LG	92
3.3	Emission spectra of curcumin in the presence of β LG	94
3.4	Quenching of tryptophan fluorescence of β LG by curcumin	97
3.5	Effect of temperature on the binding constant of β LG-curcumin	98
3.6	Förster type resonance energy transfer between β LG and curcumin	100
3.7	Effect of pH on the binding constant of curcumin to β LG	102
3.8	Effect of palmitate on curcumin- β LG complex	104
3.9	CD measurements of curcumin bound to β LG	107
3.10	HPLC profile of β LG native, heated β LG and heated β LG containing curcumin	110

3.11	Visualization of the binding of curcumin on β LG	113
3.12	SEM photograph & size distribution graph of curcumin encapsulated in β LG nanoparticle	116
3.13	CD spectra of curcumin encapsulated in β LG nanoparticle	117
3.14	SDS PAGE representing the homogeneity of α_{S1} -casein	122
3.15	Emission spectrum of curcumin in the presence of α_{S1} -casein	123
3.16	Effect of temperature for the formation of α_{S1} -casein curcumin complex	124
3.17	Induced circular dichroism spectra of curcumin- α_{S1} -casein complex	127
3.18	HPLC profile of curcumin in buffer	129
3.19	Semi logarithmic plot to ascertain the stability of curcumin in different media	130
3.20	Thermal aggregation assay of carbonic anhydrase and catalase in the presence of curcumin and α_{S1} -casein	132
3.21	Inhibition of AAPH-induced hemolysis of erythrocytes by curcumin and α_{S1} -casein bound curcumin	134
3.22	SEM photograph and particle size analysis graph of α_{S1} -casein nanoparticle loaded with curcumin	136
3.23	SEM photograph and particle size analysis graph of HSA nanoparticle loaded with curcumin	140
3.24	<i>In vitro</i> release kinetics of curcumin from β LG, HSA and α_{S1} -casein nanoparticle	141
3.25	Apparent solubility of curcumin in mixed PC micelles, HSA, β LG and α_{S1} -casein	143
3.26	Comparative fluorescence emission spectrum of curcumin in buffer, BSA and lysozyme	146
3.27	Effect of urea on the surface hydrophobicity of BSA	150

3.28	Time course of LOX-1 catalyzed reaction in the presence of CPA and determination of IC_{50} value of CPA for inhibition of LOX-1	153
3.29	Kinetics of inhibition of LOX-1 by CPA	157
3.30	Molecular docking of CPA to soy LOX-3	158
3.31	Emission spectra of CPA on titration with LOX-1 and determination of binding constant	159
3.32	Quenching of intrinsic fluorescence of LOX-1 on titration with CPA and concentration dependence of energy transfer between tryptophan and bound CPA	160
3.33	Quenching of soy LOX-1 fluorescence by CPA and determination of binding constant	161
3.34	Time course of lipoxygenase catalyzed reaction and IC_{50} value with free curcumin, PC micelle encapsulated curcumin, free THC and PC micelle encapsulated THC	164
3.35	Kinetics for the inhibition soy LOX-1 by THC	165
3.36	Effect of THC on the absorption and CD spectra of ferric lipoxygenase.	170
3.37	HPLC profile of THC in the presence of LOX-1 and linoleic acid.	171
3.38	Molecular docking of THC with soy LOX-1	172
3.39	Activity of carbonic anhydrase followed in the presence of different concentrations of curcumin	174

LIST OF TABLES

Table No.	Title	Page No.
1.1	Chronicle of major biological properties of curcumin reported for first time	6
1.2	Examples of protein dissociation constants	33
1.3	Composition of skim milk	45
3.1	Stability of curcumin at pH 7.0 in the presence and absence of β LG	91
3.2	Effect of pH on the binding of curcumin to β LG	102
3.3	Comparative secondary structural details of native β LG, β LG nanoparticle and curcumin encapsulated β LG nanoparticle	118
3.4	Half life ($t_{1/2}$) and rate constant (k) of curcumin in different solution condition	130
3.5	Comparative physical, morphological properties, solubility and release kinetics of curcumin encapsulated in different protein nanoparticles	141
3.6	Apparent solubility of curcumin in different media	143
3.7	Comparison of the curcumin emission maximum, association constant and surface hydrophobicity with different proteins	147
3.8	Comparison of ANS emission maximum, association constant and average hydrophobicity of different proteins	148
3.9	Surface hydrophobicity of different proteins determined using CPA	148

“The secret of life is molecular recognition; the ability of one molecule to recognize another through weak bonding interactions”

-Linus Pauling

ePrints@CITRI

1. Introduction

ePrints@CFTRI

Introduction

Historically, plants have shown great promise in the treatment of diseases and been a source of inspiration for novel drug compounds. There has been considerable public and scientific interest in the use of phytochemicals derived from dietary components to fight against the human diseases. Phytochemicals are synthesized as secondary metabolites in plants, and stem from two major synthetic pathways: shikimate and the acetate pathway. These phytochemicals are mainly phenolic compounds. All plant phenolic compounds share one common feature, namely an aromatic ring with at least one hydroxyl substituent, but may vary greatly in their complexity from simple phenols to the highly polymerized tannins and lignins. They occur predominantly as conjugates with sugars, glucuronic or galacturonic acids or even with other phenols that are linked to hydroxyl groups. The structural diversity of phenolic compounds results in a plethora of phytochemicals ingested by man.

The active components of dietary phytochemicals that are most often reported to be protective against various pathological conditions are curcumin, genistein, resveratrol, diallyl sulfide, S-allyl cysteine, allicin, lycopene, capsaicin, diosgenin, 6-gingerol, ellagic acid, ursolic acid, silymarin, anethol, catechins, eugenol, isoeugenol, dithiolthiones, isothiocyanates, indole-3-carbinol, isoflavones, protease inhibitors, saponins, phytosterols, inositol hexaphosphate, vitamin C, D-limonene, lutein, folic acid, beta carotene, selenium, vitamin E, flavonoids, and dietary fiber (Aggarwal and Shishodia, 2006). However, the list is not exhaustive.

Turmeric

Turmeric, the “golden spice”, has been unique for its medicinal uses and socio-religious practices since ancient times (Table 1.1). *Curcuma longa* Linn., or turmeric, a tropical plant, is a perennial herb belongs to the *Zingiberaceae* (ginger) family, which is 3–5 feet tall bearing oblong, pointed, short-stemmed leaves and funnel-shaped flowers (Figure 1.1A, 1.1B). The rhizome of turmeric (Figure 1.1C) is a valuable cash crop, native to southern and southeastern tropical Asia. Turmeric (Figure 1.1D), a rich source of phenolic compounds – curcuminoids, is widely used as a dietary spice and coloring agent in food, herbal medicine and textile industry (Srinivasan, 1952; Srimal and Dhawan, 1973). In addition to its aromatic, stimulant and coloring properties in the diet, turmeric is mixed with other natural compounds such as slaked lime and has been used topically in the treatment of wounds, inflammation and tumors. It is widely used in traditional Indian medicine to cure biliary disorders, anorexia, cough, diabetic wounds, hepatic disorders, rheumatism, and sinusitis (Jain, 1991). Turmeric is also an effective household remedy for sore throat, cough and common cold, where it is taken orally with tea or hot milk (Jagetia and Aggarwal, 2007). This nonnutritive phytochemical consumed as a dietary spice is reported to be pharmacologically safe, at doses up to 100 mg/day for centuries (Ammon and Wahl, 1991).

Curcuminoids

The rhizome of turmeric plant contains turmerin (a water-soluble peptide), essential oils (such as turmerones, atlantones and zingiberene) and the major chemical principle curcuminoids, which imparts characteristic yellow color (Heath et al., 2004). Curcuminoids can be separated from turmeric by ethanol extraction and usually

constitutes ~2.5 to 6% depending on the season of its harvest and variety. The major curcuminoids present in turmeric are curcumin (also known as curcumin I; [1,7-bis-(4-hydroxy-3-methoxy-phenyl)hepta-1,6-diene-3,5-dione]), demethoxycurcumin (curcumin II; [4-hydroxycinnamoyl-(4-hydroxy-3-methoxycinnamoyl) methane]), bisdemethoxycurcumin (curcumin III; bis-(4-hydroxy cinnamoyl) methane), and the recently identified cyclocurcumin (Figure 1.2A-E) (Kiuchi et al., 1993). Curcumin with two methoxy groups is reddish orange color, demethoxycurcumin with one methoxy group is orange-yellow in color and bis-demethoxycurcumin without methoxy group is yellow in color. The distribution of curcuminoids in Indian varieties is curcumin I (52-63%), curcumin II (19-27%), and curcumin III (18-28%).

Curcumin

Structure and Photophysical Properties

Vogel and Pellatier (1818) first reported the molecular formula of curcumin as $C_{21}H_{20}O_6$, which was later identified as diferuloylmethane (Lampe and Milobedzka, 1913). Powder of curcumin is crystalline and does not dissolve in water; however, it readily goes into solution in ethanol, dimethylsulfoxide and acetone. Curcumin is a low molecular weight compound with a molecular weight of 368.37 g/mol and melting point of 183 °C.

Curcumin shows maximum absorption between 425–430 nm in methanol (Prasad, 1997). It is a non fluorescent compound in aqueous medium and any vicinity with hydrophobic surface makes it fluorescent (Began et al., 1999; Khopde et al., 2000a). This environment dependent fluorescence property of curcumin is used to measure the cellular and differential uptake of curcumin in normal and tumor cells (Kunwar et al., 2008).

Curcumin is a *bis* α - β -unsaturated β -diketone. Under acidic and neutral conditions the *bis*-keto form predominates and at $> \text{pH } 8$, the enolate form is generally found (Jovanovic et al., 1999) (Figure 1.3A and 1.3B). Hence at $\text{pH } 3\text{-}7$, it acts as an extraordinarily potent H-atom donor. This is because, the heptadienone linkage between the two methoxyphenol rings in the keto form of curcumin contains a highly activated carbon atom and the C-H carbon bonds on this carbon are very weak due to delocalization of the unpaired electron on the adjacent oxygen. In contrast, at $\text{pH } > 8$, the enolate form of the heptadienone chain predominates and curcumin acts mainly as an electron donor, a mechanism more typical for the scavenging activity of phenolic antioxidants (Jovanovic et al., 2001).

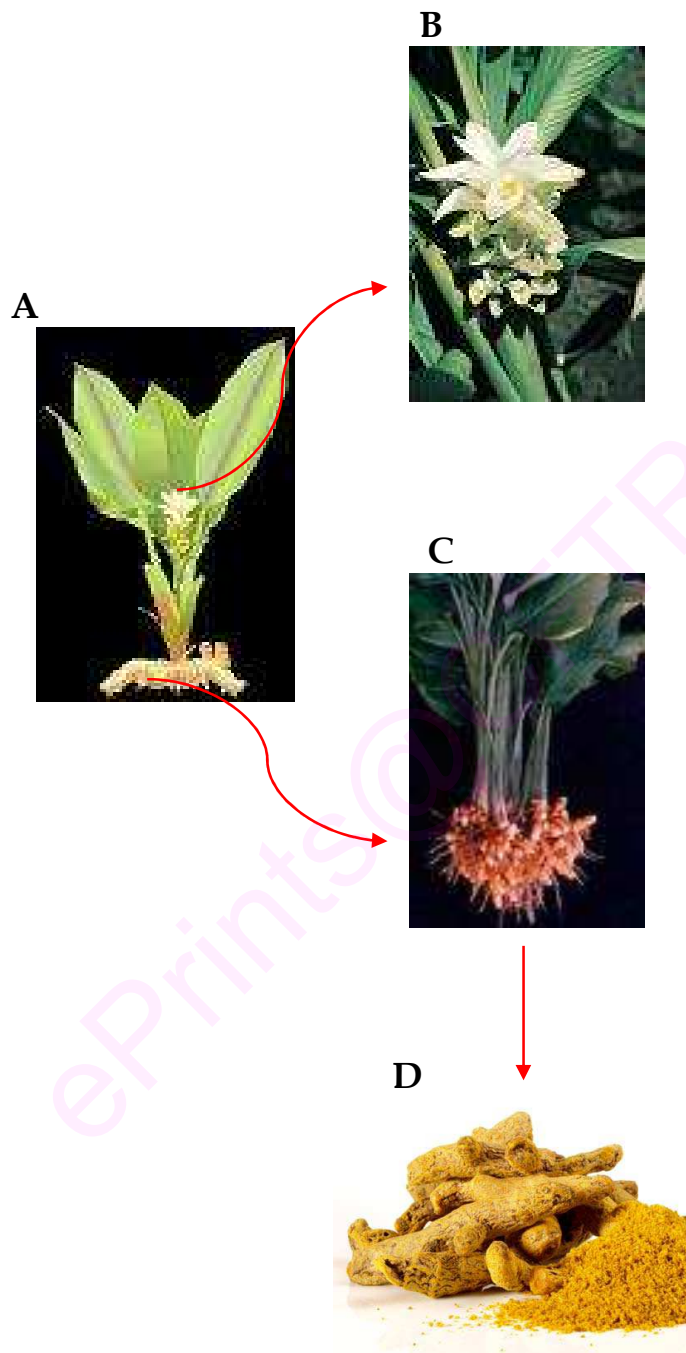
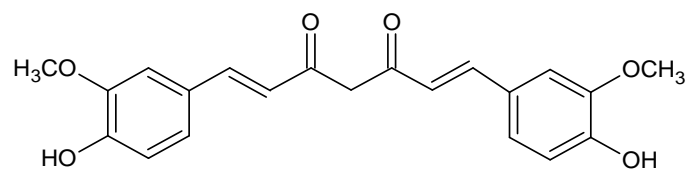


Figure 1.1. *Curcuma longa*, (A) Plant (B) Inflorescence (C) Rhizome (D) Dried and powdered rhizome.

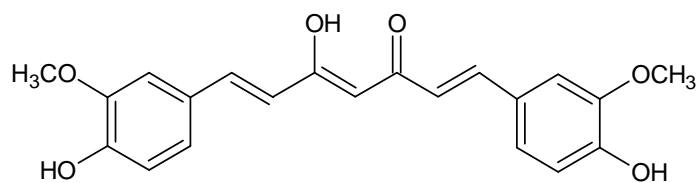
Table 1.1. Chronicle of major biological properties of curcumin reported for first time

Year	Major research findings
3000 B.C.	Discovered by Indian medicine as potent health beneficial rhizome
1280 A.D.	Identified as a wonder root for health benefits by Marco polo
1818	Curcumin isolated and characterized by Vogel and Pelletier
1973	Roughly and Whiting determine the chemical structure
1748	First recorded article referring to <i>Curcuma</i> spp., "de curcuma officinarum," published in 1748 by Loeber
1937	First article referring to use of curcumin in disease published in <i>The Lancet</i>
1941	Nematocidal activity of curcuma using <i>Paramecium caudatum</i>
1972	Anti-inflammatory and antiarthritic actions of volatile oil of <i>C. longa</i>
1982	Anti-inflammatory activity of curcumin
1988	Antitumor activity of curcumin demonstrated
1992	Anti-venom activity of against <i>Bothrops</i> and <i>Crotalus</i> venom
1992	Inhibitory effect of curcumin on the proliferation of blood mononuclear cells and vascular smooth muscle cells
1992	Curcumin as the inhibitor of leucotriene formation in rat peritoneal polymorphonuclear neutrophils (PMNL)
1994	Lipid peroxidation inhibitory activity of curcumin
1995	Antioxidative properties of curcumin and its three derivatives (demethoxycurcumin, bisdemethoxycurcumin and diacetylcurcumin)
1995	Curcumin has antiviral activity, being an HIV-1 integrase inhibitor
1998	Wound healing activity of curcumin demonstrated
1998	Antiprotozoal activity of curcumin against <i>Leishmania amazonensis</i>
1999	Antimicrobial and antimutagenic components of turmeric identified
2000	Curcumin shown to have cholesterol-lowering effect similar to that of statins
2000	Inhibition of NFκB by curcumin demonstrated by Anto and co-workers
2006	Antioxidant activities of curcumin, demethoxycurcumin and bisdemethoxycurcumin demonstrated
2007	Clinical study on pancreatic cancer in progress at M. D. Anderson Cancer Institute, USA

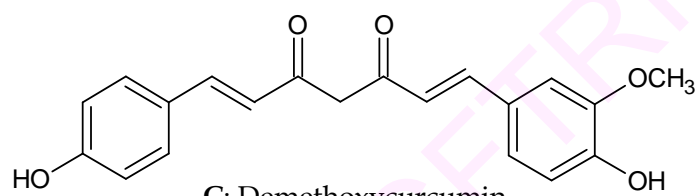
(Adopted from Patil et al., 2009)



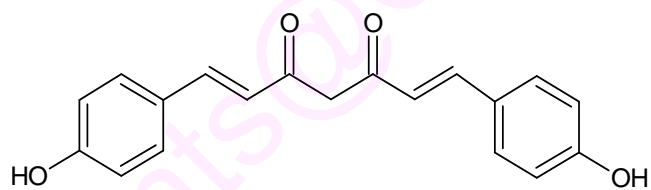
A: Keto form of curcumin



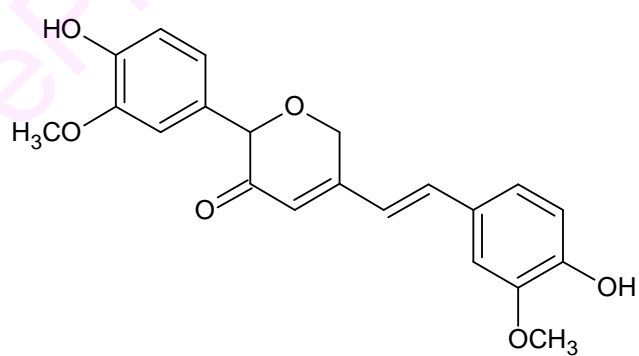
B: Enol form of curcumin



C: Demethoxycurcumin



D: Bisdemethoxycurcumin



E: Cyclocurcumin

Figure 1.2. Structure of curcuminoids

A



B

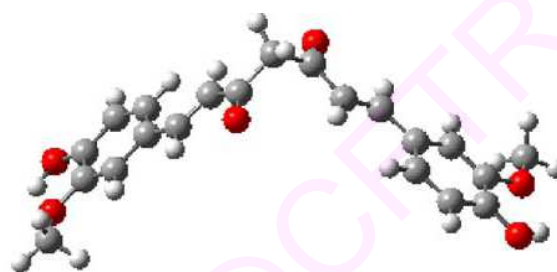


Figure 1.3. Ball and stick model of curcumin in (A) enol form (predominates at $> \text{pH } 8$)

(B) diketone form (predominates at $\text{pH} < 8$)

Biological Activities Attributed to Curcumin

Traditionally, curcumin is used as a good therapeutic agent and many of its biological effects have been scientifically confirmed (Aggarwal et al., 2007). These include antioxidant (Sreejayan, 1997), anti-inflammatory (Ammon and Wahl, 1991) anticarcinogenic and antimicrobial (Shankar and Murthy, 1979; Mazumdar et al., 1995; Brouet and Ohshima, 1995), hepatoprotective (Kiso et al., 1983), thrombosuppressive (Srivastava et al., 1985), hypoglycemic (Babu and Srinivasan, 1995), and as also its protective effects against myocardial infarction (Nirmala and Puvanakrishnan, 1996; Venkatesan, 1998) and rheumatoid arthritis (Deodhar et al., 1980) and many more. These physiological and biochemical actions of curcumin are represented in Figure 1.4. The pharmacological property of curcumin is due to its diverse range of action on different targets which in turn influences the cascade of molecular and biochemical reactions (Figure 1.5). The rationale for enormous interest is due to non toxic nature of the compound even when used in a quantity, as high as 12 g/day (Lao et al., 2006).

The properties of curcumin are due to its structure which allows interacting with many proteins and metal ions. Curcumin interacts with proteins/enzymes such as albumin (Reddy et al., 1999), human alpha1-acid glycoprotein (Zsila et al., 2004a), amyloid protein (Yang et al., 2005), ATPase (Logan-Smith et al., 2001), autophosphorylation-activated protein kinase (Reddy and Aggarwal, 1994), aminopeptidase N (Shim et al., 2003), DNA polymerase- γ (Takeuchi et al., 2006), focal adhesion kinase (Leu et al., 2003), glutathione S-transferase (Iersel et al., 1996), GST-P1 (Awasthi et al., 2000), chelates iron, copper, zinc (Baum and Ng, 2004), microtubulin (Gupta et al., 2006), nucleic acid (Zsila et al., 2004b), P-glycoprotein (Romiti et al., 1998; Chearwae et al., 2004), thioredoxin

reductase (Fang et al., 2005), topoisomerase II (Martin-Cordero et al., 2003), ubiquitin isopeptidase (Mullally and Fitzpatrick, 2002). Curcumin in aqueous medium or bound to PC micelles has shown to inhibit the activity of soy lipoxygenase (Skrzypczak-Jankun et al., 2003a; Began et al., 1998).

ePrints@CFTRI

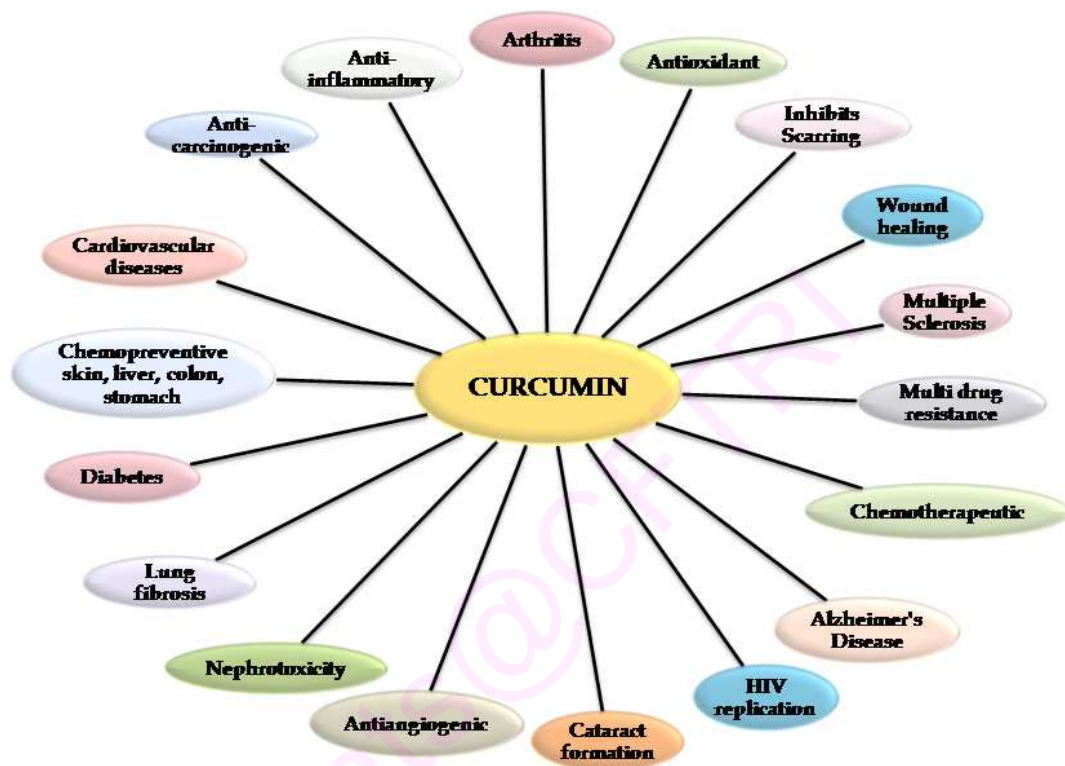


Figure 1.4. Physiological and biochemical action of curcumin

(Joe and Lokesh, 2004; Aggarwal et al., 2007)

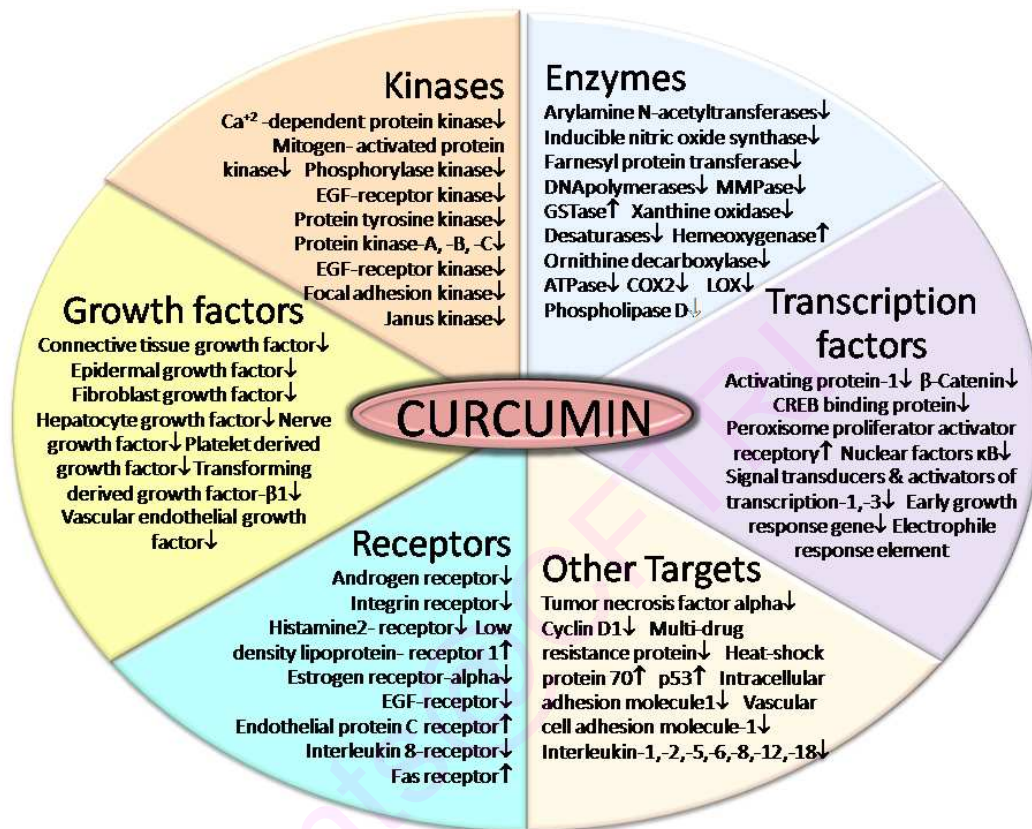


Figure 1.5. Molecular targets of curcumin (Aggarwal and Shishodia, 2006)

Limitations of Curcumin

Bioavailability

Since 1978, the pharmacokinetics and pharmacodynamics of curcumin is being investigated. Many studies to examine the uptake, distribution, and excretion of curcumin in Sprague-Dawley rats have been conducted. Nearly ~ 75% of the ingested curcumin, when administered orally at a dose of 1 g/kg is excreted in the feces with negligible amounts in the urine. Curcumin is poorly absorbed from the gut (Wahlstrom and Blennow, 1978). Curcumin is excreted in the bile, when it is administered intravenously and intraperitoneally to cannulated rats. The major biliary metabolites are glucuronides of tetrahydrocurcumin (THC) and hexahydrocurcumin (HHC) and minor biliary metabolite is dihydroferulic acid accompanied by traces of ferulic acid (Ravindranath and Chandrashekhara, 1981).

In 1999, Pan et al. investigated the pharmacokinetics of curcumin in mice. They found plasma curcumin level reach 2.25 mg/mL, within first 15 min after intraperitoneal administration of curcumin (0.1 g/kg). One hour after administration, curcumin level reach 177.04, 26.06, 26.90 and 7.51 mg/g in intestine, spleen, liver and kidney respectively and traces (0.41 mg/g) in the brain. In comparison, after oral administration of 1 g/kg curcumin, serum plasma levels peaked to 0.5 mM. Pan et al. (1999) observed curcumin-glucuronoside, dihydrocurcumin-glucuronoside, THC-glucuronoside and THC to be the major metabolites of curcumin *in vivo*. Overall, these results agree with the studies conducted by Ireson et al. (2002). Several groups have shown liver to be the major organ responsible for metabolism of curcumin (Wahlstrom and Blennow, 1978; Garcea et al., 2004). Hoehle and coworkers (2006) observed several reductive metabolites

including THC, HHC and octahydrocurcumin (OHC) and its glucuronide and sulfate conjugates, with THC being a more stable derivative compared to the parent compound. They noted the predominance of OHC in males against THC in females. All the above result suggests that curcumin undergoes extensive reduction, most likely *via* alcohol dehydrogenase before conjugation (Goel et al., 2008).

Solubility and Stability

Curcumin has a brilliant yellow hue at pH 2.5 - 7 and turns red at pH > 7. Tonnesen et al. (1986) investigated the photodecomposition of curcumin on exposure to UV/visible radiation. Photobiological activity of curcumin on *Salmonella typhimurium* and *Escherichia coli* was examined. It concluded that the observed phototoxicity makes curcumin a potential photosensitizing drug and its application in phototherapy of psoriasis, cancer, bacterial and viral diseases was suggested (Tonnesen et al., 1987). The same group checked the water solubility of curcumin in cyclodextrin complexes and its hydrolytic and photochemical stability (Tonnesen et al., 2002a). Complex formation resulted in an increase in water solubility at pH 5 by a factor of 10^4 . The hydrolytic stability of curcumin under alkaline conditions was improved by complex formation, while the photodecomposition rate was increased compared to curcumin solution in organic solvents.

The degradation kinetics of curcumin has been determined under various pH conditions (Wang et al., 1997). Ninety percent of curcumin gets decomposed within 30 min in 0.1 M phosphate buffer and serum-free medium (pH 7.2, 37 °C). Curcumin is comparatively more stable in cell culture media containing 10% fetal calf serum and in human blood. Less than 20% of curcumin gets degraded after 1 h and approximately 50% decomposes

after 8 h. The major degradation product of curcumin are *trans*-6-(4-hydroxy-3-methoxyphenyl)-2,4-dioxo-5-hexenal and the minor degradation products are vanillin, ferulic acid and feruloyl methane. Concentration of vanillin increased with time amongst all the degradation products reported (Wang et al., 1997). In a separate study, curcumin is reported to be stabilized by plasma proteins (Leung and Kee, 2009). Influence of major plasma proteins (HSA, fibrinogen, IgG and transferrin) were investigated on the hydrolysis of curcumin at pH 7.4. In the presence of transferrin and IgG, curcumin continues to undergo rapid hydrolysis but is suppressed in the presence of HSA and fibrinogen. These two proteins suppress the hydrolytic degradation of curcumin with a yield of approximately 95%. The binding constants of curcumin to HSA and fibrinogen were in the order of 10^4 and 10^5 M⁻¹, respectively. Strong binding occurs at the hydrophobic moieties of HSA and fibrinogen, excluding water (Leung and Kee, 2009).

Overcoming the Limitations of Curcumin for Usage as a Drug

A major challenge in using curcumin for treatment of diseases is its poor aqueous solubility (~ 20 µg/mL), which significantly limits its availability to the biological system (Letchford, 2008). Despite extensive research and development, poor solubility of curcumin in aqueous solution remains a major barrier for its bioavailability and clinical efficacy (Anand, 2007). Poor oral absorption due to its extremely low aqueous solubility or extensive pre-systemic metabolism may be responsible for its unfavorable pharmacokinetics (Ammon and Wahl, 1991). Keeping in view, curcumin as a promising therapeutically active agent it is pertinent to develop new formulations of curcumin, which can increase its oral absorption and enhance its therapeutic activity (Corson and

Crews, 2007). Therefore various attempts are made to increase its solubility and bioavailability.

Traditionally, turmeric is delivered orally as an emulsion in oil or milk; probably because of the hydrophobic nature of its bioactive constituents such as curcumin and turmeric oil. Several groups have investigated ways to enhance bioavailability. In studies involving rats and healthy human volunteers, piperine significantly enhanced the bioavailability of curcumin (Shoba et al., 1998). Formulation of curcumin-PC given orally to rats enhanced the bioavailability of curcumin five folds in plasma and in liver; however levels were lower in gastrointestinal mucosa (Marczylo et al., 2007). Indeed curcumin has been shown to interact with phospholipids (Began et al., 1999; Maiti et al., 2007; Kunwar et al., 2006; Marczylo et al., 2007), surfactants (Tonnessen et al., 2002b), proteins (Kumar et al., 2002) and cyclodextrin (Salmaso et al., 2007). Delivery of curcumin has been studied by its incorporation into liposome's (Li et al., 2005; Takahashi et al., 2008) and into phospholipid vesicles (Sou et al., 2008) or in the form of synthetic analogues (Sun et al., 2006). The latter was used to deliver curcumin *via* the intravenous route to bone marrow and splenic macrophages.

Curcumin is reported to possess significantly higher solubility (~740 µg/mL) in micellar solutions (Tønnesen, 2002a; Chignell et al., 1994). Alternate way to solve the problem of lack of water solubility and poor bioavailability is encapsulation in polymer-based nanoparticles (Cho et al., 2008). This approach has been used to deliver many natural products like coenzyme Q10 (Ankola et al., 2007), estradiol (Hariharan et al., 2006), ellagic acid (Bala et al., 2006) and chemotherapeutic agents such as paclitaxel (Mu and Feng, 2003) and doxorubicin (Vasey, 1999). In fact, nanoparticle formulation of paclitaxel

with serum albumin as the carrier (Abraxane) has been approved for the treatment of breast cancer (Gradishar et al., 2005). In cell culture studies, Gupta et al. (2009) has observed that silk fibroin-derived curcumin nanoparticles exhibit higher efficacy against breast cancer cells. Curcumin was encapsulated with 97.5% efficiency in biodegradable nanoparticulate formulation based on poly (lactide-co-glycolide) (PLGA) and a stabilizer polyethylene glycol (PEG)-5000 with enhanced cellular uptake by tumor cell lines and increased bioactivity *in vitro* and superior bioavailability *in vivo* than curcumin alone (Anand et al., 2010). Nanocurcumin formulation synthesized by Maitra group (Bisht et al., 2007) has shown about > 90% entrapment efficiency and ~ 40% release of curcumin from the copolymer (NIPAAM/VP/PEG-A: NIPAAM = N-isopropylacrylamide; VP = N-vinyl-2-pyrrolidone (VP); PEG-A = poly (ethyleneglycol)monoacrylate) in 24 h at physiological pH.

Structure Activity Relationship of Curcumin with its Analogues

Although curcumin possess promising therapeutic potential, various studies highlight its instability under physiological conditions. Therefore, to improve the stability and solubility of curcumin, derivatives/analogues of curcumin are being synthesized to study their physiological potency. Way back from 1970's, people are working to improve the solubility and stability of curcumin.

Water soluble semi-synthetic derivative of curcumin - sodium curcumin ate was synthesized and studied for its anti-inflammatory effect. Inflammation induced by carrageenan and formalin in albinio rats was reduced when treated with sodium curcumin ate and was better when compared with hydrocortisone acetate (Ghatak and Basu, 1972).

Curcumin and its analogues like DMC, BDMC and THC were evaluated for their effect on the modulation of signaling on inflammation and cell proliferation (Sandur et al., 2007). Suppression of tumor necrosis factor (TNF)-induced nuclear factor-kB (NF-kB) activation was in the order curcumin > DMC > BDMC while, THC was ineffective. This order on suppression was due to the presence of methoxy groups on the phenyl ring in curcumin, DMC and BDMC. THC, lacking the double bond at central seventh carbon position, was completely inactive for suppression of the transcription factor. The suppression of NF-kB activity is correlated with the down regulation of COX-2, cyclin-D1 and vascular endothelial growth factor. In contrast to NF-kB activity, no major difference was found in suppressing the proliferation of various tumor cell lines by curcumin, DMC and BDMC. This indicated the minimal involvement of methoxy groups in the growth-modulatory effects other than suppressing of TNF. THC was

found to be active in suppression of cell growth but to a lesser extent than curcumin, DMC or BDMC. There was no relationship between any of the curcuminoid, with the production of reactive oxygen species (ROS) related to suppression of NF- κ B or cell proliferation. Therefore, it was concluded that different analogues of curcumin exhibit variable anti-inflammatory and anti-proliferative activities, which did not correlate with their ability to modulate the ROS status.

The antioxidant activities of curcumin, DMC, BDMC and different hydrogenated derivatives *viz.* THC, HHC, OHC were studied and compared using 2,2-diphenyl-1-picrylhydrazyl (DPPH) radical, 2,2-azobis(2-amidinopropane)dihydrochloride (AAPH) induced linoleic acid oxidation and AAPH induced red blood cell hemolysis assays. Hydrogenated derivatives of curcumin exhibited stronger DPPH scavenging activity compared to curcumin and the reference antioxidant, trolox. The scavenging activity was in the order THC > HHC = OHC > trolox > curcumin > DMC > BDMC. Stronger antioxidant activities towards lipid peroxidation and red blood cell hemolysis were also demonstrated by the hydrogenated derivatives. The inhibition of AAPH induced red blood cell hemolysis significantly decreased in the order OHC > THC > HHC > trolox > curcumin > DMC. Results demonstrated lower antioxidant activity by demethoxy derivatives, suggesting the role of methoxyphenolic groups of curcumin in antioxidant activities. On the other hand, hydrogenation at conjugated double bonds of the central seven carbon chain and β -diketone of curcumin to THC, HHC and OHC remarkably enhanced the antioxidant activity (Somparn et al., 2007).

Curcumin exhibits anti-proliferative and anti-inflammatory activity by generating reactive oxygen species. This property of curcumin is due to the presence of functional

groups like two each of hydroxyl, methoxy and phenyl groups. To confirm the role played by each functional group Ravindran et al. (2010) synthesized analogues that varied in each of these functional groups and compared their activity. Bisdemethylcurcumin (BDC) was potent than curcumin as an anti-inflammatory agent by suppressing the TNF induced NFκB activation. BDC was a more potent anti-proliferative agent. Hispolon, a derivative of curcumin lacking an aromatic ring showed anti-inflammatory and anti-proliferative activity. Synthetic curcumin (Cur-S) was compared with BDC, hispolon, hispolon methyl ether (HME), dehydroxy hispolon (DH), hydroxyl hispolon (HH), methoxy hispolon methyl ether (MHME) and methoxy hispolon (MH) and found that anti-inflammatory activity was in the order : BDC = Hispolon > HME > HH > Cur-S > MHME > MH > DH; for anti-proliferative activity: Hispolon > BDC > MHME > Cur-S > MH > HME = HH > DH; and for prooxidant activity: BDC > Cur-S = MHME > HH > MH + HME > DH. Amongst all the compounds checked, DH was least active. Enhanced anti-inflammatory activity was observed in compounds possessing hydroxyl group for methoxy group on the phenyl rings in curcumin and anti-proliferative activity in compounds which lacked an aromatic ring at the seventh position of heptadiene backbone with addition of hydroxyl group.

BDMC and the acetylated derivative - diacetylcurcumin (DAC) are reported to be stable than curcumin in physiological medium (Basile et al., 2009). These compounds were checked for their anti-proliferative effect in HCT116 human colon cancer cells. Both the derivatives correct the spindle formation and prevent the entering of post-mitotic cells to next cell cycle (Basile et al., 2009).

Curcumin inhibits the growth of chloroquine-sensitive (CQ-S) and chloroquine-resistant (CQ-R) *Plasmodium falciparum* in culture with an IC_{50} of ~ 3.25 and $4.21 \mu\text{M}$, respectively (Reddy et al., 2005). Surolia and group (Mishra et al., 2008) synthesized potent curcumin derivatives and were evaluated for their ability to inhibit *P. falciparum* growth in culture. Several curcumin analogues examined, showed effective inhibition against *P. falciparum* growth than the parent compound curcumin. Pyrazole analogue of curcumin exhibited seven fold higher anti-malarial potency against CQ-S and nine fold higher anti-malarial potency against CQ-R. They concluded that curcumin analogues represented a novel class of highly selective *P. falciparum* inhibitors and promising candidates for the design of novel anti-malarial agents.

Since it has been suggested that the seven-carbon β -diketone linker in curcumin is responsible for its instability, Liang et al. (2009) designed and synthesized nine mono-carbonyl five-carbon linker containing analogues. Their bioactivity against lipopolysaccharide-induced TNF-alpha and IL-6 secretion was evaluated by using mouse J774.1 macrophages. The results showed that the 3'-methoxy group plays an important role in bioactivity.

The relationship between the keto and enol tautomeric forms of curcumin in binding to Abeta fibrils has been assessed (Yanagisawa et al., 2010). Weak binding of the keto analogue of curcumin to Abeta aggregates was observed, in comparison to the analogues of keto-enol tautomers. It was concluded that the keto-enol tautomerism of curcumin derivatives may be a novel target for the design of amyloid-binding agents that can be used both for therapy and for amyloid detection in Alzheimer's disease.

Lenhart et al. (2010) synthesized bivalent multifunctional A β oligomerization inhibitors (BMAOIs) containing cholesterol and curcumin, and were characterized for treatment against Alzheimer's disease. From *in vitro* assays it was concluded that the activity against A β oligomers and oxidative stress depends on the spacer length between curcumin and cholesterol and the spacer attachment on curcumin.

ePrints@CFTRI

Hydrogenated Derivative of Curcumin: Tetrahydrocurcumin

Tetrahydrocurcuminoids are the major active metabolites formed when curcuminoids are intraperitoneally administered to mice (Pan et al., 1999). Tetrahydrocurcumin (THC; 1,7- bis(4-hydroxy-3-methoxyphenyl)heptane-3,5-dione) can be prepared synthetically by reducing C=C in curcumin. The structure of THC is depicted in Figure 1.6. Double bonds conjugated to β -diketone in curcumin are reduced to tetrahydro forms by hydrogenating with PtO_2 as the catalyst. The mass of THC is 372.6 and shows maximum absorption at 225 and 282 nm in ethanol. The molar absorption coefficient at 282 nm in ethanol is $17000 \text{ M}^{-1} \text{ cm}^{-1}$ (Osawa et al., 1995). The photochemical properties of THC have been studied by Castellán et al. (2007). THC displays very low fluorescence in ethanol solution at room temperature with quantum yields of 0.9×10^{-3} .

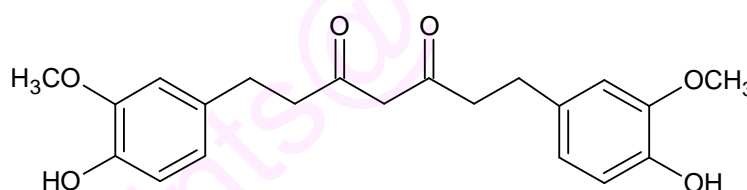


Figure 1.6. Structure of Tetrahydrocurcumin

Unlike curcumin, THC is a colorless compound and shows appreciable hydrophilicity when compared to curcumin (Khopde et al., 2000b). This property of THC renders it useful in non-colored food and cosmetic applications that currently employ synthetic antioxidants (Majeed et al., 1990). As a transformed product of curcumin, THC appears to be involved in physiological and pharmacological activity.

Curcumin being a potent antioxidant molecule, the possibility of THC in mediating antioxidant activities *in vivo*, is speculated and confirmed by several independent

studies. Significant antioxidant effects of the tetrahydrocurcuminoids obtained from turmeric has been reported (Osawa et al., 1995; Sugiyama et al., 1996; Nakamura et al., 1998). Venkatesan et al. (2000) reported that THC has higher activity than curcumin in protecting the nitrite induced oxidation of hemoglobin and lysis of erythrocytes. THC exhibits stronger DPPH scavenging activity compared to curcumin. AAPH induced hemolysis was significantly reduced when treated with THC and is stronger when compared with curcumin. The increased antioxidant activity of THC over curcumin is due to the hydrogenation at the central seven carbon chain and β -diketone moiety of curcumin (Somparn et al., 2007).

THC has also been demonstrated to be more potent than curcumin in protecting against ferric nitrilotriacetate (Fe-NTA) induced oxidative renal damage in mice (Okada et al., 2001). THC produces this protective effect to cells against oxidative stress by scavenging free radicals (Khopde et al., 2000b), inhibition of lipid peroxidation and formation of hydroperoxides (Pari and Murugan, 2004). THC is a potent antioxidant under the conditions where the radical initiators are produced in the polar water medium (Khopde et al., 2000b). THC is also reported to display chemopreventive effects on mouse colon carcinogenesis (Kim et al., 1998). In contrast to the higher antioxidant activity over curcumin, THC is completely inactive for suppression of tumor necrosis factor induced NF κ B activation (Sandur et al., 2007). THC is proposed as an anti-inflammatory and chemopreventive agent (Atsumi et al., 2005).

Strategy for Using Carrier Molecule for Ligand

Many active agents used in pharmaceuticals, food and chemical processes require temporal stabilization and protection against degradation or oxidation (Hattori et al., 1995; Iametti et al., 1995). The efficacy of such agents can be improved by increasing their solubility or by masking the unwanted properties such as toxicity or bad taste (Jain, 1989; Pothakamury and Cánovas, 1995). In other words, the unstable, insoluble bioactives would require the prevention from early degradation, an improvement in the solubility or dispersability in water or a more efficient routing to its target environment. To meet these demands carrier systems have been developed, including particulate systems like nanoparticles, microspheres, liposomes and even resealed erythrocytes. Liposomes consist of phospholipids, whereas nanoparticles may be made of natural or synthetic biocompatible polymers.

Delivery of Nutraceuticals using Nanoparticle

The nanoparticle delivery systems for nutraceuticals with poor water solubility provide opportunity for the design of systems for specific delivery of materials to targeted sites.

Nanotechnology has been introduced into several aspects of food industry including encapsulations and delivery systems which protect and deliver functional food ingredients. Nanotechnology provides possible alternative to traditional method of encapsulation in the production of supplements (Weber et al., 2000). This type of 'nanoceutical' or functional food appears to be the growth area at present and fits between foods and pharmaceuticals.

Biopolymers such as proteins, lipids or polysaccharides, are commonly used to encapsulate the bioactives in order to protect them from rapid degradation by

environmental stress (e.g. light, heat, oxygen or pH sensitivity). Among these colloidal systems those based on proteins may be very promising, since they are biodegradable and non-antigenic, relatively easy to prepare and their size distribution can be monitored easily (Kramer, 1974).

Proteins, such as gelatin, albumin, caseins, β LG or fibrin (Thies and Bissery, 1984; Gupta and Hung, 1989) are commonly used matrices to encapsulate the functional ingredients. The application of carrier systems that selectively and reversibly bind the active agent offer possibilities to stabilize and improve its release (Hattori et al., 1995). Nanoparticles with a diameter of 50 to 500 nm have the potential to deliver to specific target sites and to achieve sustained drug release. Encapsulation can modify the biodistribution and increase its bioavailability. Schematic representation of nanoparticle preparation by desolvation of an aqueous protein solution followed by crosslinking for particle stabilization is shown in Figure 1.7.

In general protein nanoparticles display a number of interesting advantages. These carriers are biodegradable and metabolizable which can bind a variety of ligands in non-specific fashion. The defined primary structure of proteins, offer various possibilities for surface modification and covalent attachment of drugs and ligands. Due to their sub-cellular size, nanoparticles offer promising means of improving the bioavailability of nutraceutical compounds, especially poorly soluble substance such as functional lipids (carotenoids, phytosterols, ω -3 fatty acids), natural antioxidants and numerous other compounds that are widely used as active ingredients in various food products. They can dramatically prolong compound residence time in the gastro-intestinal (GI) tract by decreasing the influence of intestinal clearance mechanisms and increasing the surface

available to interact with the biological support (Kavashim, 2001; Peppas, 1992; Arbos et al., 2002). They can also penetrate deeply into tissues through fine capillaries, cross the epithelial lining fenestration (e.g. in the liver) and are generally taken up efficiently by cells, thus, allowing efficient delivery of active compounds to target sites in the body (Chen et al., 2006).

Natural polymers are promising due to their safety, especially when originated from food sources. Food proteins show great promise for developing and engineering a range of new generally recognized as safe (GRAS) matrices with the potential to incorporate nutraceutical compound and provide controlled release *via* the oral route. Clear advantages of food protein matrices include their high nutritional value, abundant renewable sources and acceptability as naturally occurring food components degradable by digestive enzymes.

Structural and physicochemical properties of milk proteins favor their choice as vehicles for encapsulation and controlled release of bioactive compounds (Livney, 2010; Gunasekaran et al., 2007). Food-grade materials generally recognized as safe. They are biocompatible and biodegradable and have the potential to be used for the delivery systems in a wide variety of foods.

Food proteins can be exploited to create different interactions with nutraceuticals compounds and subsequently form three-dimensional networks to incorporate and protect these compounds in a matrix and deliver them to the site of action in active form. New strategies for stabilization of fragile nutraceuticals and development of novel approaches to site-specific carrier targeting, food-protein-based materials play an important role in increasing the efficacy of functional foods. However, greater

fundamental understanding of protein–protein and protein–nutraceutical interactions at the molecular level and their impact on functional properties of proteins is still required to ensure design of ideal nutraceuticals carriers for use in the food industry.

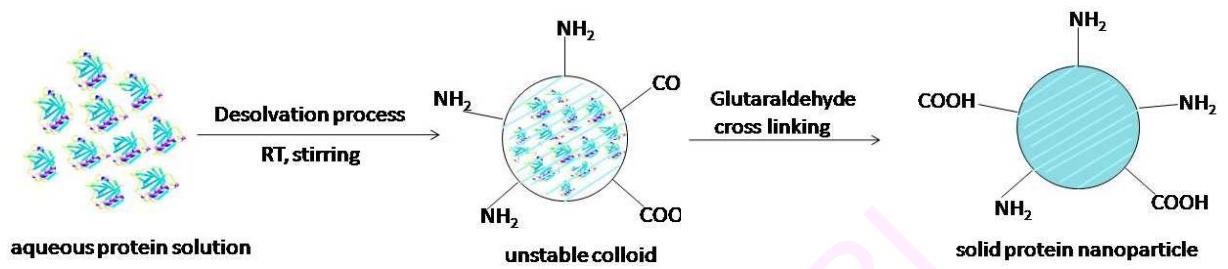


Figure 1.7. Schematic representation of nanoparticle preparation by desolvation of an aqueous protein solution followed by particle stabilization by crosslinking.

Binding of Ligands to a Macromolecule

Molecular organization and recognition is the fundamental principle of all biological processes. Molecular recognition plays central role in cellular behavior (Bongrand, 1988) and the immunological response (Eisen, 1990). This has become the basis for a wide range of bioanalytical techniques (Tijssen, 1985). Biological macromolecules are able to interact with various small and large molecules, with a high degree of specificity and with high affinity. It offers a powerful mechanism for exogenous control of biological systems. Many medications and biological probes act by binding and inhibiting a specific macromolecular target. In general, protein-ligand interactions play a major role in cellular metabolism. A ligand is usually a small molecule; however, anything that binds with specificity can be considered as a ligand. A prerequisite for a deeper understanding of the molecular basis of protein-ligand interactions is a thorough characterization and quantification of the complex formation.

Knowledge on the structure/conformation at the molecular level and the biophysical properties of protein and the ligand is required for protein-ligand interaction studies.

Binding Equilibrium

Describing protein-ligand interactions, a simple method to represent the non-covalent interaction between a protein [P] and ligand [L] is,



The equilibrium constant (also known as association constant or affinity constant) for the binding of a ligand to a protein is described by the following equation:

$$K_{\text{eq}} = \frac{[PL]}{[P][L]}$$

where K_{eq} is the equilibrium constant for the reaction, $[PL]$ is the concentration of the protein-ligand complex, $[P]$ is the concentration of the protein, and $[L]$ is the concentration of the free or unbound ligand. Association constant, K_a describes the affinity of protein $[P]$ to ligand $[L]$ in a reversible reaction.

Representation and Analysis of Ligand Binding

The dissociation constant, K_d , is given by,

$$K_d = \frac{[P]_F [L]_F}{[PL]}$$

where f denotes the concentration of free species at equilibrium. The total concentration of protein, $P_T = [PL] + [P]_F$, and the concentration of PL , may be expressed as a function of $[L]_F$, as shown below,

$$[PL] = \frac{[P]_T}{1 + K_d/[L]_F}$$

If P_t is constant, a plot of $[PL]$ versus $[L]_f$ is a rectangular hyperbola and the concentration of $[L]_F$ at which $[PL] = \frac{1}{2} [P]_T$ is equal to K_d . This is depicted in Figure 1.8A.

The dissociation constant K_d , is the equilibrium constant for the release of ligand from protein and is therefore the reciprocal of the association constant. K_d is the molar concentration of ligand at which half of the available ligand-binding sites are occupied. High value of K_a or a lower K_d value represents high affinity of ligand to protein *i.e.* more protein-ligand complex than unbound protein or ligand. When K_a is low, the affinity of ligand to protein is less with less number of binding sites occupied. Some examples of dissociation constants for known protein and ligand are given in Table 1.2.

The above parameters can be evaluated from several linearized versions, of which commonly used are the Klotz equation (Klotz, 1946),

$$\frac{1}{[\text{PL}]} = \frac{1}{[\text{P}]_T} + \frac{K_d}{[\text{P}]_T} \frac{1}{[\text{L}]_F} \quad (1)$$

and the Scatchard equation (Scatchard, 1949),

$$\frac{[\text{PL}]}{[\text{L}]_F} = K_a n - K_a [\text{PL}] \quad (2)$$

The graphical equivalents are shown in Figure 1.8B and 1.8C. The above equations refer to a case where a single protein molecule has a single binding site for ligand.

The other models used to represent and analyze the data to gain information about the binding parameters and stoichiometry are Stern-Volmer equation (Lakowicz, 1999) or its modified form (Lehrer, 1971), double logarithm regression curve (Xiao et al., 2008), Benesi-Hildebrand equation (Benesi and Hildebrand, 1949), Lehrer-Fasman equation (Lehrer and Fasman, 1967; Rao and Cann, 1981) and many more.

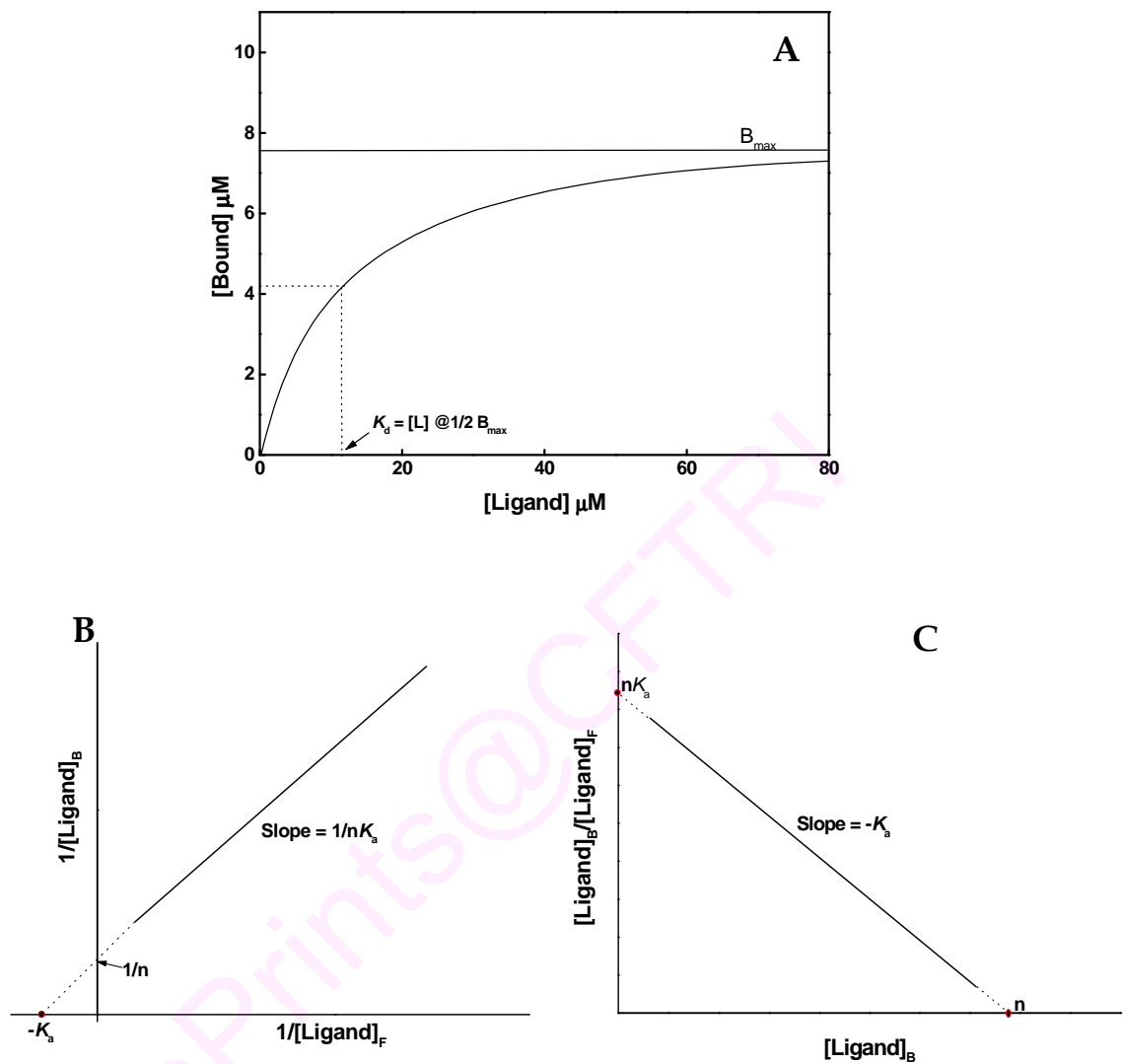


Figure 1.8. (A) Saturation curves for ligand binding to proteins. (B) Klotz plot for the equilibrium binding data. (C) Scatchard plot for the equilibrium binding data. The slopes and intercepts of the straight lines are indicated.

Table 1.2. Examples of protein dissociation constants

Protein	Ligand	K_d (M) *
Avidin (Egg white)†	Biotin	1×10^{-15}
Insulin receptor (human)	Insulin	1×10^{-10}
Nickel binding protein (E.coli)	Ni^{2+}	1×10^{-7}
Calmodulin (rat)‡	Ca^{2+}	$\left. \begin{array}{l} 3 \times 10^{-6} \\ 2 \times 10^{-5} \end{array} \right\}$

*Reported dissociation constant is valid only for the particular solution conditions under which it was measured. K_d values changes for protein-ligand interaction when solution salt concentration, pH or other conditions are varied.

†Interaction of avidin with the enzymatic cofactor biotin is among the strongest noncovalent biochemical interactions known till date.

‡Calmodulin has four binding sites for calcium. The values shown reflect the highest and lowest affinity binding sites observed in one set of measurements.

Thermodynamics of Binding

Selective binding of a low-molecular weight ligand to a specific protein is determined by the structural and energetic recognition of a protein and ligand. Thermodynamics offers insight into the energetics of protein-ligand interaction that is not readily attainable by other means. Measurement of thermodynamic parameters is important because, vast majority of ligands act through non-covalent interaction with the target protein along with the redistribution of non-covalent bonds. Since the nature of most protein-ligand interaction involves relatively weak force resulting from electrostatic attractions such as ion-ion, ion-dipole, dipole-dipole (hydrogen bonds), van der Waals (induced transient

fluctuating dipoles) or hydrophobic effects, they are reversible and thus amenable to thermodynamic analysis (Figure 1.9). Binding constant depends on the number of different forces involved. Gossypol binds reversibly with high affinity to serum albumin with the involvement of hydrogen and hydrophobic interactions (Maliwal et al., 1985). Albumin binds to genestein *via* ionic and hydrophobic forces (Mahesha et al., 2006). Curcumin binds to human serum albumin at two site, the primary site being the domain II with the involvement of hydrophobic and hydrogen bonds (Reddy et al., 1999; Zsila et al., 2003).

The most experimentally accessible thermodynamic parameter occurring during this process is either the release or uptake of heat (enthalpy). The enthalpy changes can be measured from the temperature dependence of the binding constant using the van't Hoff equation.

$$\Delta G^\circ = -RT \ln K_a = \Delta H^\circ - T\Delta S^\circ \quad (3)$$

ΔH° → Enthalpy: A measure of stability

ΔS° → Entropy: A measure of disorder

ΔG° → Spontaneity of a reaction

In terms of protein-ligand interactions, energy changes occur in the dissociation of the ligand molecules from the molecule of the solvent with the protein molecules. Ligand binding to protein is associated with changes in ΔH° and ΔS° . Change in free energy is a dual rearrangement process of protein and solvent. Rearrangement of protein involves change in degrees of freedom or exposure to water molecules and rearrangement of solvent involves a decrease in constraint and hence an increase in entropy.

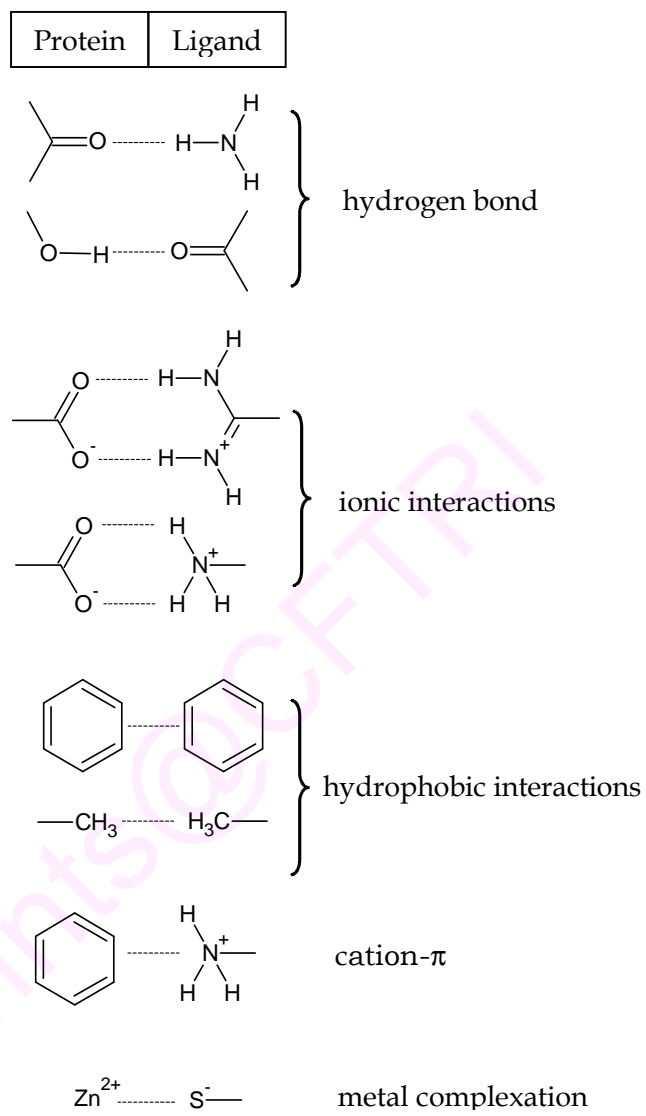


Figure 1.9. Major contribution of forces in protein-ligand interaction

(Adopted from Böhm and Schneider, 2003)

Experimental Approaches to Study the Binding

Different experimental methods have been developed to study and quantitate protein-ligand interactions. These techniques, in general, involve any one of the following principles: (i) separation of the free ligand from the protein-ligand complex/determination of the concentration of the free ligand, and (ii) detection of changes in either the physicochemical properties of the bound ligand or the physicochemical behavior of the protein (Klotz, 1973).

The former is non-spectral and direct and includes the following methods.

Nonspectral Methods

(a) Equilibrium dialysis - Equilibrium dialysis is based on the principle of separating the free ligand from the protein bound ligand. This is achieved by allowing the former to dialyze through a semi-permeable membrane until the concentration of ligand in the dialysate, *i.e.* the protein-free compartment, under ideal conditions, is equal to the concentration of unbound ligand in the retentate *i.e.* the protein-containing compartment (Davis, 1943). The bound and unbound ligand is then measured spectroscopically or by other sensitive detection methods like radioactivity and HPLC measurements. Disadvantages of this method include long equilibrium time, adsorption of the ligands on the surface of the dialysis tube and membrane. In addition, large volume of buffer and samples are required (Oravcova et al., 1996).

(b) Hummel - Dreyer method - The Hummel and Dreyer method is a direct method of measuring the ligand binding to proteins. The principle is analogous to dialysis equilibrium and is devised to detect the reversible interactions between macromolecules and the low molecular weight compounds. This involves the application of small

volume of the macromolecule with the known concentration of ligand on a size exclusion chromatography column (e. g. Sephadex G-25) which is pre-equilibrated with the same concentration of the ligand. The consequent elution profile obtained exhibits a peak of ligand bound to the macromolecule along with a trailing trough representing, the quantity of ligand withdrawn from the solution. Appearance of a trough in the elution profile thus provides a criterion of ligand binding to protein. Under these conditions, the concentration of the ligand and the protein is in constant equilibrium and hence, weak interactions can be studied (Hummel and Dreyer, 1962). Because of its simplicity and speed, this method has been used to study numerous drug interactions (Cann et al. 1989; Sebille et al., 1979). The main advantage of this method is, the ligand binding is less exposed to artifacts and there is control of free ligand concentration as an independent variable, which depends on the bound site ratio. Factors which affect the accuracy and reproducibility of the results are variation in the temperature and aggregation or polymerization when high protein concentration is used. Advancement in HPLC technology and automation has reduced the column size and volumes of the eluent making the technique more reliable and faster.

(c) Calorimetric - The calorimetric method is widely and increasingly used to assess the protein-ligand binding which includes isothermal titration calorimetry (ITC) and differential scanning calorimetry (DSC). These two methods are complimentary and are based on equilibrium thermodynamics, which allows the direct determination of the enthalpy and entropy of inter- and intra-molecular reaction (Jelesarov and Bosshard, 1999). Calorimetric technique requires no chemical modification or extrinsic probes or immobilization of the reactants. These are non-invasive and non-destructive methods

with good reproducibility of results. ITC measures the binding equilibrium by determining the heat change when a protein is titrated with a ligand (Jelesarov and Bosshard, 1999; Pierce et al., 1999). It allows the determination of binding constant, stoichiometry and binding enthalpy. The advantage of using ITC is that, it is a direct binding measurement and the theoretical equilibrium state of the system under study is not disturbed. ITC allows the studying of abnormal protein-protein and other types of protein-ligand interactions which may be useful in understanding the various disease states. ITC cannot be used to study the high affinity reactions, which otherwise, may result in aggregation.

DSC allows the measuring of heat energy uptake that takes place in a sample during controlled change in temperature. It enables the assessment of thermally induced transitions, particularly conformational transitions in biological macromolecules (Bruylants et al., 2005). DSC provides preliminary information about the changes occurring in the system.

Other methods include:

(d) Sedimentation velocity – results in change in sedimentation coefficient, a good tool for the separation and analysis of heterogeneous mixtures of the various components and detects conformational change.

(e) Sedimentation equilibrium analytical ultracentrifugation – In this technique, there is change in solution mass and allows predicting the stoichiometry, dissociation constant, Gibbs free energy and molecular mass in case of oligomers.

(f) Affinity chromatography (frontal and zonal) - The principle is similar to equilibrium gel filtration chromatography, involves the partitioning of free from the bound ligand, and allows the determination of the stoichiometry and dissociation constant.

(g) Surface plasmon resonance - a label-free, real-time, optical detection method (O'Shannessy et al., 1994) that detects changes in refractive index and change in mass bound to the surface of sensor chip (Zeder-Lutz et al., 1999). This technique is used to measure the stoichiometry, strength and kinetics of binding.

(h) Capillary electrophoresis is implemented to detect any change in shape, size or charge of protein and this allows measuring the association constant and kinetics.

Above are a few methods highlighting the non-spectral methods for studying protein-ligand interactions.

Spectral Methods

Structural and spectroscopic studies gives an in depth knowledge about the conformational change in the structure after interaction. Subtle changes occurring at the molecular level after the interaction can be analyzed using these techniques. Following are the structural and spectroscopic technique employed to study the protein-ligand interactions.

(a) X-ray crystallography - X-ray crystallography allows the examination of the three-dimensional (3D) structure (Atkins and de Paula, 2005) and conformational changes associated in the protein structure after complexing with ligand. Information can be gained about the location of all atoms in a molecule and the structural changes. The formation of protein crystals is the slowest step in x-ray crystallography. When x-ray

beams or synchrotron beams are directed at the crystal, some of the x-rays are scattered by the crystal and diffraction spots appear, forming an x-ray diffraction pattern. This pattern contains information about the position of the atoms in the crystal and forms a complex 3D electron-density map. The map is then analyzed using specialized software.

(b) Nuclear magnetic resonance - The other method for studying the three dimensional structure of protein, interaction between molecules and molecular motion is nuclear magnetic resonance (NMR). NMR allows the determination of structure of small proteins (15-30 kDa) and protein-ligand interactions (Sykes and Hull, 1973). NMR provides information on many different aspects of protein-ligand interaction ranging from structure to dynamics, kinetics and thermodynamics. The difference between NMR and x-ray crystallography is NMR can be performed in solution (Cooke and Campbell, 1988). NMR requires small volume of highly concentrated pure protein. It is based on the detection of transitions between nuclear energy levels (Cooke and Campbell, 1988). The sample is placed in a magnetic field and radiofrequency pulses are applied. This disturbs the equilibrium of nuclear magnetization and the signals to be analyzed are then detected when the system returns to equilibrium. Advantage is that, the detailed arrangement of individual atoms can be calculated from the spectra. Hydrogen atoms which are beyond the resolution of x-ray diffraction analysis in large molecules can be located and different atoms can be located separately. Two-dimensional NMR (2D NMR) is used to characterize the protein structure. In this method, the resonances are spread out in two dimensions, making it easier to detect the NMR signals of the molecule. Based on detection, 2D NMR is divided into two classes - (i) detecting

through-bond interactions between resonances (COSY, correlated spectroscopy) (ii) detecting through-space interactions (NOE, Nuclear Overhauser Effect).

(c) Electron cryo-microscopy - Electron cryo-microscopy (cryo-EM) is used to determine the biological structures of proteins and is extensively utilized in studying membrane proteins (Henderson, 2004). Cryo-EM enables analysis of the structure of molecules arranged in the form of 2D crystals, helical arrays or single particles with or without symmetry using frozen unstained specimens.

(d) Circular dichroism: Conformation of a macromolecule or the interactions between molecules in solution can be elucidated using circular dichroism (CD). This method measure the wavelength dependence of the ability of differential absorption of right and left circularly polarized light. Either the ligand must bind in a dissymmetric fashion that induces extrinsic optical activity in the chromophore of the bound ligand or the binding must result in a conformational change in the macromolecule that results in a change in its intrinsic CD spectrum. The data obtained from either of the above changes can be used to figure out the ligand binding constants. Several useful applications of CD as a tool for analyzing the properties of proteins are: (i) protein-ligand interactions (ii) thermodynamics of protein folding (iii) conformational transitions and protein aggregation (iv) folding intermediates (v) kinetics of protein folding (vi) structural characterization and secondary structure determination of proteins (Bulheller et al., 2008; Wallace and Janes, 2003).

(e) Fluorescence spectroscopy: Fluorescence spectroscopy is the most widely used method for studying protein-ligand interactions. The extensive use of this non-invasive technique is due to its high sensitivity and applicability in broad range like

conformation, binding sites, solvent interactions, degree of flexibility, intermolecular distances and rotational diffusion coefficient of macromolecules. Protein-ligand interaction studies is approached by two modes - by following the intrinsic fluorescence of the protein which is due to the presence of three intrinsic fluorors - phenylalanine, tyrosine and tryptophan residues or by introducing an extrinsic probe either by chemical coupling or by simple binding. The later method of adding an external molecule and following the fluorescence analysis is named as extrinsic fluorescence.

Intrinsic fluorescence, which is contributed by the presence of three aromatic amino acids, can be followed by exciting at the appropriate wavelength. Tryptophan fluorescence is the most commonly studied because phenylalanine has very low quantum yield and tyrosine fluorescence is weak due to quenching. Tryptophan fluorescence is followed at 295 nm whereas at 280 nm, all the three amino acids contribute to the fluorescence property. Fluorescence of tryptophan and tyrosine depends on their environment like solvent, pH, presence of a quencher or an external molecule or a neighboring group in the protein. Fluorescence quenching can be a result of many molecular interactions such as excited-state reactions, molecular rearrangements, resonance energy transfer and ground-state complex formation (Lakowicz, 1999). Resonance energy transfer (RET) is due to long-range dipolar interactions between an electron in the excited donor and an electron in the acceptor (Lakowicz, 1999). When RET occurs, the donor returns to the ground state, while the acceptor simultaneously enters a higher excited-state orbital (Lakowicz, 1999). In RET, the acceptor need not be fluorescent. The fluorescence-based method is fast and simple. Fluorescence quenching can also be used to study the structure and dynamics of protein

molecules in solution, folding and association reactions of proteins (Palazolo et al., 2000; Lakowicz, 1999). Therefore, intrinsic fluorescence is often studied to gain information about the conformation of the protein.

The use of an external molecule to study the fluorescence is called extrinsic fluorescence. The fluor to be utilized in extrinsic fluorescence studies should meet the following requirements: (i) the fluor must bind to protein (ii) the fluorescence of the probe must be sensitive to the environment (iii) it should not affect the fluorescence of the macromolecule under investigation. Commonly used fluorescent probes are ANS, *bis*-ANS, PRODAN, TNS, CPA, fluorescein.

(f) Electron paramagnetic resonance (EPR) - EPR is used to analyze the changes in the electronic environment and rotational diffusion, which gives insights on the changes in the structure and dynamics of macromolecule.

(g) Atomic force microscopy (AFM) - AFM is based on force measurements (Lee et al., 1994). This technique involves the surface imaging of force between the molecules and changes on ligand binding. Change in structure and altering of the mechanical stability of proteins upon ligand binding can be measured (Cao et al., 2007). This is used to visualize single molecule and is useful in studying the membrane proteins which are inaccessible to x-ray crystallography.

(h) Mass spectrometry (MS) - Different methods such as soft ionization methods, direct monitoring of protein-ligand interactions by electrospray ionization-mass spectrometry (ESI-MS), hydrogen-deuterium exchange methods, mass spectrometry with affinity chromatography and chemical cross linking are used to investigate protein-ligand interactions (Schermann et al., 2005).

Molecular Docking

Prediction of three dimensional visualization of interaction of ligand to protein has emerged into a wide field namely molecular modeling (Ekins et al., 2007). Advantages are, different surface models can be made and analyzed, 3-D structure can be rendered and visualized, noncovalent bonding length like the hydrogen and van der Waals distance can be measured. Comparison with the experimental data serves to test the accuracy of the calculated research and time efficiency. The shortcomings of molecular modeling are: the method is approximate, rigorous theoretical calculations and computations are involved, system is too large to be handled by one approach and modeling software is expensive. Although, methods are approximate and fail to take chemical accessibility into account and needs validation, computational approaches are becoming practicable (Ekins et al., 2007).

Milk Proteins

Milk proteins are divided into two fractions, *viz.* casein and whey proteins. Casein is the protein fraction of milk obtained from precipitation at pH 4.6, 20 °C. The liquid portion left after precipitation is termed as whey. The composition of milk is given briefly in Table 1.3.

Table 1.3. Composition of skim milk

Component	Average content (%, w/w)	Size (nm)
Water	87.1	-
Protein		
Caseins	2.6	~ 10
Casein micelles		~ 40-300
Whey proteins	0.6	~ 3-6
Lactose	4.7	~1
Mineral substances	0.7	< 0.5
Calcium	0.12	
Phosphate	0.20	

Whey Proteins

Milk whey contains a heterogeneous group of proteins that are derived either from blood or synthesized in the mammary gland. The nutritional function of these proteins is to provide amino acids required by the infants. In addition, some proteins may have a more specific function in the mammary gland or in the newborn. α -Lactalbumin is the B subunit of lactose synthetase, the enzyme that catalyzes the addition of galactose to glucose to synthesize lactose (Brodbeck and Ebner, 1966). Immunoglobulins serve to transfer passive immunity to the neonate (Larson et al., 1980). Lactoferrin may play a

role in controlling iron absorption or in the selection of the intestinal flora in the newborn intestine (Shchez et al., 1992). Although various roles have been proposed for β -lactoglobulin, including the involvement in phosphorus metabolism in mammary glands (Farrell et al., 1987) or in the transfer of passive immunity to newborn (Warme et al., 1974), no function has been definitively ascribed to this protein.

β -Lactoglobulin

Bovine β -lactoglobulin (β LG) is a major whey protein in milk present to an extent of about 50% (Hambling et al., 1992). Its concentration varies throughout lactation, it is higher in the first colostrum (between 18 to 20 mg/mL) and becomes stable during the 2nd week of postpartum (about 4 mg/mL) (Perez et al., 1990).

β LG is produced in ruminant species under the control of co-dominant alleles. As a result, the protein isolated from a cow heterozygous in the β LG gene contains two types of polypeptide chain. The genetic variants observed by Aschaffnburg and Drewry (1995) and others, though involve one or two amino acid changes, do affect the protein and hence the milk (Creamer et al., 1997). The most common genetic variants of *Bos taurus* are the A and B forms, although about a dozen variants have been observed by their different electrophoretic mobilities (Zimmermann et al., 1996). Variant A differ at Asp64 (Gly in variant B) and at Val118 (Ala in variant B). The genetic variants referred above in the ruminant species result in relatively minor amino acid differences, but the processing properties appear to be significantly affected even by these small changes. Therefore, consideration has given to remove the less favorable variants by selective breeding (Hill et al., 1997; Harris et al., 1997).

β LG has been used as a convenient small protein for many biochemical and biophysical studies. Because of its thermally unstable and molten-globule nature, β LG has been studied extensively for its physical and biochemical properties in the past 40 years (Sawyer and Kontopidis, 2000).

Molecular weight determinations have shown that the protein exists as a dimer of \sim 36400 Da under physiological conditions, but between pH 2 to 3, it tends to dissociate into monomers. Similarly, at pH value > 9 , it dissociates, although over time aggregation and precipitation occur increasingly, especially if the pH is increased further.

Structure of β LG

β LG, a small globular protein of 162 amino acid residues ($M_r \sim 18400$ Da) contains one free cysteine residue (Cys121) and two disulphide bridges (Cys66-Cys160 & Cys106-Cys119). The secondary structure of β LG comprises 15% α -helix, 50% β -sheet and 30% random coil as shown in Figure 1.10A (Hambling et al., 1992).

The protein is a typical lipocalin whose structure contains a β -barrel with eight antiparallel β -strands with $(+1)_8$ topology, labeled A-H as shown in Figure 1.10B. The so-called calyx or β -barrel is conical in shape. It is made of β -strands with A-D forming one sheet and strands E-H forming the second. A significant feature in all lipocalins is the bend in strand A by right angle such that the C-terminal end forms an antiparallel strand with H. Strands D and E form a less significant interaction completely closing central cavity, the calyx. Calyx provides the space for ligand binding. A three-turn α -helix follows strand H and lies on the outer surface of the barrel between the C-terminal end of the A strand and the H strand (Figure 1.10B). A ninth β -strand, I, antiparallel to the first strand, A, and on the other side from H, is involved in dimer formation. The

loops that connect the β -strands at the closed end of the calyx, BC, DE, and FG are generally quite short, whereas those at the open end are significantly longer and more flexible. In particular, the EF loop acts as a gate over the binding site. At low pH, it is in the “closed” position and binding is inhibited or impossible, whereas at high pH it is open, allowing ligands to penetrate into the hydrophobic binding site. The “latch” for this gate is Glu89, the residue implicated in the Tanford transition observed (Tanford et al., 1959; Brownlow et al., 1997; Qin et al., 1998a).

The three predominant crystal forms grown by salting-out at and around neutral pH have been well described (Brownlow et al., 1997; Qin et al., 1998b). Two of the crystal forms, the triclinic lattice X at pH 6 and the orthorhombic lattice Y at pH 7.5 provide data sets at 1.8 Å resolution while, the third trigonal lattice Z at pH values between pH 6 and pH 8.5, provides data to a resolution poorer than 2.3 Å. The reason for this is that, the protein undergoes a distinct change in conformation as the pH value is raised from pH 6 to pH 8. This results in uncovering of the carboxyl group of Glu89, with an increase in the reactivity of free sulfhydryl group - Cys121 (Qin et al., 1998a; Tanford et al., 1959). This behavior of Glu89 with an anomalous pKa value of 7.3 which is buried at acidic pH but exposed at basic pH is termed as Tanford transition. The free Cys121, with its reactive thiol group has a pH-dependent activity similar to that of the Tanford transition. This is involved in the denaturation and aggregation behavior of the protein (Havea et al., 2001).

The molecule has two ligand-binding sites - a central calyx domain of the β -barrel and a surface hydrophobic pocket in the groove between the α -helix and β -barrel (Yang et al., 2009). The electrostatic protein surface with the inner binding site - calyx and the outer

binding site is illustrated in Figure 1.10C. Two independent studies have revealed the calyx as the binding site for fatty acids (Qin et al., 1998b; Wu et al., 1999) while, the binding site for retinol has so far proved to be elusive. A possible binding site reported by Monaco et al. (1987) was on the outer surface of the protein between the helix and the β -barrel but crystallographic analysis revealed the calyx as the binding site (Brownlow et al., 1997).

The proposal of β LG as an oral drug carrier is supported by its ability to bind many biochemically important hydrophobic compounds (Kontopidis et al., 2004). β LG is edible and easily solubilized with good emulsifying characteristics. Its cost effectiveness, abundant availability and acceptability make it an attractive alternative protein that can be used as a carrier molecule for curcumin.

Biological Function of β LG

Although the biological functions of the protein still remain subtle, some essential functions of β LG such as cholesterol lowering, modulation of immune system, transport of retinol, fatty acid and vitamin D (Nagaoka et al., 2001; Kontopidis et al., 2004) and prevention of oxidative stress (Marshall, 2004) have been proposed and reported. In spite of large number of studies performed over the past several years, no definite biological function has been ascribed to β LG.

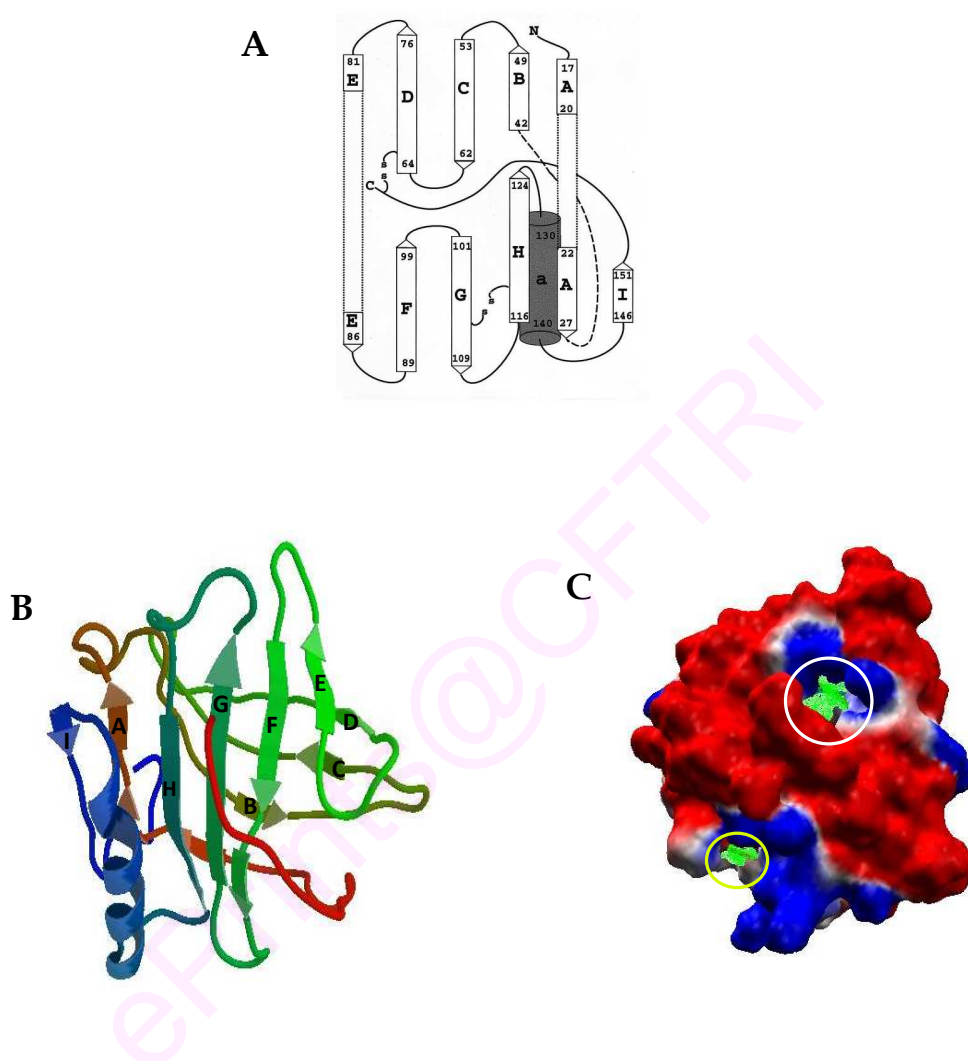


Figure 1.10. (A) Schematic diagram of secondary structural elements of β LG (adopted: Sawyer and Kontopidis, 2000). (B) Ribbon cartoon model of 3-D structure of β LG (PDB ID: 1BSY), A-H represents the β -barrel, α -helix situated in between β strands A-H and I. (C) Visualization of the central calyx (green outlined by yellow circle) and the outer binding site (green outlined by white circle) on an electrostatic protein surface.

Casein

Casein micelles are highly hydrated and sponge-like colloidal particles. Of the ~ 4 g of water/g of protein contained within the colloidal particle, ~ 15% is bound to the protein with the remainder being occluded within the particle (de Kruif and Holt, 2003; Farrell et al., 2003). About 95% of the casein is present in micellar form (average diameter is ~200 nm). It serves as the prime nutritional source of calcium, phosphate and amino acids to meet the growth and energy requirements of mammalian neonates. Linderstrom-Lang and coworkers at the Carlsberg Laboratory in 1920's, discovered that casein is composed of a mixture of individual caseins. Casein, the major protein constituent of mammalian milk, is principally a mixture of four phosphoprotein fractions - α_{S1} , α_{S2} , β and κ , termed after their electrophoretic mobility. All the caseins are phosphorylated but to variable extent - α_{S1} : 8, α_{S2} : 10-13, β : 4-5 and κ : 1 mole of phosphate. These are secreted in their numerous genetic and post-translational variations (Farrell et al., 2004). They are strongly hydrophobic in the order $\beta > \kappa > \alpha_{S1} > \alpha_{S2}$ (the latter being about as hydrophilic as most globular proteins) with the uneven distribution of hydrophobic residues. Of these, α_{S1} and α_{S2} - caseins comprise 40% and 10% of the casein content of milk respectively, and are together referred as α_S -casein (Farrell et al., 2004). α_S casein fraction constitutes the calcium sensitive fraction of milk.

The secondary structure of casein is often referred to as random coil (Farrell et al. 2006). Casein is considered as intrinsically unstructured proteins like other secretory calcium-binding proteins (Smith et al., 2004). Their physiological function in the mammary gland results from their partially folded conformation and structural transitions. Other terms used to describe the considerable conformational flexibility of the caseins include molten

globule structure (Malin et al., 2005) and rheomorphic structure (Holt and Sawyer, 1993). Recently, α_{S1} - and α_{S2} -caseins are considered as natively unfolded proteins with extended coil-like conformations (or premolten globule-like), whereas β - and κ -caseins possess molten globule-like properties (Farrell et al. 2006).

Because of the lack of rigid 3-D tertiary conformation, caseins react very rapidly to environmental changes. In mammary cells, their function is to sequester small clusters of calcium phosphate, thus preventing precipitation and calcification of the mammary milk synthesis and transport system (Horne, 2002; de Kruif and Holt, 2003). Casein functions as a transporter of inorganic calcium and phosphorous to the neonates. The lack of rigid globular structure under physiological conditions in these intrinsically unstructured proteins allows them to interact with different targets than their globular counterparts (Wright and Dyson, 1999). The factor that sets casein monomers apart from globular and fibrous proteins is the presence of exposed hydrophobic patches containing proline turns, which gets buried upon subsequent self-association with the formation of hydrophobic cores (Alaimo et al., 1999). It has the propensity to form aggregates associated with degenerative disorders like Alzheimer's disease, Parkinson's disease, dementia with Lewy body etc (Fink and Uversky, 2006). Although, casein function is largely nutritional, recent studies provide insights about the functional properties of casein exhibiting chaperone like activity. Casein acts as a chaperone very similar to small heat shock proteins thus protecting the substrate proteins against aggregation (Bhattacharyya and Das, 1999; Morgan et al., 2005) including amyloid fibril formation (Thorn et al., 2005) when placed under condition of stress, like elevated temperature or in reduced environment.

α_{S1} -Casein

α_{S1} -Casein occurs in two variant forms *viz.* A and B. α_{S1} -Casein B is a single polypeptide chain with 199 amino acid residues and the molecular weight is 23619 Da (Mercier et al., 1971). The primary sequence of α_{S1} -casein B is given in Figure 1.11A. The polypeptide chain contains three hydrophobic regions, *viz.* 1-44, 90-113 and 132-199 and two hydrophilic regions 45-89 and 114-131. The α_{S1} -casein B molecule contains eight phosphate residues, all in the form of serine monophosphates (Mercier et al., 1971). Seven of these phosphoserine residues are clustered in acidic portion of the molecule, which contains 12 carboxylic acid groups. Proline residues are evenly dispersed (8.5%) which restricts the protein to take a definite conformation (MacArthur and Thronton, 1991).

α_{S1} -Casein is considered to be a hydrophobic protein (Mercier et al., 1971) based on the Bigelow's parameter with the average hydrophobicity of ~ 1170 (Bigelow, 1967).

The secondary structure of α_{S1} -casein has been examined by various methods including CD spectroscopy, Raman spectroscopy and predictive algorithms using sequence information. As the protein does not form crystals, x-ray structure is not available. NMR studies have also proven to be problematic because of the intrinsic aggregation of the protein. Its tertiary structure has been predicted using a combination of predicted secondary structures, with molecular modeling computations based on energy minimization and is represented in Figure 1.11B (Kumonsinski et al., 1991). The protein is composed of short hydrophilic amino-terminal portion, a segment of hydrophobic β -sheet, the phosphopeptide region and a short portion of α -helix, which connects N-terminal portion to the very hydrophobic carboxyl terminal domain (residues 100 to 199)

containing extended β -strands (residues 134 to 160 and 163 to 178) (Kumonsinski et al., 1991). The high degree of hydrophobicity on C-terminus is responsible for the self association of the α_{S1} -casein monomer in aqueous solution with the subsequent formation of hydrophobic cores (Holt, 1992). Casein is an easily digestible protein with appropriate amino acid composition that is important for growth and development of infants which is the key factor for considering milk as an important source of protein.

Casein, an abundant milk protein is highly amphiphilic and self assembles into stable micellar structures in aqueous solution. Its hydrophobic portion is exposed to outside environment, due to which casein aggregates. 10-100 casein molecules gather forming submicelle, with a diameter of ~ 20 nm, 100-1000 casein molecules associate to form a structure with the diameter of ~ 90 -150 nm and further these micelles gather together to form ~ 500 nm diameter structures. These micelles are utilized as natural nanodelivery vehicles for lipid soluble vitamin.

A

```
1 RPKHPIKHQGLPQEVLNENLLRFFVAPFPEVFGKEKVNELSKDIGSE50STEDQAMEDIKQMEAESISSS  
EEIVPNSVEQKHIQKEDVPSERYLGYLE100QLLRLLKKYKVPQLEIVPNSAERLHSMKEGIHAQQKEPMI  
GVNQELAYFYPELFRQFYQLDAYPSGAWYYVPLGTQYTDAPSFSDIPNPIGSEKTTMPLW199
```

B

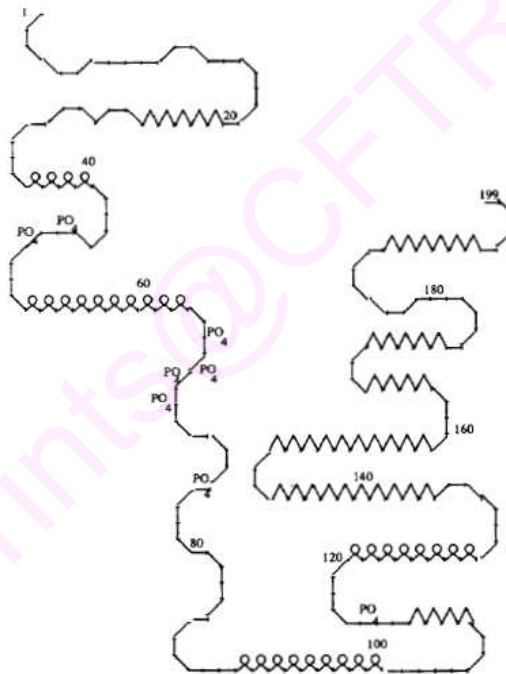


Figure 1.11. (A) Primary sequence of bovine α_{S1} -casein (ExPASy file number - P02662)
(B) Secondary structural assignments predicted by Kumonsinski et al. (1991).

Lipoxygenases

Lipoxygenases (linoleate: oxygen oxidoreductase, EC 1.13.11.12; LOXs) are a family of monomeric non-heme, non-sulfur iron dioxygenases, ubiquitous in both plants and animals. They catalyze the conversion of polyunsaturated fatty acids possessing *cis, cis*-1,4-pentadiene unit into 1,3-*cis, trans*-diene-5-hydroperoxides (Gardner, 1991).

Mammalian LOXs are implicated in the pathogenesis of several inflammatory conditions such as arthritis, psoriasis, prostate cancer (Gosh and Myers, 1998), breast cancer (Natarajan and Nadler, 1998) and bronchial asthma. They are also thought to have a role in atherosclerosis, brain aging, HIV infection, kidney disease, and terminal differentiation of keratinocytes (Kuhn and Borngraber, 1999). In plant, LOXs favor germination, participate in the synthesis of traumatin and jasmonate in response to abiotic stress (Grechkin, 1998).

Plant and animal LOXs form separate branches in the phylogenetic tree, each forming several subgroups (Brash, 1999). When arachidonic acid (eicosatetraenoic acid, C₂₀:4) is the substrate, different LOX isozymes can add a hydroperoxy group at carbons 5, 12 or 15 and therefore are designated 5-, 12- or 15-lipoxygenases. Linoleic (octadecadienoic acid, C₁₈:2) and linolenic (octadecatrienoic acid, C₁₈:3) acid are also substrates of LOXs. Soybean (*Glycine max*) lipoxygenase (LOX-1) is a 15-LOX widely used as a prototype for studying the homologous family of LOXs from tissues of different species, both in structural (Sudarshan and Rao, 1999) and kinetic investigations (Clapp et al., 2000).

Structure of Soy LOX-1

Soy LOX is a soluble cytosolic protein. The primary sequence and the 3-D structure of LOX-1 have been determined, showing it as an ellipsoid of 90×65×60 Å with 839 amino

acid residues and a molecular mass of 93480 Da (Brash, 1999). Three dimensional structure of LOX-1 shows 38% of α -helical content and 14% of β -sheet. LOX-1 is made up of two domains *viz.* eight-strand antiparallel β -barrel with 146 residues at the N-terminal termed as domain I and a 693 residue helical bundle at the C-terminal termed as domain II (Figure 1.12A). The interior of β -barrel in domain I is densely clustered with hydrophobic residues. Domain II contains two distinct stretches of π -helix. π -helix, with unusual hydrogen bonding between residues *i* and *i*+5 instead of *i*+4 is seen. The iron-containing active site is in the centre of domain II, coordinated to four conserved histidines (His499, His504 and His690) and to the carboxyl group of the C-terminal conserved isoleucine (Ile839) (Figure 1.12B). The major domain of LOX-1 contains two cavities *viz.* cavity I and cavity II which spans from the surface to the active site. Cavity I is funnel shaped, presents an ideal path for access of molecular oxygen to iron, whereas cavity II is the substrate pocket, which is the locus for all the catalytic events of the enzyme (Minor et al., 1996).

Iron plays an active role in the catalysis. Unlike the other mononuclear non-heme iron enzymes, the Fe(II) of LOX is in resting state and the active LOX contains Fe(III). Autoactivation of LOX-1 occurs in the presence of hydroperoxides resulting in the conversion of Fe(II) to Fe(III). Iron is maintained in the Fe(III) form during the steady-state turnover of the enzyme (Veldink et al., 1977). Transition in the state of iron is associated with changes in the spectroscopic properties (Pistorius et al., 1976; Slappendel et al., 1981). In presence of hydroperoxides, the Fe(II) form of the enzyme is converted to the yellow form with the iron getting oxidized to Fe(III) state. Change in the state of iron can be monitored by different experimental technique. The change in state of iron leads

to the appearance of an absorption band at 330 nm, 30% decrease in the fluorescence intensity at the tryptophan emission region and appearance of a positive circular dichroic band at 425 nm. LOX-1, with the iron in reduced state is EPR silent. In the presence of hydroperoxide product *i.e.* when the iron in the LOX-1 is in its oxidized form with the iron in high-spin ferric ion, EPR signal at $g = 6.1$ accompanied by a small but sharp signal at $g = 2$, exists.

Due to the proposed role of products of LOX in inflammation and immediate hypersensitivity, there is much current interest in inhibiting LOXs (Samuelsson, 1983). Search for new and effective natural inhibitors of LOX is still ongoing (Nuhn et al., 1991). Mammalian LOXs are the target for drug design (Ford-Hutchinson et al., 1994). Since mammalian LOXs are difficult to purify, soy LOXs have been used as the template to design the inhibitors, as extensive structural and kinetic data on soy LOX-1 are available. Soy LOX-1 is used as a model since, the substrate specificity and inhibition characteristics are similar to mammalian LOX (Borgeat et al., 1982). Soy LOX-1 is used as the model in substitute of mammalian LOX to study the structural and functional properties of LOX from various species (Brash, 1999).

Inhibitors

Inhibitors of LOX are diversified into: (i) substrate analogues (competitive, reversible inhibition) (ii) redox inhibitors which act at the catalytic iron site (iii) radical trappers which act by trapping the free radical intermediates of lipoxygenase catalyzed reaction.

Substrate analogues show competitive type of inhibition and they bind to the catalytic site. Although, redox inhibitors are very potent, its pharmaceutical value is insignificant due to their toxic side effects (Falgueyret et al., 1993).

A number of monoenoic fatty acids, which resemble fatty acid substrates, but structurally differ in *cis*, *cis*-1, 4-pentadiene unit are shown to be competitive inhibitors of LOX-1 (St. Angelo and Ory, 1984). 4-Nitrocatechol, N-alkylhydroxylamine, naphthols, disulfiram and soy isoflavones are the reductive inhibitors inhibiting LOX-1 by converting the active ferric enzyme to the inactive ferrous form (Galpini et al., 1976; Kemal et al., 1987; Clapp et al., 1985; Hausknecht and Funk, 1984, Mahesha et al., 2007). Curcumin is a potent inhibitor of soy LOX-1 (Began et al., 1998). Nordihydroguaiaretic acid (NDGA), n-propylgallate and butyl hydroxytoulene are antioxidants, function by reacting with free radical intermediates thereby acting as free radical scavengers (Tappel et al., 1952). Inhibitors of LOX-1 such as, *p*-aminophenol, catechol, hydroquinone and NDGA, are oxidized to free radical metabolites or one-electron oxidation products. They reduce the catalytically active ferric lipoxygenase to its resting ferrous form. It has been reported that these inhibitors undergo base-catalyzed auto-oxidation in the pH range 6.5-9.0 (van der Zee et al., 1989).

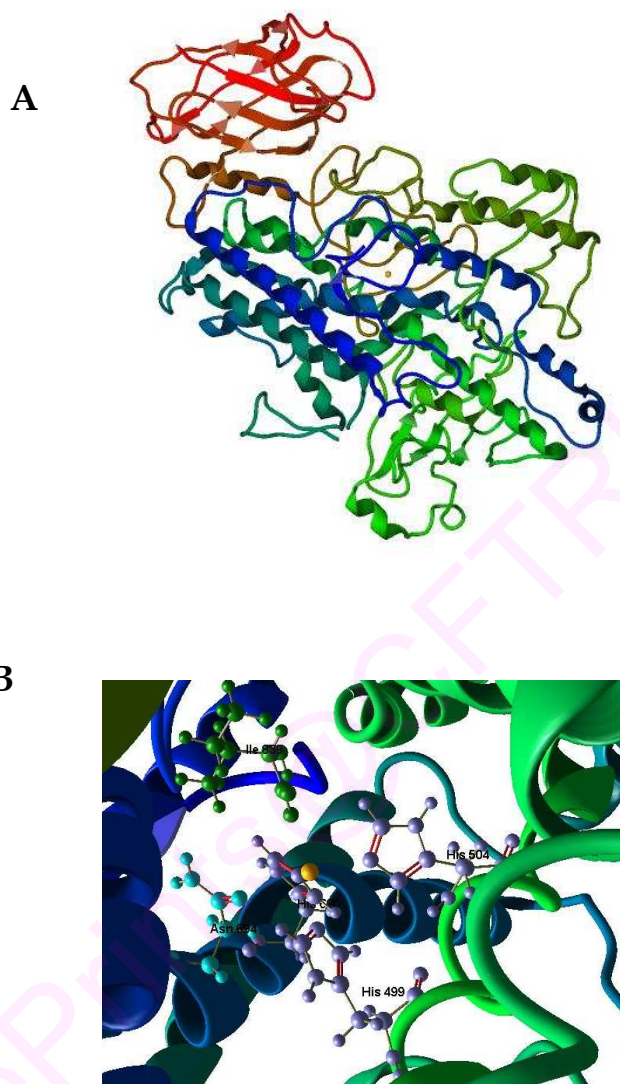


Figure 1.12. (A) Cartoon ribbon representation of the soy LOX-1 (PDB ID: 1F8Q). (B) Structure of active site: α helices with iron (yellow) coordinated to His499, His504, His690, Ile839 and Asn694.

Surface Hydrophobicity of Proteins

In proteins, hydrophobic interactions play a major role in dictating conformation, solubility, ligand binding and aggregating properties. The number and relative size of hydrophobic sites on a protein's surface, termed as 'surface hydrophobicity', prescribes the functionality of proteins *viz.* emulsifying property. The ability to measure the hydrophobicity of a protein may be useful in understanding and predicting the effects of manipulation of the sequence of structural and functional domains or during the thermal stability of food proteins. Methods to assess the surface hydrophobicity of proteins include, binding of hydrocarbons to proteins (Mohammadzadeh et al., 1969), reverse phase chromatography (van Oss et al., 1979), use of fluorescent probes (Sklar et al., 1977a & 1977b). Correlation between the surface hydrophobicity, binding constant (Cardamone and Puri, 1992) and with the surface properties (interfacial tension and emulsifying activity) of proteins (Kato and Nakai, 1980) has been established by fluorescent probe method. The fluorescent probes used in such measurements are non-fluorescent in aqueous medium and on contact with hydrophobic environment, exhibits fluorescence. Examples of such probes include 1-anilino-8-naphthalene sulfonic acid (ANS), 6-propionyl-2-(dimethylamino)-naphthalene (PRODAN), *cis*-Parinaric acid (CPA), and 2-p-touidinylnaphthalene-6-sulfonate (TNS).

cis-Parinaric acid

cis-Parinaric acid (CPA, 9,11,13,15-*cis-trans-trans-cis*-octadecaenoic acid: 18:4) (Figure 1.13) is a naturally occurring fluorescent 18-carbon polyunsaturated fatty acid with a linear polyenic structure, consisting of 4 conjugated π -electron bonds. It exhibits maximum emission at 432 nm, when excited at 320 nm (Sklar et al., 1977a). CPA differs

from other fatty acids in having conjugated double bonds. In case of other commonly occurring polyunsaturated fatty acids the double bonds are separated by methylene carbon. Because of the fluorescent properties conferred by the alternating double bonds, CPA is commonly used as a molecular probe to study biomembranes. This fatty acid is relatively non-fluorescent in aqueous environment, however, in hydrophobic environment, such as in the lipid binding site of a protein or in membranes, CPA becomes fluorescent. The fluorescent properties of CPA have been used to study its binding to fatty acid binding proteins (Schroeder et al., 1976; Sklar et al., 1976; Sha et al., 1993). CPA also has a distinct UV spectrum which is shifted by the binding of proteins such as albumin (Sklar et al., 1977b).

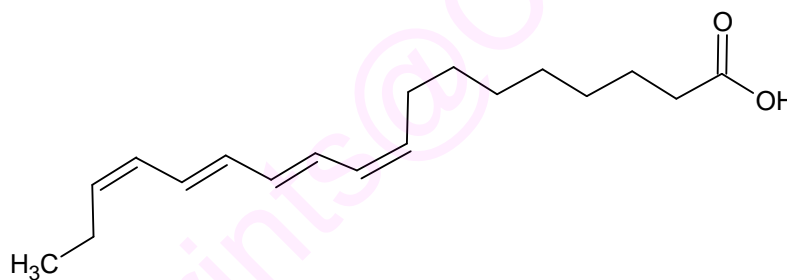


Figure 1.13. Structure of *cis*-Parinaric acid

CPA is used to study the foam stability of beer (Cooper et al., 2002) and the surface hydrophobicity and foaming characteristics of food proteins (Townsend and Nakai, 1983; Zhu and Damodaran, 1994). As the fluorescence of CPA is irreversibly lost upon oxidation, this compound has been used as a probe to evaluate lipid peroxidation (Kuypers et al., 1987, Drummen et al., 1999) and/or for the evaluation of the antioxidant activity of lipophilic compounds (Naguib et al., 1998).

CPA is reported to be cytotoxic to human leukemia cells in cell culture at concentrations of 5 μM or less. This is due to the sensitizing of tumor cells to lipid peroxidation, during which the free radicals generated react with electrons from cell membrane lipids, resulting in cell damage (Cornelius et al., 1991). It is similarly cytotoxic to malignant gliomas grown in cell culture (Traynelis et al., 1995). Normal (non-tumorous) astrocytes grown in culture are far less sensitive to the cytotoxic effects of CPA (Traynelis et al., 1995). This preferential toxicity towards tumor cells is due to a differential regulation of c-Jun N-terminal kinase, and forkhead transcription factors in malignant and normal cells (Zaheer et al., 2007).

ePrints@CFTRI

CFTRI Work on Curcumin

Curcumin, the diferuloyl methane component of turmeric and responsible for the yellow coloring, is present to an extent of 2 - 3% of the rhizome. The medicinal value of turmeric is well recognized since time immemorial in India. Curcumin, as a major bioactive component responsible for many health benefits has received attention only during the past two decades. Some of the major findings for this have come from pioneering studies in *CFTRI*.

Work has been carried out on metabolism of the active principles of spices, prompted detailed investigations on curcumin. At oral doses corresponding to 5 - 40 times human intake, about 60% of the dose administered is absorbed and metabolized within 72 h. Curcumin is transformed during absorption from the intestine. Intact curcumin was detected in the brain up to 96 h following its oral intake (Ravindranath and Chandrasekhara, 1980; Ravindranath and Chandrasekhara, 1981). The presence of curcumin, administered orally was detected in the portal blood, liver, and kidney of rats (Ravindranath and Chandrasekhara, 1982). Dietary curcumin at 0.5% caused a significant reduction in the induction of gallstones in mice and hamsters (Hussain and Chandrasekhara, 1993). The antilithogenicity of curcumin is due to their ability to lower cholesterol saturation index by altering the bile composition and also to their influence on biliary proteins (Hussain and Chandrasekhara, 1992).

Beneficial physiological effects of curcumin on their influence on lipid metabolism, digestive stimulant action (Rao et al., 2003), hypocholesterolemic effect and maintenance of erythrocyte integrity in hyperlipidemic rats and anti-inflammatory effects have been recognized. Curcumin has been shown to be an effective hypocholesterolemic agent

under various conditions of experimentally induced hypercholesterolemia/hyperlipemia in rats (Manjunatha and Srinivasan, 2007). Curcumin stabilises the erythrocyte membranes in hypercholesterolemic animals (Kempaiah and Srinivasan, 2006). Curcumin in combination with capsaicin inhibited the *in vivo* iron-induced LDL oxidation, as well as copper-induced oxidation of LDL *in vitro* (Manjunatha and Srinivasan, 2006). Experiments with streptozotocin-induced diabetic rats have shown that dietary curcumin ameliorate diabetic kidney lesions as indicated by decreased proteinuria and leaching of renal tubular enzymes, correction of the alteration in renal cellular enzymes, and countering of the altered renal membrane ATPases and fatty acid composition (Babu and Srinivasan, 1998). The nature of degraded/ altered compounds due to heat treatment of curcumin during domestic cooking has been characterized (Suresh et al., 2009).

The antioxidant properties of curcumin were studied in rats both *in vivo* and *in vitro*. Lipid peroxidation is inhibited by quenching oxygen free radicals and by enhancing the activity of endogenous antioxidant enzymes - superoxide dismutase, catalase and glutathione transferase (Joe and Lokesh, 1994). Curcumin is an effective anti-inflammatory agent reducing the incidence and severity of carrageenan induced paw edema in arthritic rats as well as delaying the onset of arthritis (Joe and Lokesh, 1997). The antioxidant activities and antioxidant capacities of curcumin, demethoxycurcumin and bisdemthoxycurcumin have been studied with *in vitro* model systems (Reddy and Lokesh, 1994a; Reddy and Lokesh, 1994b). Curcumin exhibits antioxidant activity by scavenging reactive oxygen species and enhancing the activities of endogenous antioxidant enzymes (Reddy and Lokesh, 1994c; Salimath et al., 1986).

Curcumin and its derivatives prevent the aggregation of amyloid peptides which have implications in neurodegenerative diseases such as Alzheimer's disease (Hegde et al., 2009).

Biophysical techniques like fluorescence and circular dichroism studies have been used to understand the binding and transport of curcumin with human serum albumin under physiological conditions (Reddy et al., 1999). Curcumin could be stabilized in phospholipids liposomes/ vesicles (Began et al., 1999).

Work is being currently carried out on the preparation of water soluble sugar and amino acid conjugates of curcumin. Conjugation of the phenolic hydroxyl group of curcumin to a sugar moiety renders it water-soluble whilst retaining/enhancing its *in vitro* antioxidant, antimutagenic and antibacterial properties (Parvathy et al., 2009). The protection of curcumin and its water soluble synthetic conjugates against onset of neurodegenerative diseases are being currently pursued.

CFTRI in 1975, initiated program on postharvest technology and quality studies on turmeric. During subsequent years, improved curing methods and technology for processing, oleoresin extraction, and extraction of curcumin were developed. CFTRI has also played a major role in establishing the safety of curcumin in foods (Jayaprakasha et al., 2006). Improved HPLC methods have been developed for determination of curcumin, demethoxycurcumin and bisdemethoxycurcumin (Jayaprakasha et al., 2002). Recovery of curcuminoids from spent turmeric oleoresin has been successfully carried out (Jayaprakasha et al., 2004).

Aim and Scope of the Present Investigation

Curcumin, a polyphenolic compound derived from dietary spice turmeric, possess diverse pharmacological effects including anti-inflammatory, antioxidant, antiproliferative and antiangiogenic activities. Pronounced influence of curcumin on health has been the subject of numerous studies. Curcumin with many health benefits is still not approved as a therapeutic agent due its low solubility, stability and bioavailability. Encapsulation of bioactive molecules in nanoparticles could improve its biodistribution and solubility. To achieve good bioavailability, bioactive molecules must be soluble in water and stable in gastrointestinal tract. Binding to proteins may improve the solubility of many hydrophobic bioactive compounds and protect these compounds during processing and storage. Food based nanocomplexes improve bioavailability and stability of bioactives, providing protection against degradation by environmental stress (e.g. light, heat, oxygen or pH sensitivity). Protein nanoparticles, being biodegradable and metabolizable serve over other carriers, as they can incorporate a wide variety of small molecules in a nonspecific fashion. Nanocomplexes of protein, such as serum albumin, bovine β -lactoglobulin (β LG) capable of binding hydrophobic molecules serve as base materials for the encapsulation and controlled release of bioactive compounds. As β LG is known to bind different types of compounds, it may improve their solubility and stability. The present investigation is aimed to gain more information on exploring possible medium/carrier to increase the solubility and stability of curcumin. Further, studies on the binding of curcumin with milk proteins - β LG and α_{S1} -casein are carried out by biophysical studies.

cis-Parinaric acid (CPA) is a fluorescent, 18-carbon polyunsaturated fatty acid with a linear polyenic structure, consisting 4 conjugated π -electron bonds. CPA is used as a fluorescent probe to estimate the surface hydrophobicity of proteins, due to its fluorescence enhancing property, after binding to hydrophobic surface. Due to the similarity in the fluorescence property of curcumin and CPA, surface hydrophobicity for known proteins was compared with CPA and curcumin. The main aim was to evaluate whether curcumin could be used as a fluorescent probe/fluorophore to assess the surface hydrophobicity of proteins similar to CPA. Incidentally, the structural similarities of CPA with the linoleic acid led to the investigation for the possible inhibition of soy LOX-1 with CPA.

Tetrahydrocurcumin (THC), the reduced derivative of curcumin, is the major metabolite *in vivo*. It is known to possess potent antioxidant activity in comparison to curcumin. Curcumin is a strong anti-inflammatory agent. Inflammation is mediated by the products released by the metabolism of unsaturated fatty acids. This occurs *via* lipoxygenase or cyclooxygenase pathway. Curcumin is known to be an inhibitor of lipoxygenase enzyme. It is requisite to understand the structural requirements for the exertion of such physiological activity by analogues. Therefore to understand the structural relationship, curcumin and THC are selected and the potency to inhibit the soy LOX-1 is compared and evaluated. As a transformed product of curcumin, THC appears to be involved in physiological and pharmacological activity.

Curcumin is a known chelator of metal ions. The effect of curcumin on activity of metalloenzyme is studied. For this purpose, zinc containing enzyme - carbonic

anhydrase is selected and investigated for the modulation of activity in the presence of curcumin.

The main objectives of the present investigation are:

- (i) To understand the structural and molecular basis of interaction of curcumin with proteins
- (ii) To understand the role of ligands like metal ions in the modulation of curcumin action

In pursuit of these aims, the following studies were conducted: (i) Interaction studies of curcumin with β LG and α_{S1} -casein and encapsulation of curcumin in different protein nanoparticle, to assess the suitability of curcumin as a tool to measure the surface hydrophobicity of proteins in comparison with CPA and inhibition studies of CPA with soy LOX-1 (ii) Molecular basis of interaction of curcumin with proteins – study with tetrahydrocurcumin and soy LOX-1 (iii) Effect of curcumin on carbonic anhydrase - a zinc containing enzyme.

It is expected that these studies will lead to a better understanding of the curcumin interaction with proteins and could eventually provide a platform for improving the stability and solubility of curcumin.

ePrints@CFTRI

2. Materials and Methods

Materials and Methods

HEPES, curcumin, dephosphorylated casein, anilino naphthalene sulphonic acid (ANS), bovine serum albumin (BSA), phosphatidylcholine (PC) from egg yolk, sodium deoxycholate, β LG, ovalbumin, palmitic acid, linoleic acid, Tween 20, carbonic anhydrase, catalase, Trizma base, Sephadex G-100, DEAE Sephadex A-50, glycine, urea, β -mercaptoethanol, glutaraldehyde and sodium dodecyl sulphate were procured from Sigma chemicals (St. Louis, MO, USA). 2,2'-azo-bis(2-amidinopropane hydrochloride) (AAPH) and ANS were from Aldrich chemical co. *cis*-Parinaric acid was from Molecular Probes Inc. (Junction city, OR, USA). All other chemicals were of analytical grade. All the solutions were freshly prepared. The solutions used for spectrophotometric and HPLC measurements were passed through 0.22 μ filters. All spectrophotometric measurements were made in a UV 1601 double beam spectrophotometer, using 1 cm path length quartz cells. Fluorescence measurements were made on a Shimadzu RF 5000 spectrofluorimeter attached to a circulating Peltier thermostat. A 10 mm path length quartz cell was used. The solution in the cuvette was stirred continuously with the help of Hellma cuv-o-stir[®]. All the measurements were carried out at 25 °C, unless mentioned.

Palmitic acid stock solution was prepared in absolute ethanol, purged with nitrogen gas and kept in dark at -20 °C, until use. Concentration of β LG dissolved in 50 mM Tris HCl buffer, pH 7.0, was determined by absorbance measurement at 278 nm using either $E_{1\text{mg/mL}}^{1\%} = 0.93$ or $\epsilon_{278\text{ nm}} = 17600\text{ M}^{-1}\text{ cm}^{-1}$ (Dufour, 1992). Stock solution of CPA was prepared by dissolving CPA in absolute ethanol with constant purging of nitrogen. The concentration of CPA was calculated using $\epsilon_{303\text{ nm}} = 76000\text{ M}^{-1}\text{ cm}^{-1}$.

Purity of Curcumin

Curcumin obtained from Sigma (curcumin I = 80%) was further separated from other curcuminoids, by thin layer chromatography. The mobile phase was 5% methanol in chloroform. The spotted samples were resolved into three bands, of which the upper band corresponds to the curcumin I (curcumin). The band was scraped and dissolved in methanol. The sample was centrifuged to get the curcumin solution. The purity of curcumin was ascertained by subjecting the sample to RP-HPLC. C18 (5.0 μ , 4.5 mm \times 250 mm) Waters® column (Waters, Milford MA, USA), equipped with a 1525 binary pump and Waters 2996 photodiode array detector was used. The solvents used were 5% aqueous methanol (solvent A) and acetonitrile containing 0.1% Trifluoroacetic acid (solvent B). The column was washed at a flow rate of 1 mL/min, with solvent A for 20 min. Sample was injected and eluted over a time span of 15 min with a gradient of 50–70% of solvent A. Elution was monitored at 425 nm. Curcumin concentration was determined using $\epsilon_{425 \text{ nm}} = 54954 \text{ M}^{-1} \text{ cm}^{-1}$. The concentration of alcohol was maintained below 1.5%.

Preparation of THC

Tetrahydrocurcumin was synthesized from selective reduction of olefinic bonds between carbon 1 & 2 and carbon 6 & 7 without affecting the keto enol moiety at 3, 4 and 5 carbon atoms in curcumin molecule. A solution of curcumin (5.0 g) in acetone (30 mL) was hydrogenated at room temperature and 20 psi pressure over 5% Pd/BaSO₄ catalyst for 5 h. The filtered solution was concentrated and the compound was isolated by crystallization from ethanol to afford tetrahydrocurcumin as a white amorphous solid (Yield 78%, purity 97%), m. p., 92-93 °C. ¹H NMR (CDCl₃): 6.85 (dd, 2H, *J* = 5 and 8 Hz,

H-5'), 6.65 (dd, 2H, $J = 2$ and 8 Hz, H-6'), 6.69 (dd, 2H, $J = 2$ and 5 Hz, H-2'), 5.63 (br, s, 2H, 4'OH), 5.46 (s, 1H, H-4), 3.87 (s, 6H, H-3', -OCH₃), 2.87 (t, 4H, $J = 8$ Hz, H-1,7), 2.57 (t, 4H, $J = 8$ Hz, H-2,6), 15.50 (br, s, 1H). ¹³C NMR (CDCl₃): 192.91, 146.16, 143.74, 132.25, 120.52, 114.08, 110.70, 99.48, 55.57, 40.04, 31.00.

Concentration of THC dissolved in ethanol was calculated using $\epsilon_{282\text{ nm}} = 17600\text{ M}^{-1}\text{ cm}^{-1}$.

Purification of α_{S1} -Casein from Bovine Milk

Bovine milk α_{S1} -casein was purified to homogeneity as previously described (Rasmussen et al., 1992). The concentration of α_{S1} -casein solution made up in 0.01M HEPES buffer, pH 7.4 was determined spectrophotometrically, using $E_{1\text{ mg/mL}}^{1\%} = 1.05$ at 280 nm. Protein solution was centrifuged to remove any aggregates, before use.

Purification of Soy Lipoxygenase

Soy LOX-1 was purified from defatted soy flour according to the method of Axelrod et al. (1981) with some modifications (Sudharsan and Rao, 1997). 50 g defatted soy flour was extracted with 500 mL of ice cold sodium acetate buffer (0.2 M, pH 4.5) for 1 h. The extract was centrifuged at 5000 rpm for 30 min. The pH of the supernatant was adjusted to 6.8 with NaOH and the solution was clarified after centrifuging for 30 min at 8000 rpm. All steps were carried at 4 °C.

Precipitation

To the above clarified solution, ammonium sulphate precipitation was carried. Initially, 30% ammonium sulphate precipitation was carried out along with constant stirring. Supernatant solution was collected after centrifuging at 8000 rpm for 30 min at 4 °C. To the supernatant, ammonium sulphate was added to raise the concentration to 60% and

was allowed to equilibrate for 1 h. Protein precipitated at this stage was dissolved in and dialyzed against 20 mM phosphate buffer, pH 6.8 with three to four changes of buffer.

Ion Exchange Chromatography

The dialyzed protein solution was centrifuged to remove any aggregates. The supernatant was applied on a DEAE Sephadex A-50 column (25 × 4 cm) pre-equilibrated with 20 mM phosphate buffer, pH 6.8. The column was washed with 5 bed volumes of buffer (linear gradient - 20-170 mM phosphate buffer, pH 6.8). The protein was eluted by applying linear gradient of 170-240 mM phosphate buffer, pH 6.8. The fraction containing maximum activity was pooled and protein was concentrated to 70% ammonium sulphate. The precipitate was dialyzed against three changes of 20 mM phosphate buffer, pH 6.8.

Gel permeation chromatography

The dialyzed protein solution was loaded on Sephadex G-100 column (90 × 2.5 cm), pre-equilibrated with 20 mM phosphate buffer, pH 6.8. Elution was carried out using same buffer. Protein fractions which showed maximum activity was pooled and stored as 70% ammonium sulphate precipitate. Before using enzyme the pellet was dissolved and dialyzed against 20 mM phosphate buffer, pH 6.8.

Homogeneity and Molecular Weight Determination

Homogeneity of the protein/enzyme was checked by 12% SDS-PAGE (Laemmli, 1970). PAGE, under native conditions, was done without SDS and β -mercaptoethanol. The gels were stained for protein using coomassie stain and destained using acetic acid, methanol and water mixture in the ratio of 1:4:5.

Assay of Soy LOX-1

LOX-1 activity was determined by following the increase in absorbance at 234 nm due to the formation of hydroperoxide (product, $\epsilon_{234 \text{ nm}} = 25000 \text{ M}^{-1} \text{ cm}^{-1}$). The substrate was prepared according to the method of Axelrod et al. (1981). The amount of enzyme required to form 1 μM of hydroperoxide per min under the conditions of assay, was taken as one unit of activity.

The specific activity was 180-200 $\mu\text{moles}/\text{min}/\text{mg}$ of protein. The concentration of LOX-1 was calculated using the $E_{1\%}^{1 \text{ cm}} = 14.0$ (Axelrod et al., 1981).

Assay of Carbonic Anhydrase

The carbonic anhydrase assay is based on the hydrolysis of *p*-nitrophenyl acetate to *p*-nitrophenol and acetate at pH 7.6. 1.9 mL of 15 mM Tris sulfate buffer is mixed with 1 mL of 3 mM *p*-nitrophenyl acetate solution. To this diluted carbonic anhydrase solution is added and the solution is mixed thoroughly. The absorbance is read at 348 nm for 5 min. $\Delta A_{348 \text{ nm}}/\text{min}$ is calculated and units/mg is calculated using the following formula.

$$\text{Units/mg} = \frac{(\Delta A_{348 \text{ nm}}/\text{min Test} - \Delta A_{348 \text{ nm}}/\text{min Blank}) (1000)}{(5.0) (\text{mg of enzyme/mL RM})}$$

1000 = Conversion to micromoles

5 = Millimolar extinction coefficient of *p*-nitrophenol at pH 7.6 at 0 °C

RM = Reaction Mix

Stability Measurements

Encapsulations of curcumin in mixed PC micelles were prepared according to the method of Began et al. (1998), in 50 mM Tris HCl, pH 7.2. Stability of free curcumin, α_{51} -

casein bound curcumin, BSA bound curcumin and mixed PC micelles bound curcumin was established by incubating curcumin in 50 mM Tris-HCl, pH 7.2 or in the presence of other above mentioned components at 30 °C with intermittent mixing. Concentrations of proteins were 1 mg/mL and the concentration of PC was 1 mM. 20 µL of the incubated sample containing 65 µM curcumin was injected to HPLC column (C18 column, 250 × 4.5 mm, 5µ, Waters) at different intervals of time and monitored at 425 nm by applying the gradient as described earlier (Jayprakash et al., 2002).

To study the stability of curcumin at pH 7.0 with time, curcumin in buffer (Tris HCl, 50 mM) or in 1 mg/mL βLG were incubated at 30 °C. The concentration of curcumin at different time intervals was calculated by absorbance measurement at 425 nm. The half-life ($t_{1/2}$) was calculated by fitting the data to first order reaction. Since binding measurements were carried out at pH 7.0, the stability of curcumin in the presence of βLG was studied at pH 7.0.

Solubility Measurements of Curcumin in Different Medium

Solubility measurement of curcumin in the presence of BSA, α_{S1}-casein, βLG (each 1 mg/mL) and mixed PC micelles (1 mM) in Tris-HCl 50 mM, pH 7.0 buffer was carried. To protein or mixed PC micelles solution, 0.8 mg/mL curcumin was accurately weighed and added to a 50 mL stoppered conical flask. The solution was vortexed and incubated at 15, 28, 40, and 50 °C in a water bath. The mixing was accomplished in a shaker. The solution was equilibrated for one hour. The equilibrated solution was centrifuged at 8000 rpm for 20 min to pellet undissolved curcumin. The concentration of curcumin was calculated by measuring the absorbance of supernatant at 425 nm. Apparent solubility of

curcumin was calculated by plotting the graph of log mole fraction solubility versus temperature. The Y-intercept on the plot gives apparent solubility.

Stability of THC

To check stability, a known concentration of THC was incubated in different pH solutions. Buffers were 0.1 M phosphate (pH 5.8 and 7.0) and 0.1 M borate buffer (pH 9.0). Stability was measured by taking the absorbance at 280 nm at different time intervals.

Fluorescence Measurements of Curcumin and β LG

Steady state fluorescence of curcumin was measured by fixing the curcumin concentration at 10 μ M and adding aliquots of β LG from the stock solution, in the concentration range 0 to 38 μ M. The emission spectra were recorded from 450 to 600 nm, with the excitation wavelength fixed to 430 nm. The fluorescence intensities of the sample were corrected from the fluorescence intensity of the curcumin solution without β LG. Similar experiments were carried out using denatured β LG. β LG was denatured by incubation at 80 °C, in a preheated water bath for 10 min and then cooling immediately. Binding studies of curcumin with denatured β LG were carried out at 25 °C. Increase in fluorescence intensity of curcumin at 505 nm was recorded. The data recorded at maximum emission wavelength was used to analyze the binding parameters from the following equation (Gatti et al., 1995),

$$1/\Delta FI = 1/\Delta FI_{\max} + 1/K_a \Delta FI_{\max} [\beta LG] \quad (4)$$

where, ΔFI is the change in the curcumin fluorescence in the presence of β LG, ΔFI_{\max} is the maximal change in fluorescence intensity; K_a is the binding constant and $[\beta LG]$ is the

concentration of protein added. The binding constant was calculated to examine the effect of pH on the binding of curcumin to β LG at different pH values (5.5, 6.5, 7.0).

Intrinsic fluorescence of β LG was measured at 335 nm. The concentration of β LG was fixed at 2.95 μ M; the spectra for each addition of curcumin were recorded from wavelength range 305-570 nm, when excited at 295 nm. At this low concentration of protein, β LG exists predominantly as a monomer (Zimmerman et al., 1970). The fluorescence intensities of the sample were corrected for inner filter effect by the addition of ligand to N-acetyl tryptophanamide solution. Quenching, as a function of curcumin concentration, was analyzed in terms of binding of curcumin to β LG using established procedures (Rao and Cann, 1981). Assuming that the binding of curcumin causes the same degree of quenching and that binding is statistical, the intrinsic curcumin binding constant is given by the equation,

$$K = \beta / (1 - \beta) \cdot 1 / C_f \quad (5)$$

where, $\beta = Q / Q_{\max}$ and $C_f = C_T - n\beta T$, in which Q is the corrected percentage quenching; Q_{\max} , the maximal quenching; C_f , the molar equilibrium concentration of unbound curcumin, C_T , the molar constituent concentration of curcumin; T , the molar constituent concentration of β LG; and n is the binding stoichiometry. The K value is given by the slope of a plot of $\beta / (1 - \beta)$ against C_f . Q_{\max} has been determined by the extrapolation of double reciprocal graph of $1/Q$ vs. $1/C$. In both the cases, the data are fitted to a straight line by the method of least squares. Stoichiometry was determined by plotting $\log [F_0 - F / F - F_\infty]$ vs. $\log [\text{curcumin}] \mu\text{M}$, as described by Chipman et al., (1967) where, F_0 , F , F_∞ are the fluorescence intensities at zero, finite and infinite concentrations of the quencher.

Fluorescence Measurements with Curcumin and α_{S1} -Casein

All the measurements were made using 0.01 M HEPES buffer, pH 7.4, at 25 °C. The concentration of the protein used was 3 μ M. Samples with curcumin were excited at 430 nm and the emission was measured at 510 nm or recorded between 465 - 600 nm. The changes in fluorescence intensity due to curcumin were followed as a function of fixed concentration of casein and dephosphorylated casein. The binding parameters were calculated using the Scatchard's procedure (1949).

For ANS binding studies, ANS stock solution (7.6 mM) was prepared in methanol, and 2 μ L was titrated against α_{S1} -casein (3 μ M). Excitation and emission wavelengths were at 350 and 500 nm, respectively. Binding constants for phosphorylated and dephosphorylated caseins were calculated using a Scatchard plot. Appropriate blanks were subtracted to obtain the fluorescent enhancement caused by the probe.

For change in anisotropy measurements, curcumin (10 μ M) was titrated with 10 μ L increments of α_{S1} -casein (0-20 μ M). The data were obtained by setting the excitation and emission wavelengths at 430 and 510 nm, respectively. For anisotropy measurements, intensities of horizontal and vertical components of the emitted light (I_{\parallel} and I_{\perp}) were corrected for the contribution of scattered light as described (Mahesha et al., 2006).

Fluorescence Measurements of CPA with LOX-1

Association constant for the binding of CPA to LOX-1 was determined by following the fluorescence enhancement of the ligand. CPA concentration was fixed to 1.1 μ M and 5 μ L aliquots of LOX-1 were added from 0.12 mM stock in the concentration range 0-4.0 μ M. The buffer used was 0.1 M borate, pH 9.0. The excitation wavelength was set to 325

nm. The temperature was maintained at 25 °C. The spectra were taken in the range 350-650 nm. The association constant for the binding of CPA to LOX-1 was calculated from mass action plot (eq. 5).

Intrinsic fluorescence quenching of LOX-1 was carried out on titration with CPA. The excitation wavelength was set to 295 nm, with the slit width of 5 and 10 nm, respectively. The concentration of LOX-1 was fixed to 0.37 μ M. 1 μ L aliquots of CPA were added from 2.75 mM stock in ethanol in the concentration range 0-11 μ M. From the mass action plot the association constant for the binding of CPA to LOX-1 was calculated.

Effect of Temperature

The driving force for the binding of curcumin to β LG/ α _{S1}-casein was analyzed by following the change in temperature range 15-45 °C or 17-47 °C, on the binding constant of curcumin with β LG/ α _{S1}-casein. If the enthalpy changes (ΔH°) do not vary significantly over the temperature range studied, then its value and entropy (ΔS°) can be calculated from the van't Hoff equation (eq. 3).

Surface Hydrophobicity Measurements

10 mg/mL stock solutions of BSA, α _{S1}-casein, β LG, ovalbumin and soy LOX-1 was prepared in 20 mM phosphate buffer, pH 7.0. Curcumin was titrated against these different protein solutions. The excitation wavelength was 430 nm with the slit widths of 5 and 10 nm. The increase in fluorescence with the addition of protein at respective emission maxima was recorded. The slope of the plot of fluorescence intensity versus protein concentration (mg/mL) gives the surface hydrophobicity (Kato and Nakai,

1980). Surface hydrophobicity of proteins using curcumin was calculated in the presence of denaturant like urea.

The binding constant for these proteins with curcumin were calculated using the Scatchard procedure (eq. 2). The K_a was used to compare the surface hydrophobicity of different proteins (Cardomone and Puri, 1992).

Fluorescence Resonance Energy Transfer Measurements

According to Förster theory of energy transfer (FRET), the efficiency of energy transfer E is related to the distance (r_0) between acceptor and donor, and also the critical energy transfer distance (R_0), by the equation,

$$E = R_0^6 / (R_0^6 + r_0^6)$$

where, R_0 is a characteristic distance, called the Förster distance or critical distance, at which the efficiency of transfer is 50%, computed from the relation,

$$R_0^6 = 8.8 \times 10^{-25} K^2 N^{-4} \Phi J,$$

where K^2 is the spatial orientation factor describing the relative orientation in space of the transition dipoles of the donor and acceptor ($K^2=2/3$), N is the refractive index of the medium ($N=1.45$), Φ is the fluorescence quantum yield of the donor in the absence of the acceptor ($\Phi=0.118$) and J is the overlap integral between the donor fluorescence emission spectrum and the acceptor absorption spectrum. J is given by,

$$J = \sum F(\lambda) \epsilon(\lambda) \lambda^4 \Delta\lambda / \sum F(\lambda) \Delta\lambda,$$

where, $F(\lambda)$ is the fluorescence intensity of the donor at wavelength λ , $\epsilon(\lambda)$ is the molar absorption coefficient of the acceptor at wavelength λ and its unit is $M^{-1} \text{ cm}^{-1}$. Then the

energy transfer efficiency E is,

$$E = 1 - F/F_0, \quad (6)$$

where, F_0 = Fluorescence intensity of β LG alone and F = Fluorescence intensity of β LG with ligand.

The percentage energy transfer was also calculated using the eq. 6 by adding aliquots of β LG in the range 0-0.5 mg/mL to fixed concentration of curcumin. The Y-intercept on the plot of β LG against % energy transfer gives the total percentage energy transfer.

Circular Dichroism Measurements

CD spectra in the ranges of wavelength 195-260, 260-320 and 320-500 nm were recorded on a Jasco J-810 spectropolarimeter with continuous flushing of dry nitrogen. While measurements in far UV were carried out using 1 mm path length quartz cell, 10 mm path length quartz cells were used for near UV and the visible range. An average of 3 scans at a speed of 10 nm/min with a bandwidth of 1 nm and a response time of 1 s were recorded. The concentration of protein used was 0.2 mg/mL in far UV and 1 mg/mL in near UV and visible range. The secondary structural analysis was done with the help of the program in the instrument (Yang et al., 1986). The induced CD spectra were obtained by subtracting the CD spectra of the ligand-protein mixture from the spectra of protein alone. A mean residue weight of 115 is used to calculate the molar ellipticity value. The equilibrium constant of curcumin- α_{S1} -casein complex was calculated from the mass action plot (eq. 5).

Effect of Palmitate on Binding of Curcumin β LG

To equimolar concentration of curcumin and β LG, 2 μ L aliquots of palmitic acid from different stock solution in ethanol were added to the curcumin- β LG complex to get the

palmitic acid/ β LG ratio in the range 0-2. Change in curcumin fluorescence was monitored by taking the emission spectra in the range 460-600 nm, after excitation at 430 nm. Blank titrations were carried out by addition of palmitic acid to curcumin in 50 mM Tris HCl buffer, pH 7.0.

Effect of Curcumin on the Heat Denaturation of β LG

β LG (1 mg/mL) was dissolved in 20 mM phosphate buffer, pH 6.6. The solution was cooled immediately following heating to 85 °C for 10 min. For the reaction containing curcumin, equimolar concentration of curcumin was added to β LG solution. The unbound curcumin was removed by centrifuging the sample. The solution was then heated to 85 °C for 10 min and cooled immediately. Gel filtration was performed using a TSK-Super SW2000 (4.6 mm \times 300 mm, 4.0 μ) column. The column was equilibrated with phosphate buffer before injecting 20 μ L of the above sample. The sample was eluted isocratically in the same buffer. The flow rate was maintained at 0.2 mL/min at 25 °C. Detection was at 280 nm.

Biological Activities of α_{S1} -Casein bound Curcumin

Chaperone Activity

Thermally induced aggregation of carbonic anhydrase and catalase were studied by measuring the increase in absorbance of carbonic anhydrase and catalase. Protein solutions were prepared in 10 mM sodium phosphate buffer, pH 7.0. Carbonic anhydrase and catalase solution with α_{S1} -casein, curcumin and α_{S1} -casein-curcumin complex, held at 25 °C, were mixed in the cuvette, before placing into the thermostatic cell holder, maintained at 50 °C and 55 °C for carbonic anhydrase and catalase, respectively. The extent of aggregation was measured by recording the apparent

absorbance at 400 nm as a function of time. The reference cuvette contained all the components except the substrate proteins.

Inhibition of Hemolysis by α_{S1} -Casein Bound Curcumin

Blood obtained from a healthy donor was centrifuged at 2000 rpm for 10 min to separate RBC from plasma. The RBCs were washed three times with phosphate buffered saline at pH 7.4. The 5% suspension of RBCs in PBS was incubated under air atmosphere at 37 °C for 5 min, before adding 50 mM AAPH in PBS solution to initiate the hemolysis. The reaction mixture was incubated at 37 °C with intermittent shaking. The extent of hemolysis was determined spectrophotometrically at 540 nm as described earlier (Kuang et al., 1994). In the case of anti-hemolysis experiments, free curcumin and/or α_{S1} -casein bound curcumin was incubated along with the RBC suspension, half an hour before the addition of AAPH. The results obtained from three individual sets of experiments, were found reproducible with 10% deviation.

Inhibition of Soy Lipoxygenase by THC and CPA

Preparation of PC micelles and encapsulation of curcumin or THC was carried out according to Began et al. (1998). For inhibition experiments, THC and curcumin were added to 0.2 M borate buffer containing the enzyme. To the above, 100 μ M linoleic acid was added and the absorbance followed at 234 nm for three minutes. The percentage inhibition was calculated from the Δ OD at the end of three minutes. Kinetics of inhibition was analyzed by Lineweaver-Burk plot (L-B) and inhibition constant was calculated from the replot of (L-B) and Dixon plot. The data obtained were fitted to a straight line by the method of least square. Similar to THC, inhibition experiments were carried out using CPA.

Absorbance Measurements

Ferric-the active form and ferrous-the inactive form of LOX-1 can be detected by spectral changes between 300-500 nm. The ferrous form of lipoxygenase was converted to ferric form by adding 160 μM of linoleic acid. Aliquots of THC, dissolved in methanol, were added in 160 and 320 μM concentration range. The reference cuvette contained all the components except the enzyme. After mixing the components, spectra were recorded in the visible range.

Circular Dichroism Measurements

CD measurements were carried in Jasco J-810 spectropolarimeter calibrated with ammonium salt of d-10-camphor sulfonic acid. The iron state of lipoxygenase was followed in the visible range using a 10 mm path length quartz cell. An average of 3 scans at a speed of 10 nm/min with a band width of 1 nm and a response time of 1 s was recorded. The concentrations used were similar to that carried out with spectrophotometric experiments. Spectra were baseline corrected from the spectrum of THC in buffer. The mean residue ellipticity $[\theta]_{\text{MRW}}$ was calculated using 115 as mean residue weight.

HPLC Measurements

To characterize THC state after the inhibition reaction, reverse phase HPLC (RP-HPLC) was carried out. Reaction was carried out in 0.2 M borate buffer in the presence of enzyme, 100 μM linoleic acid substrate and THC. At the end of 10 minutes, an equal amount of ether was added. The reaction mixture was vortexed thoroughly to extract THC. The ether extract was then dried and the residue was dissolved in minimal amount of methanol. The sample was injected to a C18 column. The buffers and

conditions used are similar to that explained under the purity of curcumin. Sample (20 μL) was injected and eluted over a time span of 20 min. Elution was monitored at 282 nm. The peak of THC was collected and analyzed using mass spectrometry. Control, containing all the components except substrate, was also carried out.

Atmospheric Pressure Chemical Ionization-Mass Spectrometry (APCI-MS)

The peak collected from HPLC was passed into the atmospheric pressure chemical ionization mode of Waters® Corporation mass spectrometer (model Q-TOF Ultima). The corona current applied was 6.6 μA with the spray voltage of 100 V. Source temperature was 120 °C with the probe temperature of 500 °C. Data was analyzed using Mass Lynx version 4.4 software provided by the manufacturer.

Preparation of Encapsulated Curcumin in $\beta\text{LG}/\alpha_{\text{S1}}$ -Casein/ HSA Nanoparticle

The nanoparticle of βLG was prepared according to the method of Gunasekaran et al. (2007).

100 mg of purified βLG or α_{S1} -casein was dissolved in 10 mL of 10 mM NaCl (pH 9.0 for βLG or pH 8.0 for α_{S1} -casein). The solution was stirred for 1 h. With the help of burette acetone was added to the βLG or α_{S1} -casein till the solution became turbid. The drop wise addition of acetone was accompanied with continuous stirring. The solution was stirred for additional 2 h. To this 5 μL of 8% glutaraldehyde was added and stirred for 4 h. For the preparation of HSA nanoparticles, 200 mg of HSA was weighed and dissolved in 2 mL of 10 mM NaCl (pH 8.5) solution. The solution was kept for stirring for 10 min at 500 rpm. To this 8 mL of ethanol was added drop by drop. The solution was stirred for 60 min, at 25 °C. 0.588 μL of 8% glutaraldehyde/mg of HSA was added and kept for stirring for 24 h. The precipitate obtained with either βLG or α_{S1} -casein or

HSA, was collected by centrifuging the sample for 20 min at 20000 rpm. The precipitate was repeatedly washed 3-4 times with acetone. The lyophilized sample was stored at 4 °C. The particles were dispersed in water before use. Dispersion was done using sonicator. To the particles, dispersed in water containing 0.002% sodium azide, a known amount of curcumin was added. The solution was vortexed, along with sonication before being kept for equilibration. The unbound curcumin was removed by centrifuging the sample at 8000 rpm for 20 min, which pulls down only the undissolved curcumin.

Encapsulated sample or the control was characterized using scanning electron microscope (SEM) (Leo 435 VP, Cambridge, UK). For SEM analysis, a drop of the sample was placed on a microscopic cover slip, vacuum dried, coated with gold before being observed under microscope. The morphology of the nanoparticle was evaluated. Average size and distribution of the nanoparticle was determined using Zetasizer Nanoseries, (Nano ZS, Malvern Instruments Ltd., Malvern, UK). The measurements were carried out at 25 °C. The dispersion pH was 7.0 for both the control and the sample containing the curcumin. An average of 10 measurements was used to report the size.

Encapsulation Efficiency and *In Vitro* Release of Curcumin Bound to β LG Nanoparticle

Encapsulation efficiency of curcumin bound to β LG was determined by adding curcumin (0.25 mg) in 10 mg/mL solution of β LG nanoparticle. The solution was equilibrated for 30 min in an incubator equipped with shaker, maintained at 25 °C, for 30 min. The solution was centrifuged for 20 min at 8000 rpm to pellet the undissolved

curcumin. The pellet was carefully dissolved in known amount of methanol and curcumin was quantified, spectrophotometrically, at 425 nm.

$$\text{Encapsulation Efficiency (\%)} = \frac{(\text{Total amount of curcumin} - \text{free curcumin})}{\text{Total amount of curcumin}} \times 100$$

Quantity of curcumin loaded in nanoparticles was calculated by deducting the amount recovered in the methanol fraction from the total amount of curcumin added.

The *in vitro* release of curcumin was carried out as follows. Curcumin loaded nanoparticle was incubated at 37 °C with gentle agitation. The sample was centrifuged at 8000 rpm for 20 min, to remove any unbound curcumin. The unbound curcumin, settled as pellet, was carefully collected and dissolved in methanol. Its absorbance at 425 nm was checked to calculate the amount of unbound curcumin. Similar experiments were carried out in acidic conditions (pH 2.0 with 0.9% NaCl).

The percentage of curcumin released was arrived at from the formula,

$$\text{Release (\%)} = \frac{[\text{Curcumin}]_{\text{rel}}}{[\text{Curcumin}]_{\text{tot}}} \times 100$$

where, $[\text{Curcumin}]_{\text{rel}}$ is the concentration of curcumin released in 24 h and $[\text{Curcumin}]_{\text{tot}}$ is the total amount of curcumin entrapped in the nanoparticle.

Loading of curcumin to α_{S1} -casein and HSA nanoparticle, its characterization, encapsulation efficiency and *in vitro* release of curcumin was followed as mentioned under β LG-curcumin nanoparticle preparation.

Molecular Docking Studies of Curcumin to β LG

Based on experimental results, docking experiments were carried out to visualize the binding site of curcumin to β LG. To generate the binary complex of curcumin- β LG the

crystal structure of the complex of β LG-palmitate available at 2.5 Å resolution (labeled 1B0O in Brookhaven Protein Data bank) was chosen as template (Wu et al., 1999). The binding site and the mode of binding was identified by an automated public domain software package ArgusLab 4.0.1 (Mark Thompson and Planaria Software LLC) that performs the molecular constructions, calculations and visualizations. The possible binding conformations and orientations were analyzed by clustering methods. Flexible docking was carried out using the genetic algorithm implemented by the program ArgusLab (AScore scoring method). This dock engine was set to perform an exhaustive search for automated docking with complete ligand flexibility to elucidate the mode of interactions between curcumin and β LG. The water molecules and palmitate were removed and the hydrogen's were added using the builder module of ArgusLab. The ligand structure was constructed in and submitted to the PRODRG site to get optimized structure (Schuettelkopf and van Aalten, 2004). The docking search was done for the whole protein without defining the target area or protein pocket. Geometry optimization was carried out with grid resolution of 0.4 Å and grid spacing of $35.76 \times 47.68 \times 41.95$ Å. The pose with the minimal energy was taken as the optimal binding mode. To evaluate the effectiveness of the ArgusLab dock engine, redocking of palmitate back to β LG was done and the resultant best pose was compared with the corresponding crystal structure of palmitate- β LG complex (PDB: 1B0O). The best returned pose revealed similar interactions. This validated the docking accuracy needed for further studies with curcumin.

Molecular Docking Studies of THC/ CPA to Lipoxygenase

The coordinates of lipoxygenase with bound epigallocatechin (EGC) (Skrzypczak-Jankun, 2003b) was obtained from the protein data bank (PDB ID : 1JNQ). The optimized structure of THC and CPA was obtained from Dundee server - PRODRG. Molecular docking was computed using the Molecular Virtual Docking Software (MVD 2010. 4. 0. 2), which performs the docking and calculations (Molegro Virtual Docker, Molegro ApS, Denmark). The binding cavities were identified using the algorithm provided by the manufacturer. Flexible docking was carried out and evaluated using the program MolDock Score. The dock engine was set to perform an exhaustive search for automated docking with complete ligand flexibility to elucidate the mode of interactions. The possible binding conformations and orientations were analyzed from the pose clustering.

Statistical Analysis

Data are presented as means \pm standard deviation. For all of the measurements, a minimum of three to four replicates was taken for data analysis. Using the software Origin 6.1, all of the values were averaged and plotted.

3. Results and Discussion

ePrints@CFTRI

***3.1. Interaction of Curcumin with
 β -Lactoglobulin and α_{S1} -Casein and its
Encapsulation in Nanoparticle***

3.1.1. Interaction Studies of Curcumin with β -Lactoglobulin and its Nanoparticle Preparation

Purity of Curcumin

Commercially available curcumin is a mixture of three naturally occurring curcuminoids with curcumin as the main constituent. The purity of curcumin was ascertained by RP-HPLC. The retention time of the purified compound was 5.9 min (Figure 3.1).

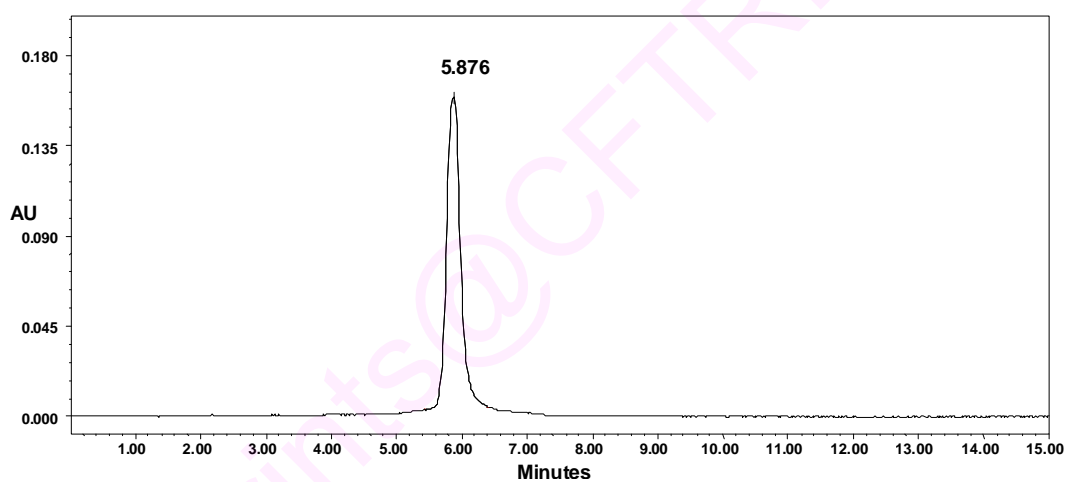


Figure 3.1. RP-HPLC profile showing the purity of curcumin. C18 column was used and the detection was at 425 nm. The elution was carried out using 5% methanol and 0.1% trifluoroacetic acid in acetonitrile.

Stability of Curcumin

The effect of β LG on the stability of curcumin was followed in buffer at pH 7.0. Half-life of curcumin in buffer is 30.8 min (Table 3.1). In the presence of β LG, the half-life of curcumin increased by 6.7 times to 206 min indicating the protection of curcumin from

hydrolytic degradation. Curcumin degrades rapidly under physiological conditions *in vitro* (Wang et al., 1997). Binding of curcumin to proteins may help in improving solubilization and arresting the degradation. The binding of curcumin to β LG delayed its hydrolytic degradation. Human serum albumin has also been reported to help enhance the stability of curcumin in solution (Leung and Kee, 2009). Curcumin in fetal calf serum has good stability with a half life of 8 h (Wang et al., 1997). Fetal calf serum has several uncharacterized proteins that could bind curcumin, although, the major protein is serum albumin. The stability of curcumin in various proteins follows the order: fetal calf serum ($t_{1/2} = 480$ min, pH 7.2) > bovine serum albumin ($t_{1/2} = 373$ min, pH 7.2) > α_{S1} -casein ($t_{1/2} = 340$ min, pH 7.2) > β LG ($t_{1/2} = 206$ min, pH 7.0). β LG bound curcumin is stable compared to free curcumin in aqueous medium. Stability of vitamin D3 bound to β LG is reported to be enhanced compared to the free vitamin (Forrest et al., 2005). Our results along with previous reports suggest that β LG protected curcumin from degradation and increased its half-life in aqueous solution. Investigation of the binding of curcumin to β LG is of interest as β LG is believed to act as a natural transporting molecule.

Table 3.1.

Stability of curcumin at pH 7.0 in the presence and absence of β LG

Curcumin	k (min^{-1})	t_{half} (min)
Buffer	0.022	30.8
β LG	0.0034	206

Spectroscopic Studies of Curcumin with β LG

Absorbance Measurements

The absorption spectrum of β LG in buffer is shown in Figure 3.2A. β LG shows a maximum at 278 nm. Curcumin in aqueous medium shows less absorption over the absorption in ethanol or in the presence of β LG. This is depicted in Figure 3.2B.

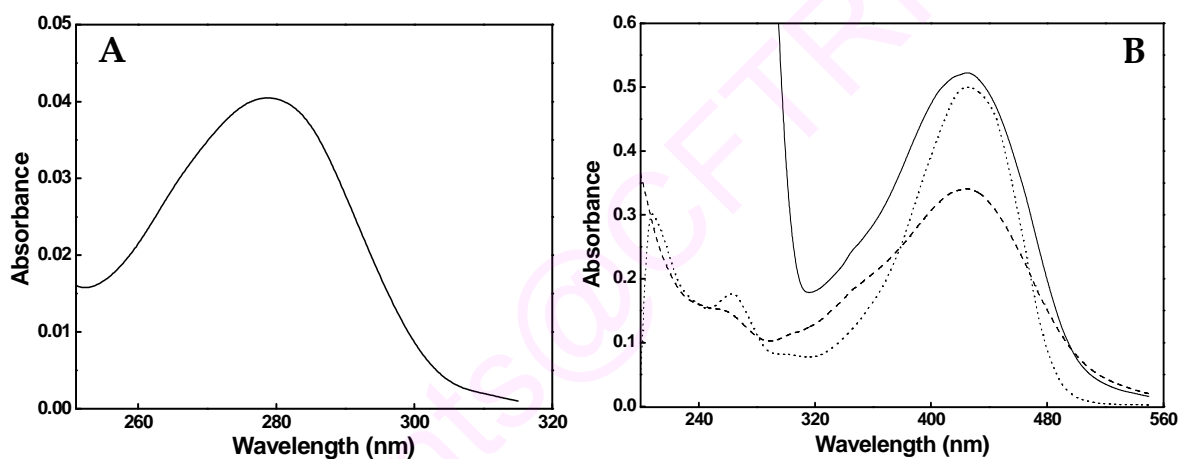


Figure 3.2. (A) Absorption spectra of β LG in 50 mM Tris HCl buffer, pH 7.4. (B) Absorption spectra of (- - - -) curcumin in buffer, (...) curcumin in ethanol and (—) β LG-curcumin complex.

Fluorescence Measurements

Curcumin in buffer when excited at 430 nm was weakly fluorescent with a nonspecific, feeble and broad spectrum centered at ~ 530 nm. Addition of β LG to curcumin solution ($10 \mu\text{M}$) resulted in a shift in the emission maximum from ~ 530 nm to 500 ± 1 nm and increased relative fluorescence intensity (Figure 3.3A). The fluorescence intensity increased linearly with increase in β LG concentration until the concentration ratio of curcumin- β LG reaches 1:4 (Figure 3.3B). The change in fluorescence intensity at 500 nm was recorded and the data plotted according to eq. 4 (Figure 3.3C). The binding constant of curcumin to β LG at 25°C , pH 7.0 is estimated to be $1.1 \pm 0.1 \times 10^5 \text{ M}^{-1}$. Fluorescence of curcumin which depends on the polarity of the environment showed solvent dependent shift in the emission maximum. Shift in the emission maximum from longer to shorter wavelength and increased fluorescence intensity indicate the movement of curcumin from a polar to a less polar environment (Figure 3.3A). This observation is in good agreement with the reports on binding of curcumin with proteins such as α_{S1} -casein (Section 3.1.2) and serum albumin. The binding of curcumin to human serum albumin exhibits emission maximum at 500 nm (Reddy et al., 1999). The shift in the emission maximum along with increase in fluorescence intensity indicated that the binding of curcumin was hydrophobic in nature.

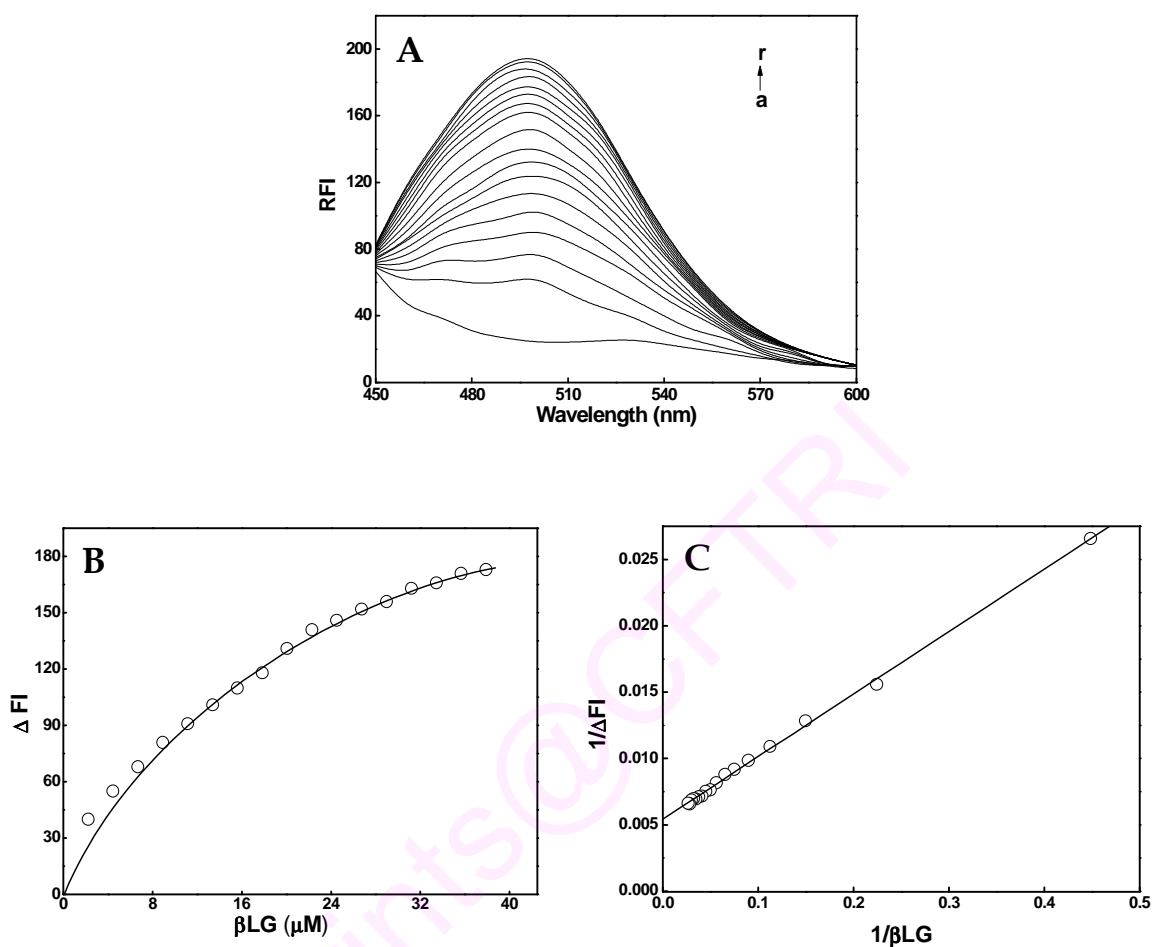


Figure 3.3. (A) Emission spectra of curcumin showing blue shift on binding to β LG. 10 μ M curcumin was titrated against increasing concentration of β LG (a-r, 0-38 μ M), Excitation wavelength was set at 430 nm, Excitation and emission slit widths were 5 and 10 nm. (B) Plot of fluorescence intensity as a function of β LG concentration. Maximum protein to ligand ratio for complex formation was 1:4. (C) Double reciprocal plot to calculate the binding constant as described in experimental section ($R=0.99$).

Fluorescence Quenching Measurements

Curcumin in buffer though weakly fluorescent when excited at 430 nm (emission maximum at ~530 nm) does not fluoresce when excited at 295 nm. However, in presence of β LG, a new fluorescent peak was observed around 500 nm reminiscent of the emission spectrum of curcumin when excited at 430 nm (Figure 3.4A). The addition of incremental aliquots of curcumin, resulted in a gradual decrease in the fluorescence intensity centered at 335 ± 1 nm. The second fluorescent peak centered at 500 nm corresponds to the characteristic spectral region of curcumin. An isoemissive point was observed at 446 nm. The binding parameter was calculated by analyzing the quenching data. Figure 3.4B shows the mass action plot from which the binding constant is calculated to be $1.04 \pm 0.1 \times 10^5 \text{ M}^{-1}$. A stoichiometry of 1:1 was obtained. This was calculated according to Chipman et al. (1967) and is shown in Figure 3.4C.

The appearance of a fluorescence band in the spectral region characteristic of curcumin (centered at 500 nm) may be due to the energy transfer between the donor residues (aromatic amino acids) of the protein and the acceptor (curcumin). β LG has two tryptophan and four tyrosine residues per monomer (Andrade and Costa, 2002) that contribute to the fluorescence of β LG. On addition of curcumin to β LG, decrease in the tryptophan fluorescence intensity along with a concurrent increase in the fluorescence intensity centered at 500 nm was observed. At 295 nm, there is selective excitation of tryptophan residues. Trp19 is in an apolar environment on β A strand at the base of binding pocket lying between 3.0 to 4.0 Å from the guanidine group of Arg124, while the partly exposed Trp61 lies on C-D loop near the entrance of β barrel and the Cys66-Cys160 bridge (Andrade and Costa, 2002). Curcumin probably binds in an apolar

environment closer to Trp19 quenching the emission of Trp19 without causing any shift in the emission peak, when excited at 295 nm (Andrade and Costa, 2002). Palmitate and retinoic acid are reported to bind to β LG, with an association constant of $10 \times 10^6 \text{ M}^{-1}$ and $5 \times 10^6 \text{ M}^{-1}$ (Sawyer and Kontopidis, 2000).

Effect of temperature on the association constant of curcumin to β LG was studied. Figure 3.5A shows the mass action plot for the curcumin- β LG system at different temperatures using an intrinsic quenching analysis. Thermodynamic parameters were calculated from the van't Hoff plot based on temperature dependence studies of the association constant in the range of 15-45 °C (Figure 3.5B). ΔS° value was $18.7 \text{ cal mol}^{-1}$, while ΔG° value is $-6.8 \text{ kcal mol}^{-1}$ at 25 °C. Temperature dependence studies on the binding of curcumin to β LG revealed a decrease in the binding constant with the increase in temperature suggesting the involvement of hydrophobic interactions. Curcumin- β LG complex formation is accompanied by positive entropy changes, an indication of the binding process being entropically driven. Similar thermodynamic parameters are reported in relation to the binding of curcumin to α_{s1} -casein (Section 3.1.2.). On the basis of the characteristic signs of thermodynamic parameters for various interactions, it can be inferred that positive entropy changes are associated with hydrophobic interactions (Ross and Subramanian, 1981).

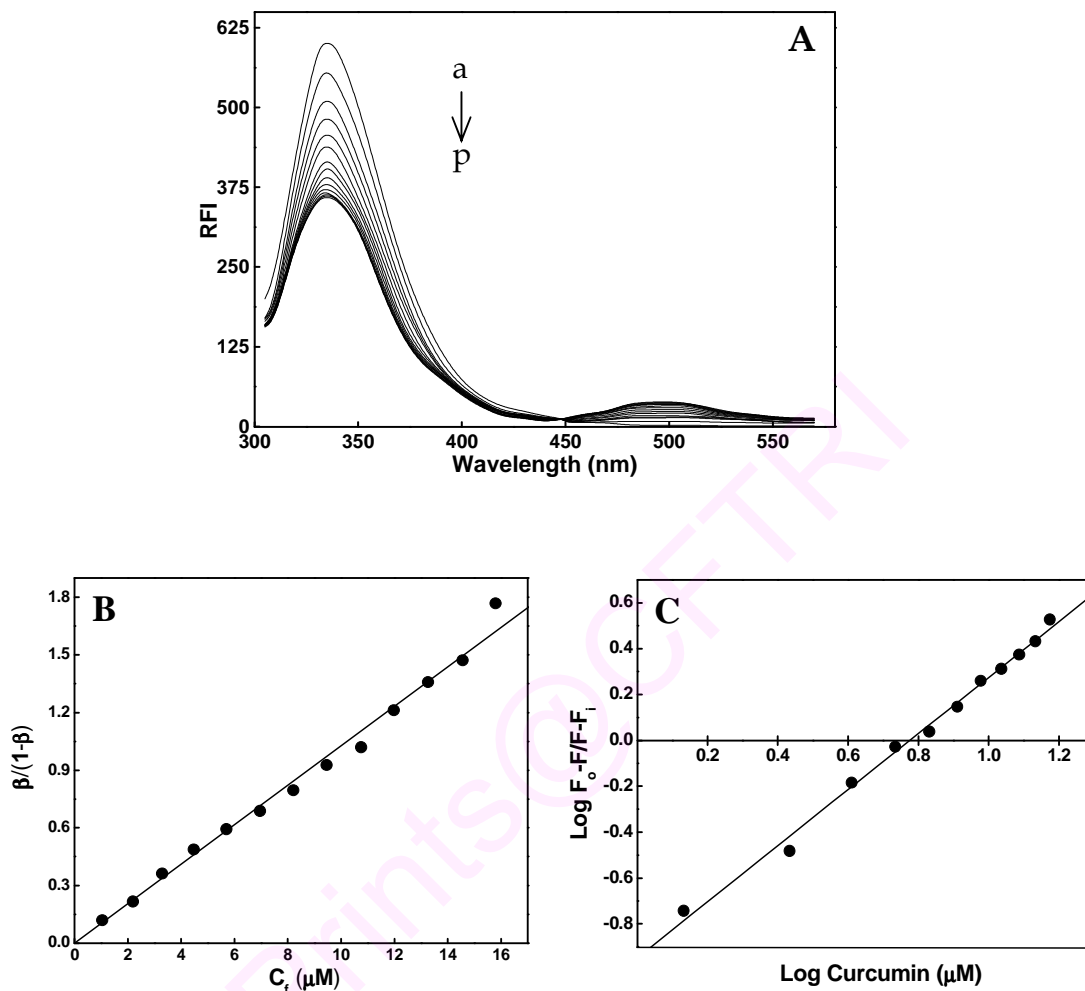


Figure 3.4. (A) Intrinsic fluorescence emission spectra of β LG and bound curcumin. Excitation wavelength was set at 295 nm, Protein concentration was fixed to 2.95 μ M and the temperature was maintained at 25 $^{\circ}$ C. Aliquots (2 μ L) of curcumin were added in the concentration range 0-20.4 μ M (a-p). (B) Mass action plot, slope gives the binding constant. (C) Plot to calculate the stoichiometry.

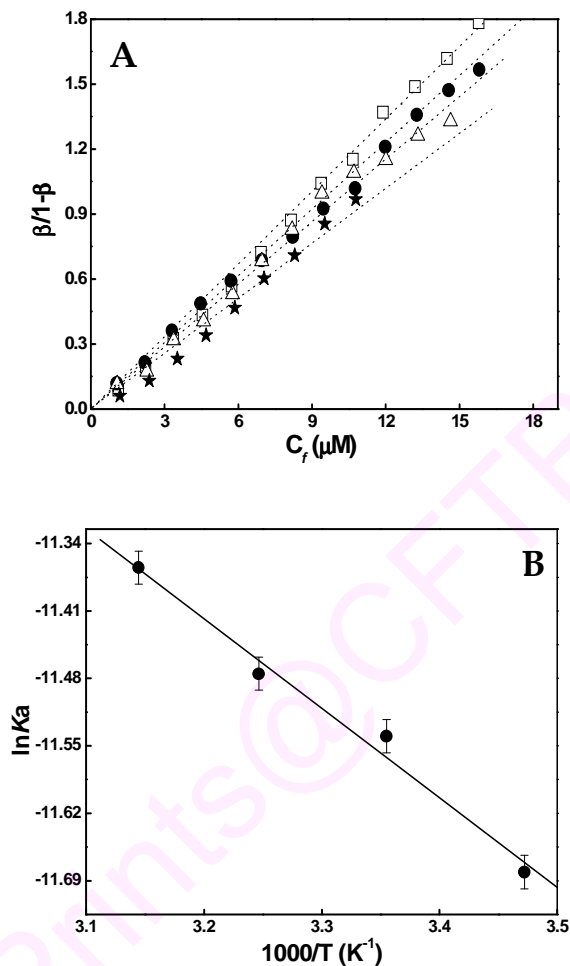


Figure 3.5. (A) Mass action plot for the binding of curcumin to β LG at, 15 ($-\square-$), 25 ($-\bullet-$), 35 ($-\triangle-$) and 45 °C ($-\star-$). (B) van't Hoff plot, to calculate the free energy and entropy. The error bars represent the mean and standard deviation of experiments in triplicate.

Fluorescence Resonance Energy Transfer Measurements

To reveal the binding site of curcumin, resonance energy transfer experiments were carried out. Fluorescence resonance energy transfer through Förster (FRET) mechanism occurs when the emission spectrum of protein overlaps with the absorption spectrum of ligand (Mahesha et al., 2006). Figure 3.6A shows the overlap spectrum. There was a fairly good overlap between the emission spectra of equimolar concentrations of β LG and the absorption spectra of curcumin. Addition of curcumin resulted in the quenching of the fluorescence intensity indicating Förster energy transfer. By integrating the spectra in the wavelength range 310-540 nm, the overlap integral J is computed to be $2.4 \times 10^{-14} \text{ M}^{-1} \text{ cm}^3$ and energy transfer efficiency E is 0.27. The total percentage energy transfer is calculated by plotting β LG concentration (mg/mL) versus the percentage energy transfer. The Y-intercept which gives the energy transfer value is 27% (Figure 3.6B). The distance between the donor and the acceptor (r_o) is 32 Å, higher than 26.8 Å, the maximal critical distance (R_o). The higher value of r_o suggests a static type of quenching with non-radiation energy transfer between curcumin and β LG. Förster distance (R_o) and the distance between the donor and the acceptor (r_o) obtained compare well with previous studies. Similar values of r_o and R_o have been obtained for β LG B variant and curcumin ($r_o=33.8 \text{ Å}$, $R_o=25.9 \text{ Å}$) (Mohammadi et al., 2009). Since, β LG contains two Trp residues; both have to be taken into account while calculating the efficiency of energy transfer and the distance between the donor and the acceptor depends on the efficiency of energy transfer.

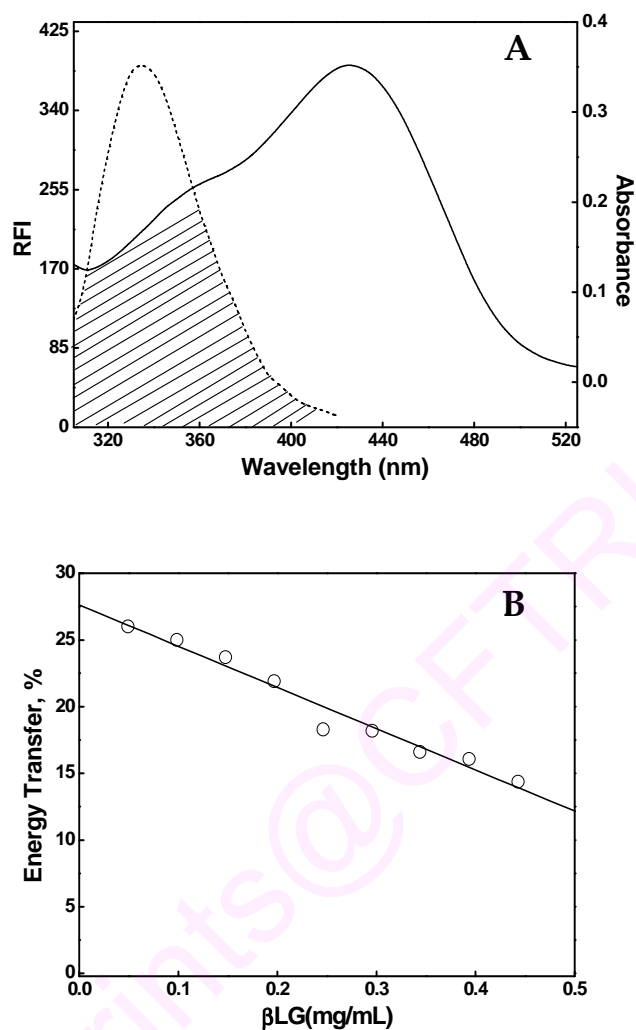


Figure 3.6. (A) Overlap spectra for representing the Förster type resonance energy transfer between β LG and curcumin. Emission spectrum of β LG in buffer in the wavelength range of 305-400 nm, excitation wavelength was 295 nm (---), Absorption spectrum of curcumin in buffer (—). Spectrum was immediately taken after adding curcumin to buffer. (B) Plot of energy transfer between tryptophan of β LG (mg/mL) and curcumin.

Effect of pH on the Binding of Curcumin to β LG

Effect of pH on the binding of curcumin to β LG was analyzed by determining its association constant (Figure 3.7A and 3.7B). There is a precipitous decrease in association constant when the pH is decreased from 7.0 to 5.5 from 1.1×10^5 to $1.1 \times 10^3 \text{ M}^{-1}$ (Table 3.2). The decrease in the association constant with decrease in pH indicated inaccessibility of the ligand binding site to curcumin. Similarly, alkyl sulfonate ligands are reported to bind to β LG at pH 6.8, with no binding observed at pH 3.0 (Busti et al., 1999). At acidic pH, the EF loop (85-90) of β LG is in closed conformation rendering the hydrophobic cavity inaccessible to the entry of ligands. With the increase in pH, the EF loop folds back opening the gate for the access to the binding of ligands (Qin et al., 1998a). At pH 7.0, the lid for the calyx is open with increased molecular volume/area (Qin et al., 1998a) allowing curcumin to get into the hydrophobic pocket. This lends credence to our suggestion that curcumin may be binding at the hydrophobic pocket of the central calyx. Earlier studies of pH titration with β LG and palmitate have clearly shown that the binding site for palmitate is within the central calyx at neutral pH. At lower pH, EF loop is in closed conformation and is stabilized by hydrogen bonds involving Ser116. Titration of Glu89 in EF loop at unusual high pH ~ 7.3 is due to deprotonation, which folds back the EF loop with a consequent solvent exposure of Glu side chain (Qin et al., 1998a). Hence, opening of EF loop appears to be a prerequisite for the binding of curcumin to β LG.

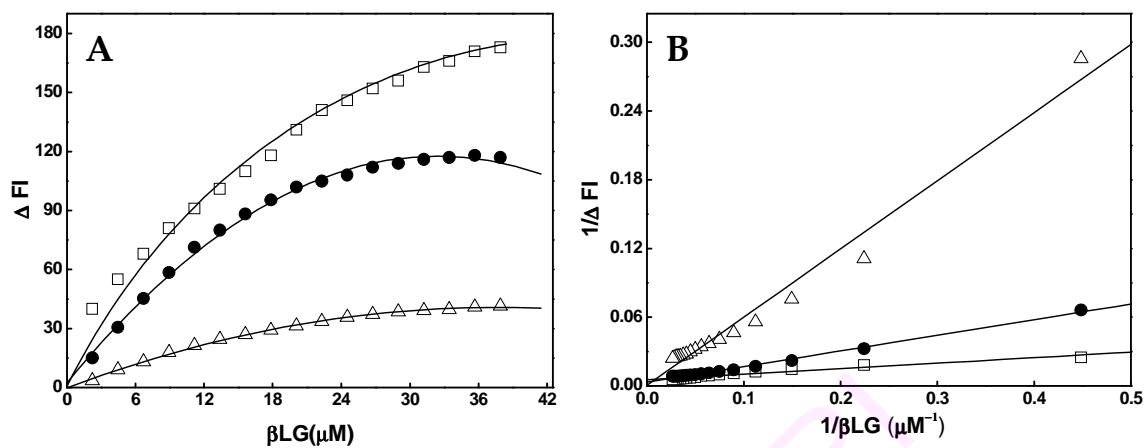


Figure 3.7. Effect of pH on the binding constant of curcumin to βLG . (A) Plot of fluorescence intensity as a function of βLG concentration. (B) Double reciprocal plot to calculate the binding constant.

Table 3.2. Effect of pH on the binding of curcumin to βLG

pH	K_a (M^{-1})
5.5	1.1×10^3
6.5	2.4×10^4
7.0	1.1×10^5

Curcumin-βLG Spectrum in the Presence of Palmitate

The binding site for palmitate in βLG is reported to be within the β-barrel lined by hydrophobic residues (Wu et al., 1999). The effect of curcumin binding to βLG in the presence of palmitate was investigated. Figure 3.8A shows the spectra of curcumin-βLG in the presence of palmitate. A solution containing equimolar ratio of βLG and curcumin has an emission maximum at 500 ± 1 nm, when excited at 430 nm. Addition of aliquots of palmitate to curcumin-βLG complex, led to a red shift in emission maximum from, 500 to 505 nm, with simultaneous decrease in fluorescence intensity of curcumin. Figure 3.8B shows the mole ratio plot of [palmitate/βLG] against the normalized values of fluorescence intensity. The intensity decreased till the ratio of protein to palmitate reaches 1, with no perceptible decrease in the intensity, thereafter. The red shift in emission maximum along with the decrease in fluorescence intensity indicated an alteration in the binding environment of curcumin. X-ray crystallographic studies have shown the binding of palmitate to the central cavity of the βLG, formed by eight anti-parallel β-strands (Wu et al., 1999). Hydrophobic interactions are the predominant contributing factors for the affinity of fatty acids to βLG. Even though the binding constant of palmitate to βLG is high when compared to the binding constant of curcumin to βLG, there is no significant decrease in the fluorescence intensity, even with excess addition of palmitate to curcumin-βLG solution.

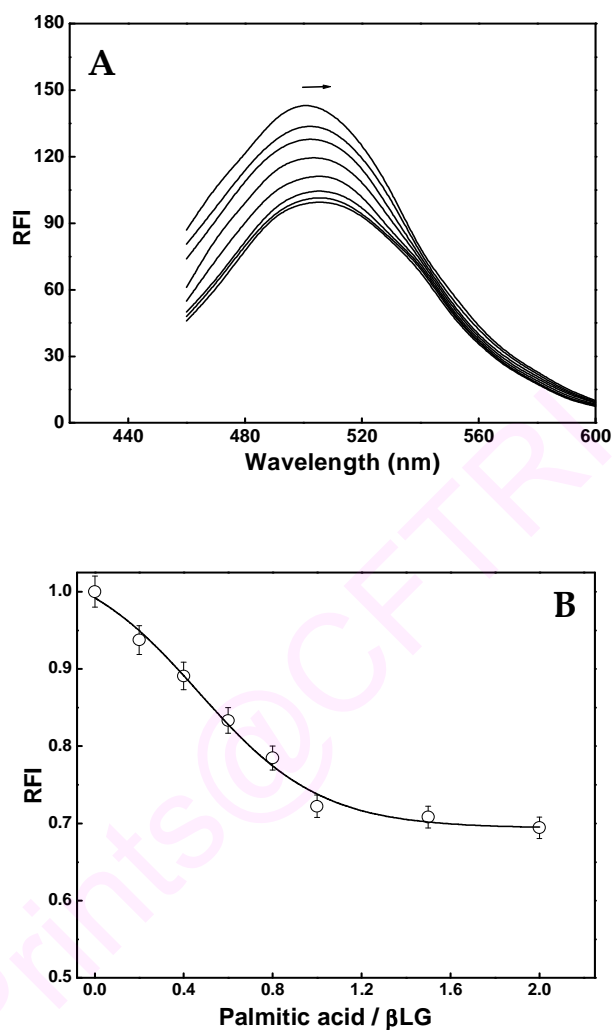


Figure 3.8. (A) Effect of palmitate on curcumin- β LG complex. Shift in the emission maximum of curcumin fluorescence on addition of palmitate from 500 to 505 nm (represented by arrow), Excitation wavelength was 430 nm, Excitation and emission slit widths were set at 5 & 10 nm, concentration of curcumin and β LG each were 10 μ M. (B) Mole ratio plot of palmitate/ β LG against normalized values of relative fluorescence intensity showing decrease in fluorescence intensity of curcumin on addition of palmitate.

Binding Studies of Curcumin with Denatured β LG

Titration of curcumin against denatured β LG was carried out at pH 7.0, and the fluorescence spectra recorded. The fluorescence emission maximum was 505 nm indicating a +5 nm shift relative to the curcumin bound to native β LG. The change in fluorescence intensity at 505 nm was used for calculating the binding constant. The binding constant of curcumin with denatured β LG was found to be $7.0 \pm 0.2 \times 10^2 \text{ M}^{-1}$, which is very low compared to that of native β LG. The low binding observed may be attributable to the nonspecific binding of curcumin to denatured β LG. In presence of denatured β LG, curcumin (when excited at 430 nm) exhibits emission maximum at 505 nm attributable to the loss in β LG structure. Conformational changes in the structure of β LG are extensive at the transition temperature of $\geq 70 \text{ }^\circ\text{C}$ (Belloque and Smith, 1998). The D strand in the calyx participates in unfolding during thermal denaturation resulting in the diminishing of calyx binding ligands such as palmitate and retinol (Yang et al., 2008). Therefore, heat treatment averts the binding of ligands to the central calyx.

CD Spectral Studies

The far UV CD spectrum of native β LG in 50 mM Tris HCl at pH 7.0, revealed a broad band with minimum at $\sim 215 \text{ nm}$ (Figure 3.9A) characteristic of the presence of prominent β structure. The near UV CD spectrum showed two sharp negative bands centered at ~ 292 and $\sim 284 \text{ nm}$ with two smaller bands located at ~ 277 and $\sim 266 \text{ nm}$ (Figure 3.9B). Curcumin did not exhibit any CD bands in aqueous solution. On interaction with β LG, it becomes asymmetric resulting in the appearance of induced bands in the visible region of 350–500 nm. The CD spectra of curcumin in presence of β LG are given in Figure 3.9C. The induced negative and positive bands were observed

at ~389 and ~450 nm, respectively. There are many examples of induced band formation for curcumin bound to protein (Reddy et al., 1999; Zsila et al., 2004a). No change in the secondary and tertiary structure was observed on addition of curcumin to β LG. In case of β LG B variant, curcumin is shown to induce change in the helix and random coil content at pH 6.4 (Mohammadi et al., 2009). However, the authors concluded that the changes observed are not significant and reflect conformational adjustments.

ePrints@CFTRI

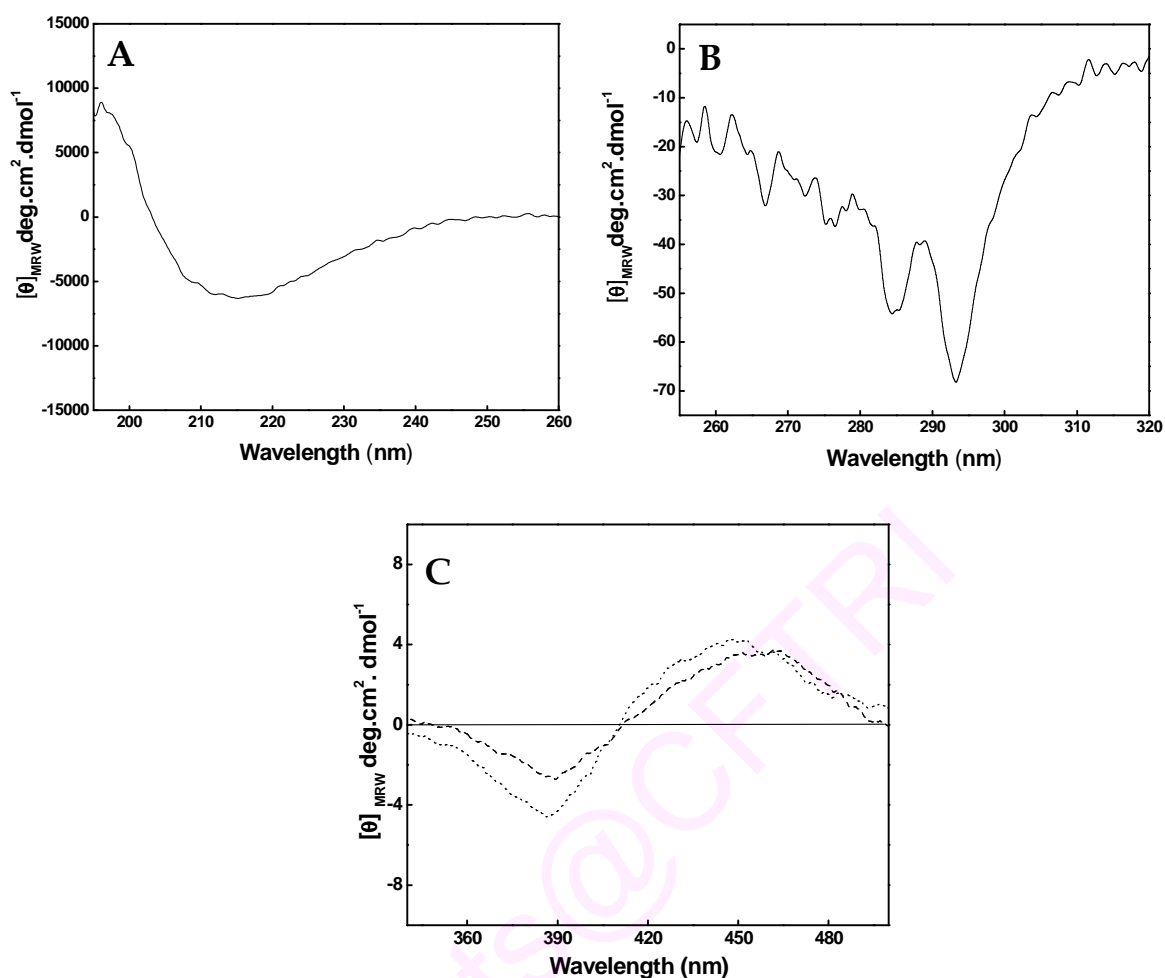


Figure 3.9. CD measurements of curcumin bound to β LG. The path length of the quartz cell was 1 mm for far UV and 10 mm for near and visible range. (A) Far UV spectrum of β LG was recorded in the wavelength range 195–260 nm. Concentration of the β LG is 0.2 mg/mL. (B) Near UV CD spectrum of β LG recorded in the wavelength in the range 320–260 nm. The concentration of the protein is 1 mg/mL. (C) Induced CD spectra of curcumin after binding to β LG recorded in the wavelength range 320–500 nm. The concentrations of curcumin were 7.5 μM (---) and 15 μM (.....) and β LG is (1 mg/mL). Tris HCl buffer (50 mM), pH 7.4, is used in all the CD measurements. All the readings were taken at 25 °C.

HPLC Measurements

To study the effect of curcumin on monomer-dimer equilibrium of β LG, gel permeation HPLC has been carried out. The HPLC profile shown in Figure 3.10, shows that native β LG eluted at 23.5 min. Native β LG, in presence of equimolar concentration of curcumin, has an identical profile as β LG alone. Heated, denatured β LG when injected to the HPLC column eluted in two major peaks; the larger peak had a retention time of 19.6 min, indicative of aggregation. Similarly heated β LG, in presence of equimolar concentration of curcumin, exhibited a major peak eluting at 23.5 min as well as a small peak at 19.6 min. Compared to native β LG, the peak area of heated β LG in presence of curcumin is reduced by 8%. Thus, aggregation of β LG, in the presence of curcumin, is either prevented or delayed.

Native polyacrylamide gel electrophoresis (PAGE) and SDS-PAGE analysis of the denatured β LG, in presence and absence of curcumin, under non-reducing and reducing conditions, did not reveal any difference in the band pattern between the control and the sample containing curcumin. Curcumin neither affected the state of association of β LG nor did it alkylate the cysteine residues.

Heating of β LG at (65 °C) neutral pH, resulted in the formation of aggregates due to scrambling of the disulfide linkages inside the protein core involving the free Cys121 (Creamer et al., 2004; Prabhakaran and Damodaran, 1997). The appearance of a weak band is reported on heating at 65 °C for 45 min, corresponding to the dimer (Hoffmann and van Mil, 1997). The band corresponding to trimer is seen only after heating at 65 °C for 4 h. In the current study, β LG, in absence or presence of curcumin, was heated at 85 °C for 10 min, cooled in an ice bucket and analyzed by HPLC, native PAGE or SDS-

PAGE (under reducing or non-reducing conditions). The absence of any band in native PAGE and SDS-PAGE could mean that the aggregates were not detected with coomassie blue staining, considering the short time of heating. However, the aggregates could be detected by HPLC at 19.6 min. The aggregated proteins were not characterized. Curcumin might be providing a hydrophobic surface to Cys121, which may delay the aggregation process rather than preventing it. Curcumin is reported to irreversibly inhibit thioredoxin reductase by alkylating the cysteine and selenocysteine, present in the active site of the enzyme (Fang et al., 2005).

ePrints@CFTRI

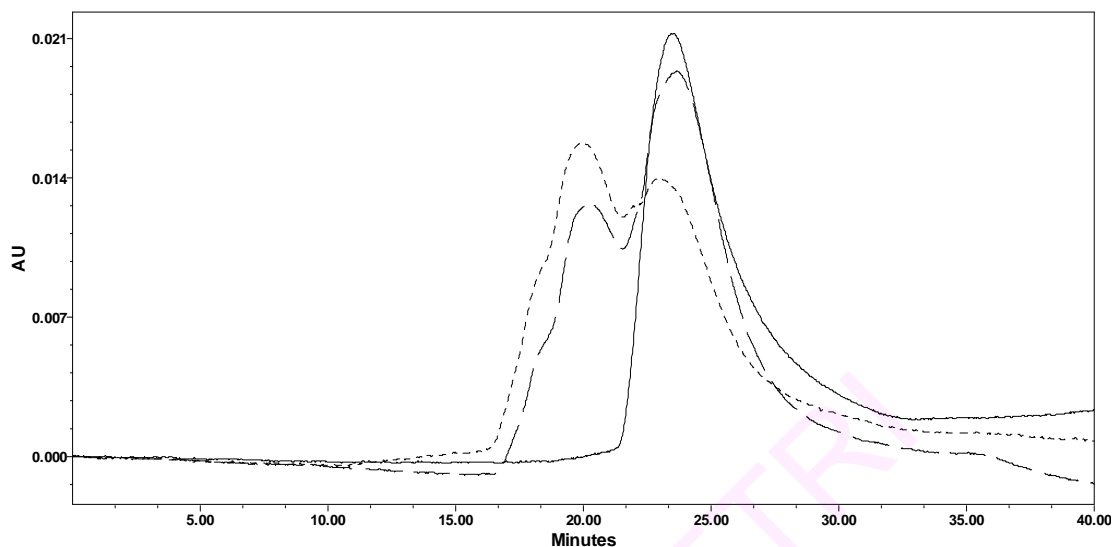


Figure 3.10. HPLC profile of (—) β LG native, (.....) heated β LG and (----) heated β LG containing curcumin. Concentration of β LG is 1 mg/mL in 20 mM phosphate buffer, pH 6.6. The solution after heating to 85 °C for 10 min, was cooled immediately. Gel filtration was performed using a TSK-Super SW2000 (4.6 mm \times 300 mm, 4.0 μ) column. The column was equilibrated with phosphate buffer and 20 μ L of the above sample was injected. The sample was eluted isocratically in the same buffer. The flow rate was maintained at 0.2 mL/min at 25 °C. Detection was at 280 nm.

Visualization of the Binding Site: Docking Studies

Results of spectroscopic studies and effect of pH indicate that curcumin probably binds to β LG at the central calyx. Based on the experimental data, computational docking studies were performed to understand the binding site location and mode of binding of curcumin to β LG. The docking of curcumin to palmitate deprived β LG was investigated. Palmitate is known to bind to the central calyx of the β LG molecule (Wu et al., 1999). The representative build derived from the best pose with the minimal binding energy of $-12.60 \text{ kcal mol}^{-1}$ is shown in Figure 3.11A. The size of the calyx was found to be large enough to accommodate curcumin which agrees with the spectroscopic data. No poses of the binding of curcumin within the surface hydrophobic patch on β LG were obtained. A careful inspection of the binding site (Figure 3.11B) suggested the closer contact of methoxy phenyl moiety of curcumin with the aromatic amino acid residues. The total number of hydrophobic contacts made by curcumin with the protein is 21. The central calyx of β LG is lined by hydrophobic amino acid residues that are gated by the protonation/deprotonation of Glu89 of the EF loop. Effect of pH on the binding of curcumin and the binding measurements with denatured β LG indicate the lower binding affinity of curcumin to β LG with decrease in pH, pointing to the restriction in entry and binding of curcumin to the internal cavity of β LG. Within the van der Waals contact, curcumin molecule is lined by hydrophobic residues such as Ile, Leu, Val and Met that line the wall of the calyx and Phe105 in an orientation suitable to establish π - π interaction with the phenolic ring of curcumin. Lys60 is in the near vicinity of the methoxy group of curcumin. Lys60 and Lys69 are known to be involved in hydrogen bonding with palmitate (Wu et al., 1999). Pro38 is in contact with the hydroxyl group of

curcumin. Pro38 is known to make contact with 3-hydroxy group of cholesterol (Kontopidis et al., 2004). Figure 3.11C shows the electrostatic surface model of β LG with curcumin bound in the central calyx. Our results suggest the binding of curcumin to β LG is predominantly due to hydrophobic contacts within the calyx.

ePrints@CFTRI

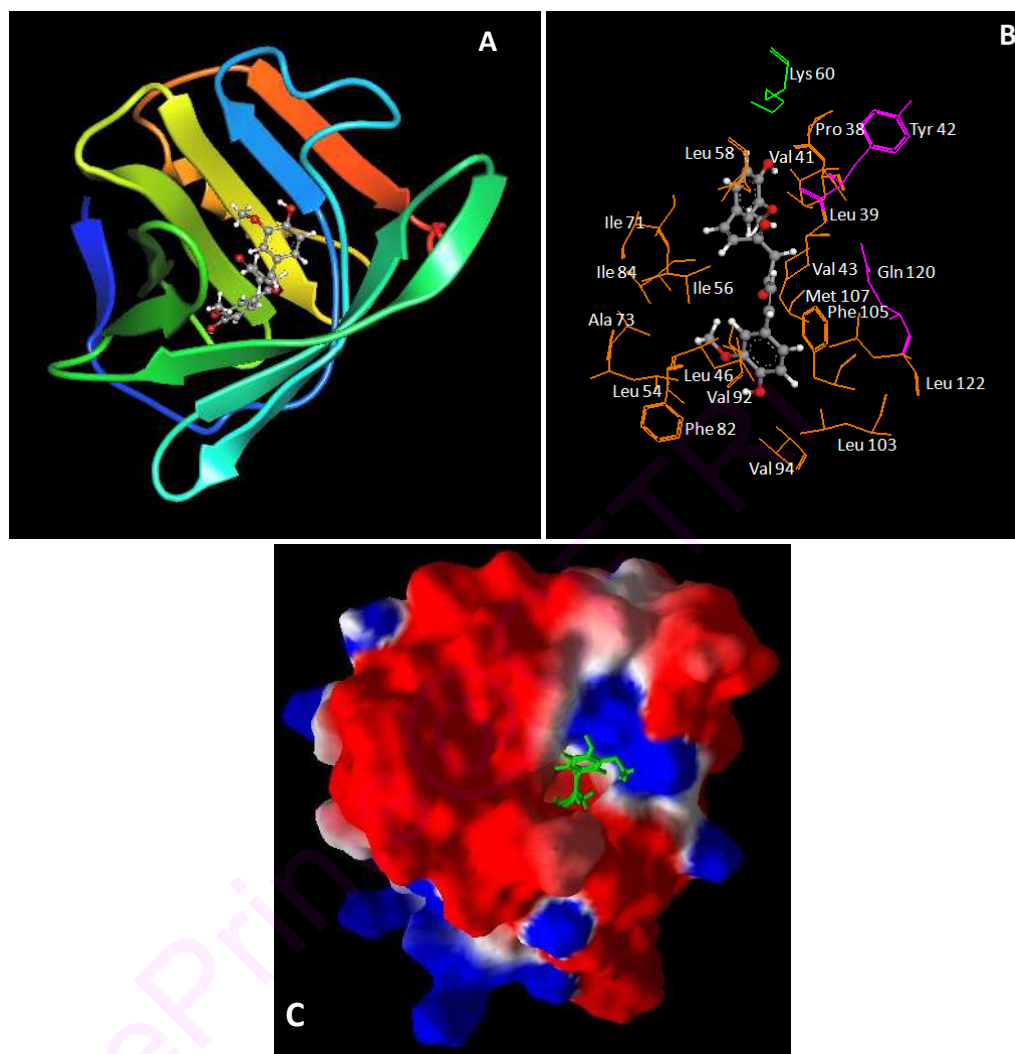


Figure 3.11. Molecular docking studies (A) Cartoon ribbon model structure of β LG showing the binding of curcumin (ball and stick) to central calyx. (B) Amino acid residues surrounding the curcumin molecule. (C) Electrostatic surface model of β LG showing bound curcumin (green: capped structure) in the central calyx.

Nanoparticle Preparation and Measurements of In Vitro Release of Curcumin from β LG Nanoparticle

β LG, a major whey protein that constitutes 10–15% of the total proteins in bovine milk, exhibits good emulsifying property due to its amphiphilic nature (Gunasekaran et al., 2007). β LG is proposed to be utilized for encapsulation as well as controlled release of bioactive compounds by preparing hydrogels or nanoparticles based on its superior gelling property (Chen et al., 2006). The proposal of β LG as an oral drug carrier is supported by its ability to be a natural carrier of many biochemically important hydrophobic compounds, such as retinol and its derivatives, palmitate, cholesterol and vitamin D (Kontopidis et al., 2004). β LG is edible and easily solubilized with good emulsifying characteristics. Its cost effectiveness, abundant availability and acceptability make it an attractive alternative protein that can be used as a carrier molecule for curcumin.

Nanoparticles of curcumin encapsulated in β LG have been prepared and the solubility and *in vitro* release of curcumin from β LG nanoparticle have been studied. The morphology of the prepared nanoparticles of β LG is analyzed using scanning electron microscope (SEM). The SEM images in Figure 3.12A and 3.12B correspond to β LG alone and curcumin encapsulated by β LG particles, respectively. Figure 3.12C shows the graphical representation of the size distribution of the β LG nanoparticles. The particles are polydispersed with the average size being 142 ± 5 nm. They are spherical in shape and no significant physical change is observed, relative to control (β LG). The average size of β LG nanoparticle is reported to be in the range of ~ 60 nm (Gunasekaran et al., 2007). The size of the particles decreases with increase in pH (Gunasekaran et al., 2007).

Encapsulation of curcumin in the nanoparticles was confirmed by the appearance of fluorescence spectrum at 505 nm, when excited at 430 nm.

Circular Dichroism Measurements

The far UV CD spectrum of native β LG in 50 mM Tris HCl buffer, pH 7.0, shows a broad band with minimum at 215 nm, indicating prominent β structure. The spectrum of β LG nanoparticle shows a shift of the minimum from 215 nm to 208 nm (Figure 3.13A). A blue shift in the spectrum occurs when there is rearrangement of disulfide bridges (de Jongh et al., 2001). Comparative details of secondary structure elements of native β LG, β LG nanoparticle and curcumin encapsulated β LG nanoparticle are given in Table 3.3.

The spectrum of the native β LG in 50 mM Tris HCl, pH 7.0, shows two sharp negative bands centered at \sim 292 and \sim 284 nm that can be ascribed to tryptophan vibrational fine structure. The two smaller bands located at \sim 277 and \sim 266 nm could be due to tyrosine. The near UV CD spectrum of β LG nanoparticle is given in (Figure 3.13B). The tertiary structure of the protein is disrupted, probably due to the exposure to organic solvent at basic pH (9.0) during the preparation of the nanoparticle.

The induced CD spectra of curcumin encapsulated in β LG nanoparticle is given in Figure 3.13C. An induced positive band and a negative band at \sim 450 nm and 395 nm were observed, respectively. There was an increase in the two induced bands concomitant with rise in curcumin concentration in the range, 10 to 70 μ M, confirming the encapsulation of curcumin.

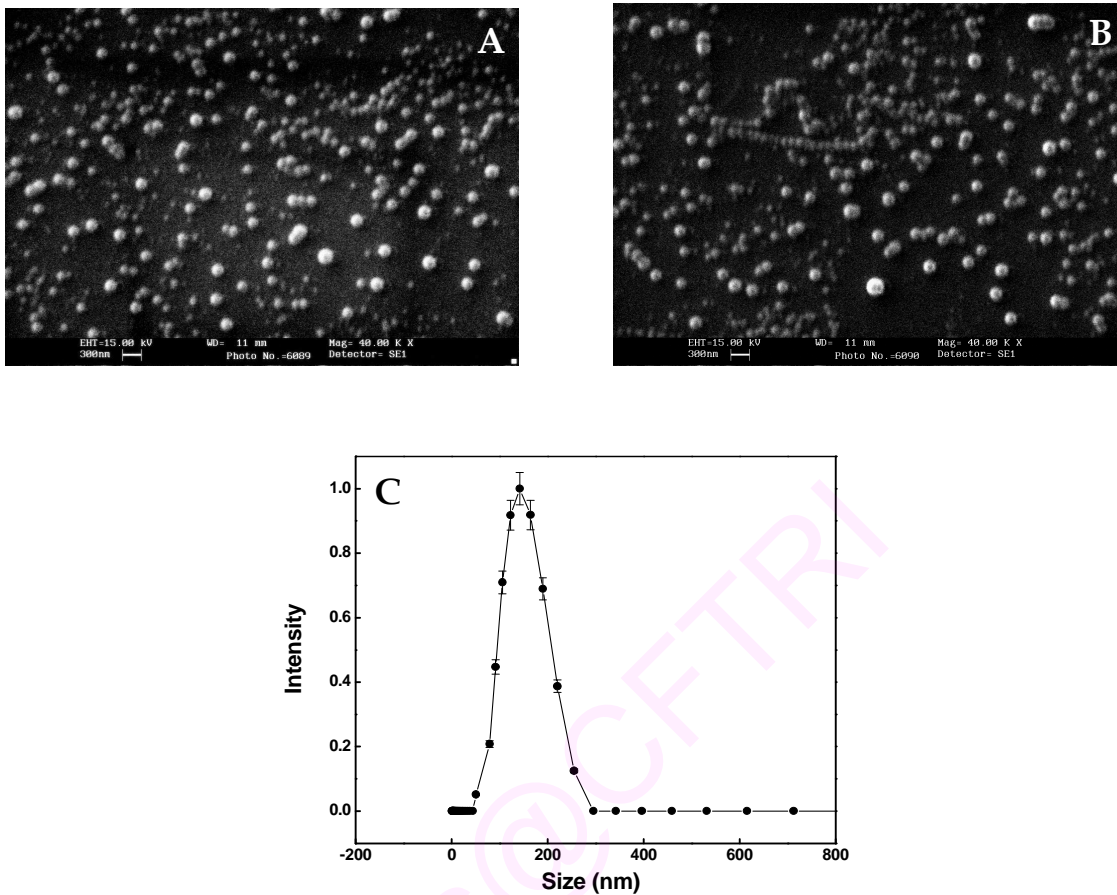


Figure 3.12. Scanning electron microscopic photograph of (A) β LG nanoparticle and (B) β LG nanoparticle loaded with curcumin. The sample was vacuum dried, coated with gold before viewing under microscope. (C) Graphical representation of particle size distribution of curcumin encapsulated in β LG nanoparticle at pH 7.0. Average size of particles was 142 ± 5 nm. Similar results were obtained with β LG nanoparticle. The error bars represents the mean and standard deviation of experiments in duplicate.

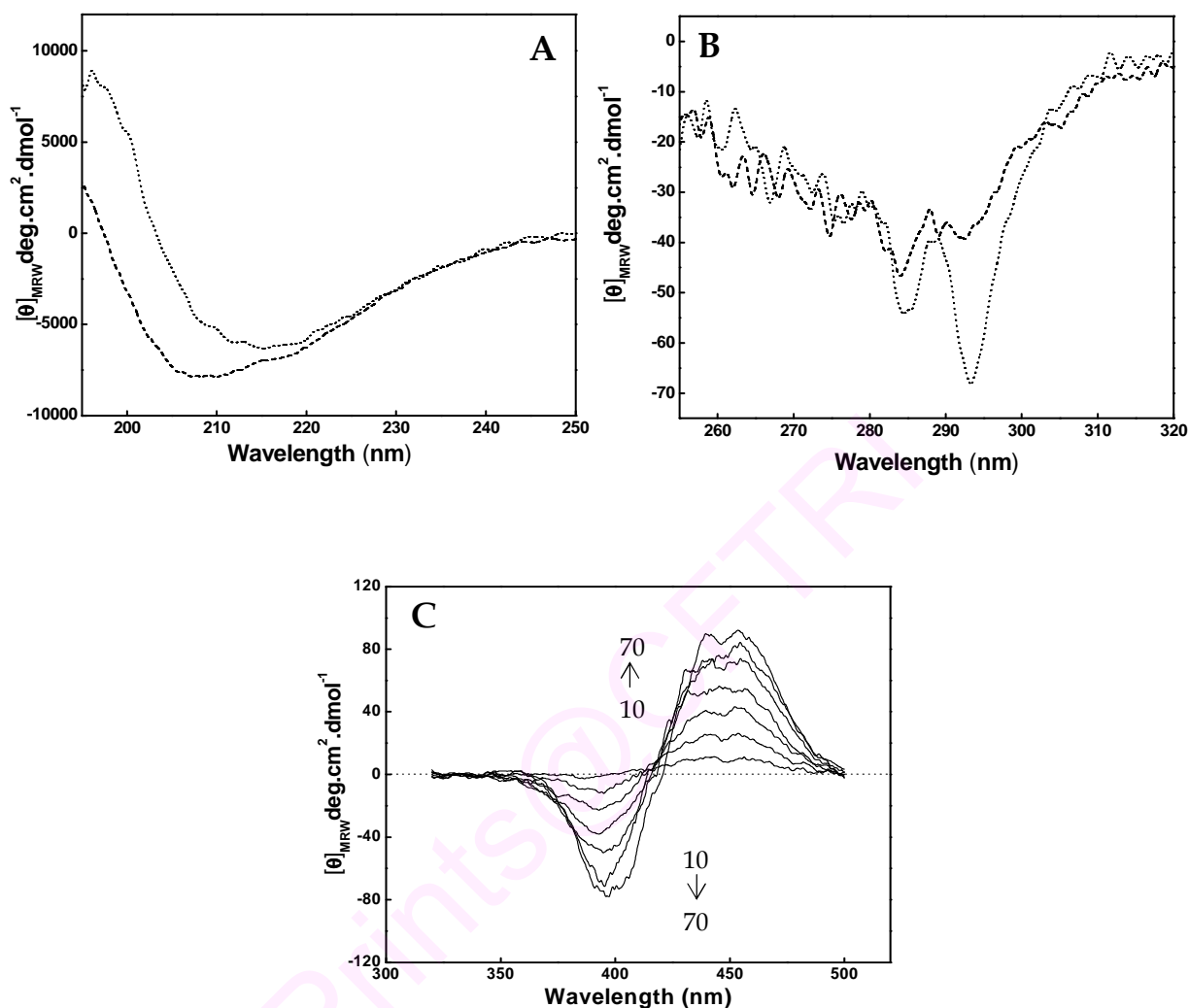


Figure 3.13. (A) Far UV CD spectra of free BLG (.....) and BLG nanoparticles (-----). The concentration of protein is equal to 0.2 mg/mL. (B) Near UV CD spectra of free BLG (.....) and BLG nanoparticles (-----). The concentration of the protein is 1 mg/mL. (C) Induced CD spectra of curcumin encapsulated in β LG nanoparticle. The concentration of β LG nanoparticle is 1 mg/mL in 50 mM Tris HCl buffer, pH 7.0. and the concentration of curcumin is from 10 to 70 μM (the arrow mark indicates the increasing concentration of curcumin).

Table 3.3. Comparative secondary structural details of native β LG, β LG nanoparticle and curcumin encapsulated β LG nanoparticle

Secondary structure element	Free β LG (de Jongh et al., 2001) (%)	β LG native (%)	β LG nanoparticle (%)	Curcumin encapsulated β LG nanoparticle (%)
Helix	15	20	10.5	10.9
Beta	54	50.4	54.8	51.8
Turn	12	13.2	2.6	4.2
Random	10	16.4	32	33
RMS		28.9	17.7	15.6

Solubility of curcumin in aqueous solution is very low (30 nM) (Sahu et al., 2008). The solubility of encapsulated curcumin in β LG nanoparticle increased significantly to $\sim 625 \mu\text{M}$. In surfactant micellar solution, the solubility of curcumin is enhanced to $\sim 740 \mu\text{g/mL}$; in contrast with the solubility of curcumin in aqueous solution ($20 \mu\text{g/mL}$) (Chignell et al., 1994). The encapsulation efficiency of curcumin within the β LG nanoparticle is found to be $> 96\%$.

Curcumin was released from β LG nanoparticles up to $\sim 16\%$, under *in vitro* conditions after 24 h (Figure 3.24). *In vitro* release kinetics was analyzed to study the release of curcumin from β LG nanoparticles at neutral pH. The *in vitro* release of curcumin from β LG nanoparticles was found to follow zero order kinetics. The zero order release constant, k_0 was 1.17 M s^{-1} . Overall, our results indicated that encapsulation of curcumin with β LG enhanced solubility with slow release of curcumin *in vitro*. *In vitro* release of curcumin from β LG nanoparticles was also checked under acidic conditions (pH 2.0). No release of curcumin was observed, over a period of 48 h, from the nanoparticles. The characteristics of curcumin encapsulated in β LG nanoparticles are tabulated in Table 3.5.

In conclusion, we report the detailed spectroscopic study on the interaction of curcumin with β LG and preparation of curcumin encapsulated in β LG nanoparticles. Curcumin probably binds to the central hydrophobic cavity of β LG surrounded by hydrophobic amino acids forming a 1:1 complex. Enhancement of the solubility and stability of curcumin, when bound to β LG, may be helpful in improving the bioavailability of curcumin *in vivo*. Curcumin bound β LG can be an effective carrier for curcumin as both are food components.

3.1.2. Interaction of Curcumin with α_{S1} -Casein and its Nanoparticle

Preparation

α_{S1} -Casein from bovine milk was purified and the homogeneity was confirmed by SDS-PAGE (Figure 3.14).

Fluorescence Measurements

Curcumin fluorescence in aqueous solution is very weak. The spectrum reveals a broad maximum at ~ 530 nm when excited at 430 nm. Addition of small increments of α_{S1} -casein results in a sharper fluorescence peak with increased intensity of ~ 25 times that of curcumin alone (Figure 3.15A). The emission maximum of curcumin shifts toward blue to 510 nm and remains constant during titration; emission intensity was enhanced with increasing curcumin concentration (Figure 3.15B). The fluorescence of curcumin is sensitive to the polarity of its surrounding environment. These results suggest that curcumin is transferred from a hydrophilic to a more hydrophobic environment. The Scatchard plot derived using eq. 2 is given in Figure 3.15C. The association constant (K_a) estimated from the plot is $2.01 \pm 0.6 \times 10^6 \text{ M}^{-1}$. With dephosphorylated α_{S1} -casein, the association constant was found to be $2.3 \pm 0.5 \times 10^6 \text{ M}^{-1}$, which is very similar to that of phosphorylated α_{S1} -casein. The similarity in association constants suggests that the phosphate groups are not involved in the binding process. The surface hydrophobicity of α_{S1} -casein did not change due to dephosphorylation. This was ascertained by ANS binding measurements with α_{S1} -casein and dephosphorylated α_{S1} -casein. The binding constant for ANS with α_{S1} -casein was $1.8 \pm 0.4 \times 10^4 \text{ M}^{-1}$, and with dephosphorylated α_{S1} -casein, the binding constant was $2 \pm 0.4 \times 10^4 \text{ M}^{-1}$. The hydrophobicities of phosphorylated and dephosphorylated α_{S1} -casein are similar. The anisotropy of

curcumin obtained from fluorescence polarization measurements did not change on binding to α_{S1} -casein. The driving force for the binding of curcumin with α_{S1} -casein was estimated by following the changes in the K_a values in the temperature range from 17 to 47 °C. The results are given in Figure 3.16A. The results show an increase in K_a with a decrease in temperature. The free energy change, ΔG° at 27 °C, calculated from the association constant obtained from the slope of the curve, was -8.65 kcal mol⁻¹. The van't Hoff plot is given in Figure 3.16B. The ΔH° and ΔS° for the binding reaction were estimated to be -1.28 kcal mol⁻¹ and 24.7 cal mol⁻¹, respectively. The obtained thermodynamic parameters reveal that interaction is driven by an increase in entropy and that the enthalpy of binding is very small. A positive ΔS° value is taken as evidence for hydrophobic interaction (Ross and Subramanian, 1981). Curcumin remains un-ionized under the experimental conditions (pH 7.4, pKa value = 8.28).

Hence, electrostatic interactions can be excluded from the binding process. Therefore, hydrophobic interactions are largely responsible, as evidenced by thermodynamic measurements. Similar results have been reported for curcumin-human serum albumin (HSA) interactions (Reddy et al., 1999).

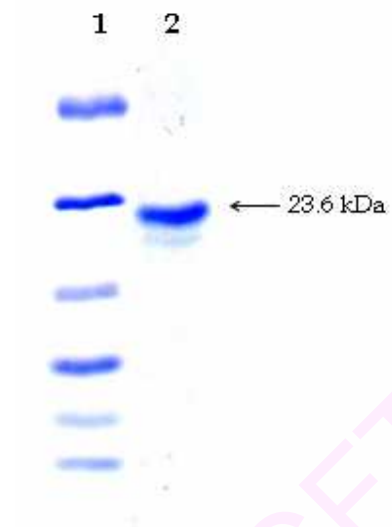


Figure 3.14. SDS PAGE representing the homogeneity of α_{s1} -casein. Molecular weight marker is shown in lane 1.

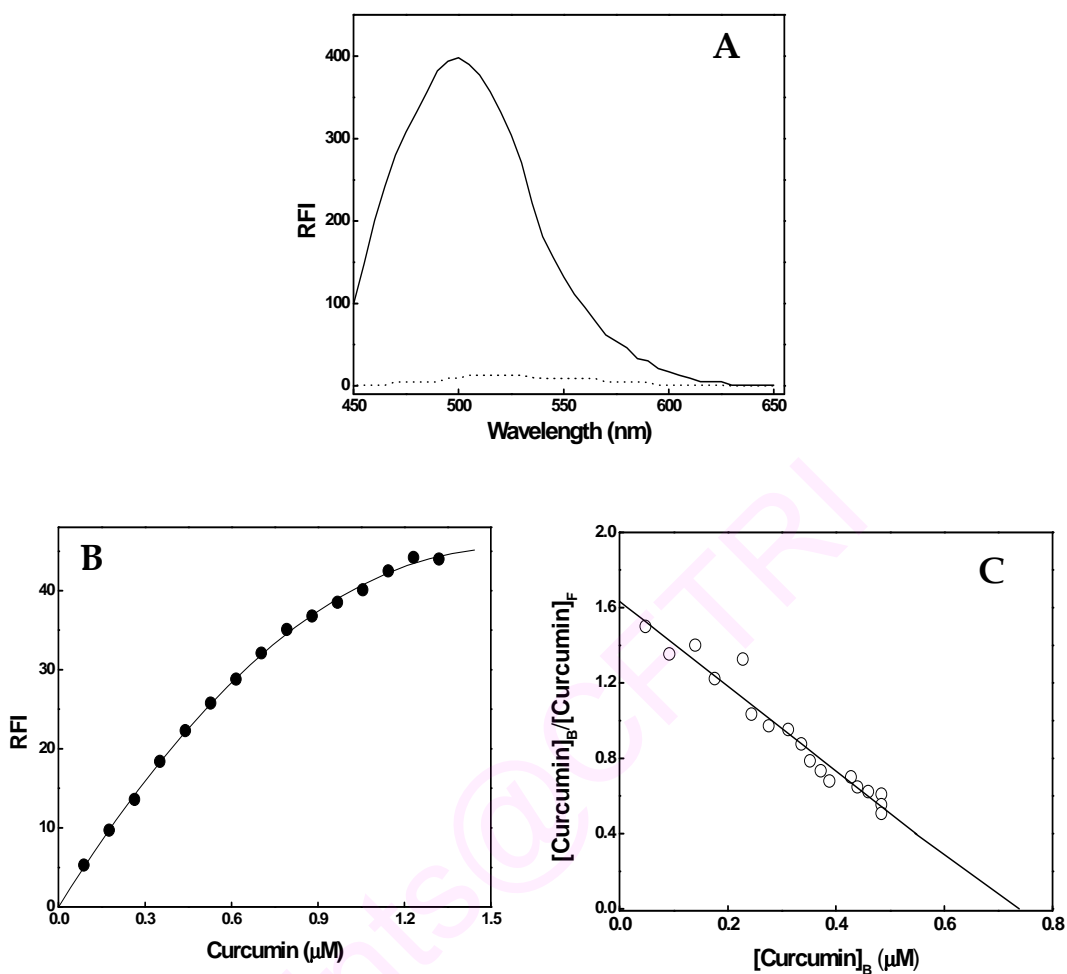


Figure 3.15. (A) Fluorescence spectra of 10 μM curcumin at pH 7.4 in the absence (...) and in the presence of 30 μM α_{S1} -casein (—). Excitation wavelength was 430 nm, Excitation and emission slit width were 5 and 10 nm, respectively. (B) Fluorescence enhancement of curcumin bound to α_{S1} -casein. 2 μL aliquot of curcumin from 0.11 mM stock in methanol was titrated against 3 μM α_{S1} -casein in 10 mM HEPES buffer, pH 7.4. Excitation wavelength is 430 nm and emission wavelength is 510 nm. (C) Scatchard plot for determining binding of curcumin to α_{S1} -casein.

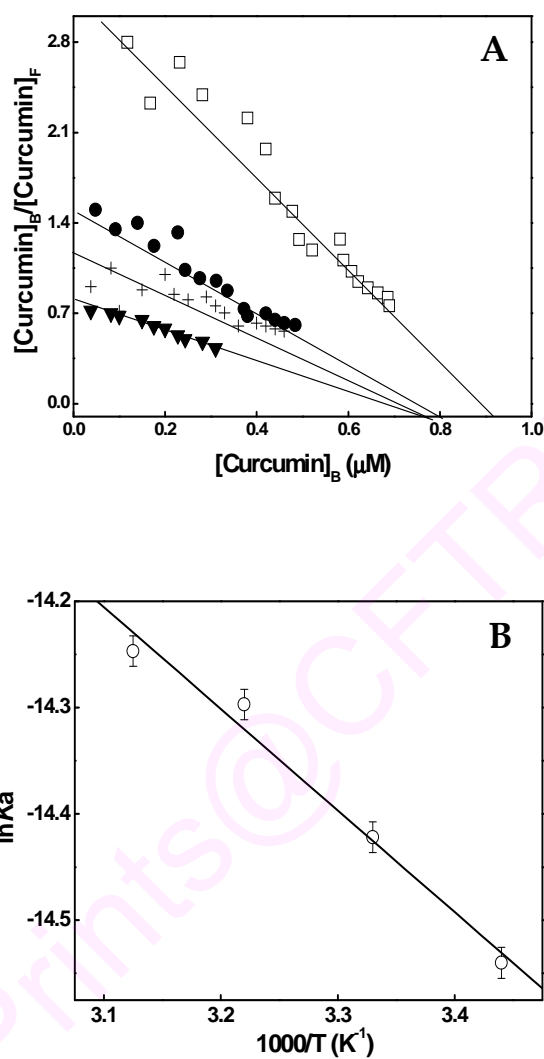


Figure 3.16. (A) Effect of temperature (-□-) 17 °C, (-●-) 27 °C, (-+-) 37 °C, (-▼-) 47 °C. (B) Variation of $\ln K_a$ for the formation of α_{S1} -casein curcumin complex monitored at 510 nm. Line plot indicates the fit according to van't Hoff Plot.

Circular Dichroism Measurements

Far-UV CD studies of α_{S1} -casein show no change in the secondary structure upon addition of curcumin, indicating the preservation of structure. Neither curcumin nor casein exhibits any CD band in the region of 340-500 nm. However, curcumin became optically active on binding to α_{S1} -casein, exhibiting CD bands in the region of 340-500 nm, suggesting the asymmetric environment of curcumin with the emergence of induced bands in the characteristic absorption region. The CD spectra of α_{S1} -casein in the presence of various concentrations of curcumin are given in Figure 3.17A. Addition of curcumin, in small increments, to α_{S1} -casein resulted in the appearance of two oppositely signed weak, extrinsic CD bands with a zero crossover point at 407 nm. The longer wavelength band at 442 nm was positive, whereas the shorter wavelength band, at 388 nm, was negative. The existence of two equal-intensity opposite bands is probably due to the excited state interaction called exciton coupling due to the mutual rotation caused by the two feruloyl moieties around the central methylene group (Berova et al., 1993).

Figure 3.17B shows the variation in the molar ellipticity value at 442 nm, as a function of curcumin concentration. The mass action plot is given in Figure 3.17C. The association constant was calculated to be $6.3 \pm 0.4 \times 10^4 \text{ M}^{-1}$. The above spectroscopic result indicates that curcumin binds to α_{S1} -casein at two different binding sites, characterized by association constants of $2.01 \pm 0.6 \times 10^6$ and $6.3 \pm 0.4 \times 10^4 \text{ M}^{-1}$. The two different association constants obtained indicate two binding sites on α_{S1} -casein, one saturated at 2 μM (from fluorescence data) and the other site saturated at 25 μM curcumin (from CD data). Curcumin has a β -diketone moiety, flanked by two phenolic groups, that helps it

bind to proteins through hydrophobic interactions. The carboxyl-terminal of α_{S1} -casein (100-199 residues) predominantly contains hydrophobic amino acids, which may be involved in the binding process. Residues 14-24 in α_{S1} -casein are hydrophobic in nature and form a surface "patch" of hydrophobicity capable of interacting with fluorescent probes in solution (Creamer et al., 1982). Curcumin may probably be binding at these two sites, with two different ranges of affinity through hydrophobic interaction.

ePrints@CFTRI

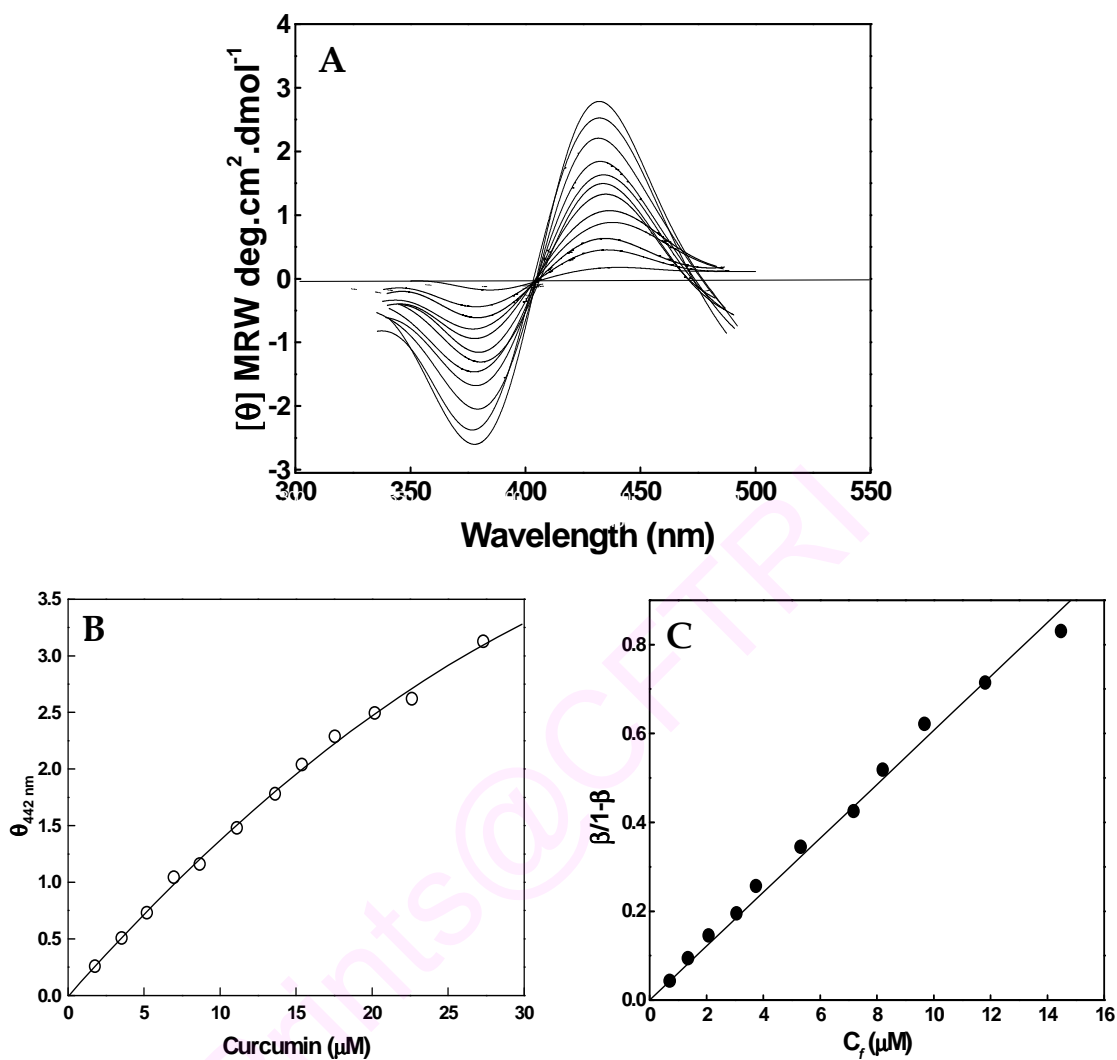


Figure 3.17. (A) Induced circular dichroism spectra of curcumin- α_{S1} -casein complex. α_{S1} -casein concentration in 10 mM HEPES buffer, pH 7.4. α_{S1} -Casein was titrated against 2 μL aliquots of 2.5 mM stock curcumin solution Curcumin concentrations were in the range of 2-25 μM . (B) Variation of ellipticity values at 442 nm as a function of curcumin concentration. (C) Plot of $\beta/1-\beta$ vs. C_f for α_{S1} -casein-curcumin complex.

Stability of α_{S1} -Casein Bound Curcumin

The stability of curcumin in solution was followed in 50 mM Tris buffer, pH 7.2. The improved stability of curcumin in the presence of α_{S1} -casein, BSA, and mixed PC micelles was followed by RP-HPLC. Curcumin in buffer undergoes rapid degradation when incubated at 30 °C. Figure 3.18 shows the HPLC pattern for the degradation of curcumin in buffer at zero time and 30 min. At zero time, a single peak is detected at 425 nm, with a retention time of 5.9 min. With progress in time; several small peaks are seen at lower retention times with concomitant decrease in the native curcumin peak at 5.9 min (Figure 3.18). About 90% of the curcumin is decomposed rapidly in buffer at the end of 30 min. At this pH, a proton is removed from the phenolic group, thereby leading to loss in the structure of curcumin molecule (Wang et al., 1997). Figure 3.19 shows the semilogarithmic plot of residual curcumin (%) versus time (min) under the various test conditions. In the presence of α_{S1} -casein, about 45% of curcumin remains undegraded at the end of 6 h of incubation. The half-life of curcumin was calculated from the graph, and the results are given in Table 3.4. Curcumin in buffer has a half-life of 8.8 min. In the presence of α_{S1} -casein, the half-life is increased ~ 39-fold to 340 min. The stability in the presence of BSA is similar to that in the presence of α_{S1} -casein. The maximum stability of curcumin is seen in the presence of mixed PC micelles (half-life = 2779 min). The structure of curcumin is protected in the presence of α_{S1} -casein, thus enhancing the stability of curcumin *in vitro*. Curcumin is reported to strongly bind at the hydrophobic moieties of HSA and fibrinogen, and this prevents its hydrolysis (Leung and Kee, 2009). Curcumin is relatively stable in the cell culture medium containing 10% fetal calf serum and in human blood (Wang et al., 1997).

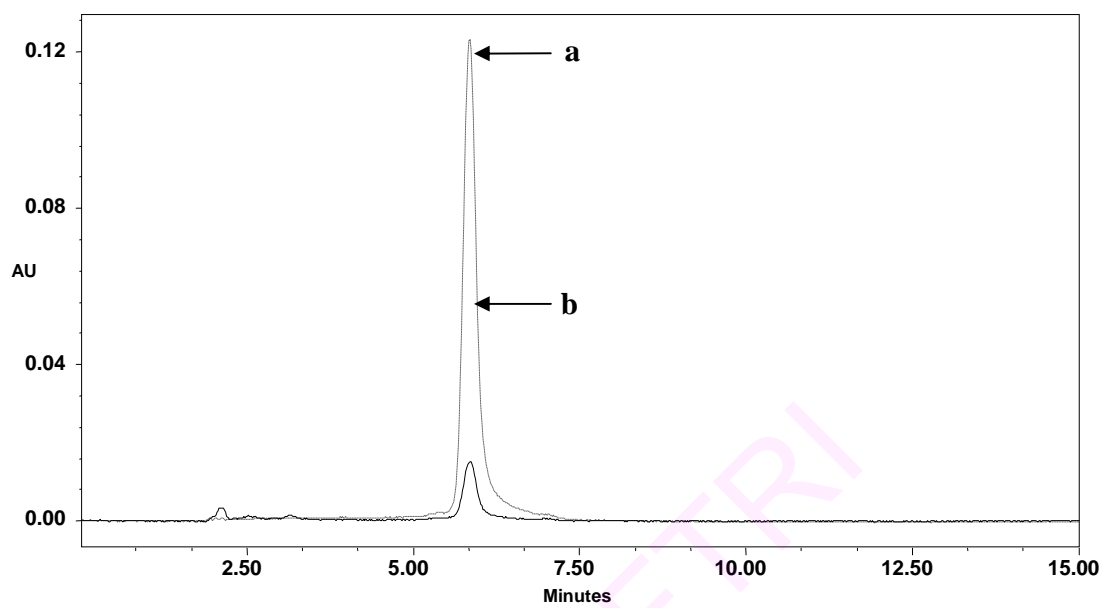


Figure 3.18. HPLC profile to show the curcumin in buffer (a) 0 min (b) degraded curcumin after 30 min.

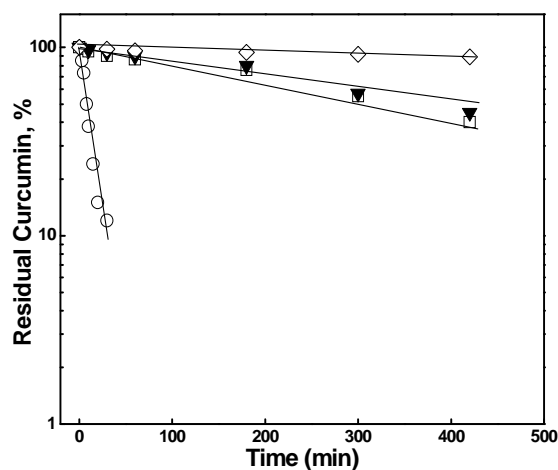


Figure 3.19. Semilogarithmic plot to ascertain the stability of curcumin in different media (-○-) Tris HCl, 50 mM, pH 7.2, (-□-) α_{S1} -casein, (-▼-) bovine serum albumin, (-◇-) mixed phosphatidylcholine micelles. The data are normalized to 100 at 0 time. The data points are fitted as first order linear regression and the rate constants (k) were calculated from the linear fit data.

Table 3.4. Half life ($t_{1/2}$) and rate constant (k) of curcumin in different solution condition

Curcumin medium*	Rate constant (k) ($\times 10^{-3} \text{ min}^{-1}$)	$t_{1/2}$ (min)	R	SD
Buffer	78.5	8.8	0.97	0.09
α_{S1} -Casein	2.04	340	0.99	0.02
BSA	1.86	373	0.99	0.02
Mixed PC micelles	0.25	2779	0.98	0.004

* Tris HCl buffer pH 7.2

Chaperone Activity

In vitro assay methods for molecular chaperone activity are generally followed by the prevention of thermal aggregation in substrate proteins. Previously, it has been reported that casein prevents the thermal aggregation of many substrate proteins by providing hydrophobic surfaces to the unfolding proteins (Bhattacharyya and Das, 1999). We have investigated the effect of curcumin binding on the chaperone activity of α_{S1} -casein. A solution of carbonic anhydrase or catalase is used as substrate protein. On heating, the solution becomes turbid, indicating the formation of aggregates. Figure 3.20A and 3.20B shows the kinetic traces of the apparent absorbance of carbonic anhydrase and catalase, at 400 nm, in the presence of α_{S1} -casein. As revealed from the figure, the chaperone activity of α_{S1} -casein is enhanced. Curcumin alone does not prevent aggregation of carbonic anhydrase or catalase. The concentration of casein was limited to prevent aggregation by ~40-50%. With the addition of 7.5 or 15 μM curcumin to form the curcumin- α_{S1} -casein complex, decreases in aggregation by 11 ± 1 and $22 \pm 2\%$, respectively, of carbonic anhydrase, were seen. The presence of 7.5 or 15 μM curcumin in the curcumin- α_{S1} -casein complex resulted in protection against aggregation of catalase by 12 ± 1 and $20 \pm 1\%$, respectively.

Curcumin may provide more hydrophobic surface, favoring the interaction of α_{S1} -casein to the partially unfolded proteins through its solvent-exposed hydrophobic surfaces. Kumar et al. (2005) has reported the modulation of chaperone activity of α -crystallin by curcumin in diabetic rat lens. Curcumin, a powerful antioxidant, is reported as a strong inducer of the heat shock response (Calabrese et al., 2003). In the concentration range of 3-10 μM , curcumin acts as a co-inducer for heat shock proteins (Ohtsuka, 2005).

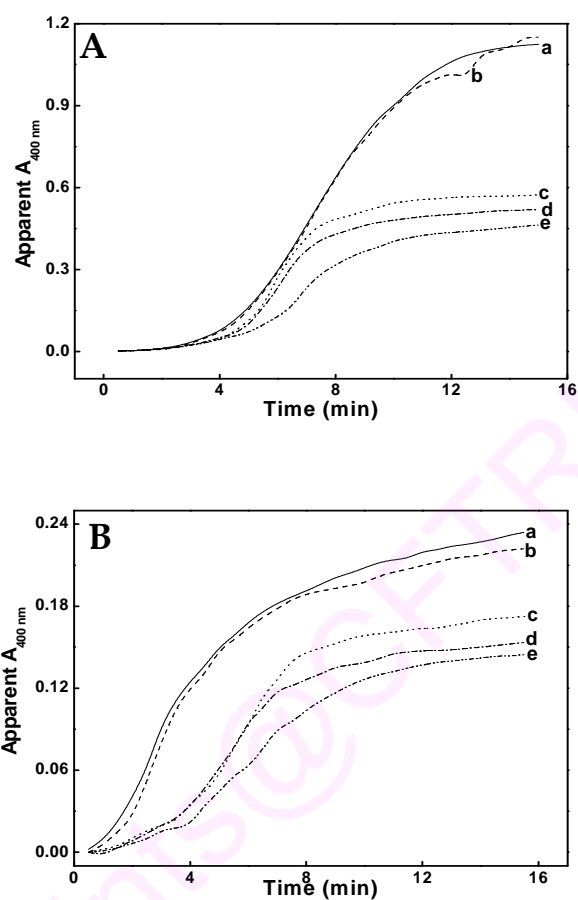


Figure 3.20. Thermal aggregation assay (A) (a) carbonic anhydrase (0.22 mg/mL), (b) carbonic anhydrase and curcumin (15 μ M), (c) carbonic anhydrase and α_{S1} -casein (0.15 mg/mL), (d) carbonic anhydrase, α_{S1} -casein and curcumin (7.5 μ M), (e) carbonic anhydrase, α_{S1} -casein and curcumin (15 μ M). (B) (a) catalase (1 mg/mL), (b) catalase and curcumin (15 μ M), (c) catalase and α_{S1} -casein (0.2 mg/mL), (d) catalase, α_{S1} -casein and curcumin (7.5 μ M), (e) catalase, α_{S1} -casein and curcumin (15 μ M). Values are the means of triplicates.

Inhibition of Hemolysis by α_{S1} -Casein Bound Curcumin

Erythrocytes have been used as a model to investigate oxidative damage in biomembranes, due to their susceptibility to free radical mediated peroxidation (Liu and Ng, 2000). Erythrocyte hemolysis is initiated by AAPH, a water-soluble azo compound, which is a peroxy radical initiator that generates free radicals by itself, decomposing to alkyl radicals, at physiological temperature. In this study, the biological property of curcumin, in preventing hemolysis, after binding to α_{S1} -casein was investigated. The inhibitory effect of curcumin is shown in Figure 3.21. About 30% inhibition of hemolysis is seen when 10 μ M curcumin alone is used. α_{S1} -Casein (10 μ M), by itself, also shows 25% inhibition toward AAPH-induced RBC hemolysis by an unknown mechanism. On binding of curcumin to α_{S1} -casein, the inhibition is 57%. The above result indicates the additive effect in protecting hemolysis. On the binding of curcumin to α_{S1} -casein, the antioxidant property of curcumin is retained. Curcumin and α_{S1} -casein independently contribute to antihemolysis action. Curcumin is a known inhibitor of free radical-induced hemolysis of RBC (Deng et al., 2006). Curcumin *per se* either scavenges the free radicals or may induce the endogenous antioxidant enzymes promoting the inhibition of hemolysis (Reddy and Lokesh, 1994c).

In conclusion, curcumin binds to α_{S1} -casein with two binding sites, one with high affinity and one with low affinity and binding is predominantly hydrophobic. The stability of curcumin is enhanced due to interaction. The chaperone-like activity of α_{S1} -casein is slightly enhanced on binding to curcumin. The inhibition of hemolytic activity by curcumin is not affected.

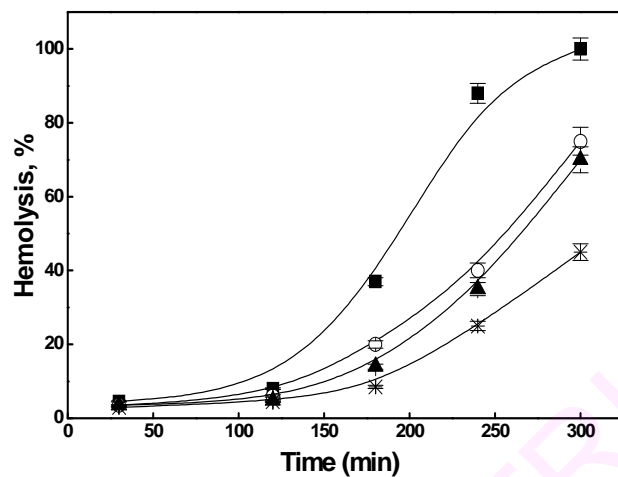


Figure 3.21. Inhibition of AAPH-induced hemolysis of erythrocytes by curcumin and α_{S1} -casein bound curcumin. 50 mM AAPH (-■-), 10 μ M α_{S1} -casein (-○-), 10 μ M curcumin (-▲-), 10 μ M each of α_{S1} -casein and curcumin (-×-). Data points are expressed as means (\pm SE) of triplicates.

Encapsulation of Curcumin in α_{S1} -Casein Nanoparticle

Casein, the major milk protein, has excellent emulsification and water holding capacity. Microspheres of casein prepared by crosslinking with glutaraldehyde have been used for the oral delivery of anticancer drugs such as doxorubicin, mitoxantrone (Willmott et al., 1992; Knepp et al., 1993). Purified α_{S1} -casein protein nanoparticles were prepared by cross linking with glutaraldehyde. The particles were less polydispersed as revealed from SEM measurements. The morphology of the prepared nanoparticles of α_{S1} -casein alone and with curcumin is represented in Figure 3.22A and 3.22B. Average size of the particles was $\sim 166 \pm 5$ nm. The graphical representation of size distribution of particles is illustrated in Figure 3.22C. The structure of casein micelles in milk has an average size distribution of < 200 nm (Sahu et al., 2008). Physical, morphological properties, solubility and release kinetics of curcumin encapsulated in α_{S1} -casein nanoparticle is tabulated in Table 3.5.

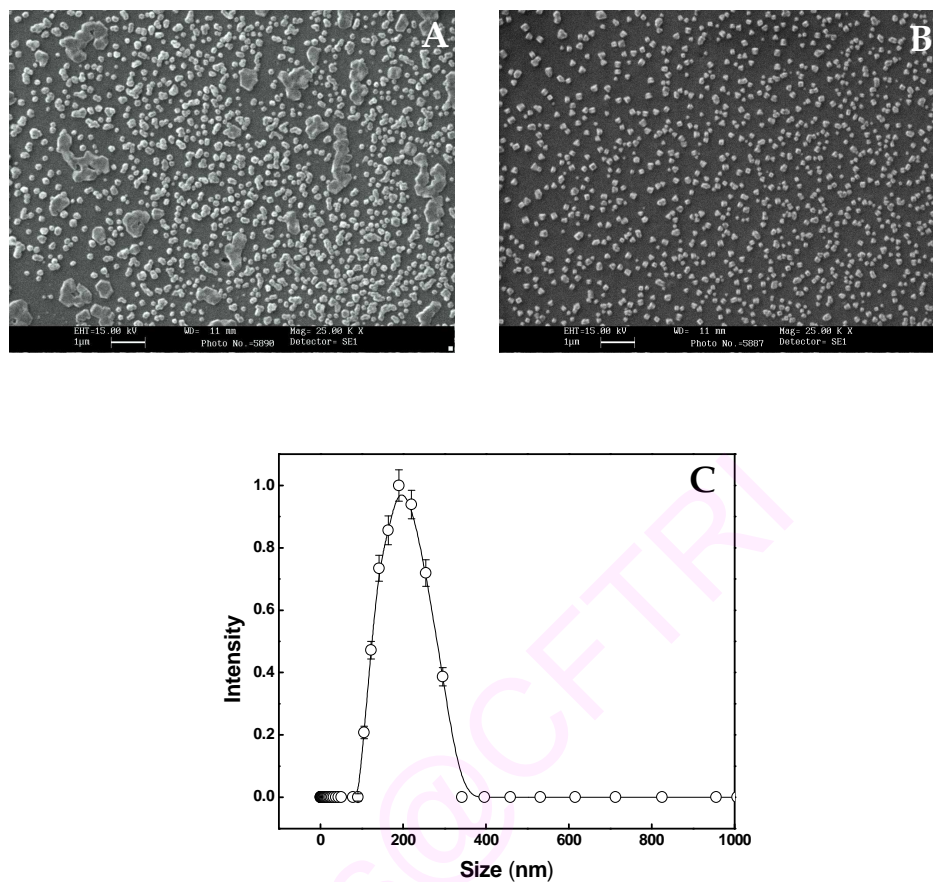


Figure 3.22. Scanning electron microscopic photograph of (A) α_{S1} -casein nanoparticle and, (B) α_{S1} -casein nanoparticle loaded with curcumin. The sample was vacuum dried, coated with gold before viewing under microscope. (C) Graphical representation of particle size distribution of curcumin encapsulated in α_{S1} -casein nanoparticle at pH 7.0. Average size of particles was $\sim 166 \pm 5$ nm. Similar results were obtained with α_{S1} -casein nanoparticle. The error bars represents the mean and standard deviation of experiments in duplicate.

Encapsulation of Curcumin in Human Serum Albumin Nanoparticle

Serum albumin is the main component of blood with concentration up to ~5 g/100 mL. It is a widely investigated protein, due its ability to bind reversibly and selectively, an incredible variety of insoluble, bioactive endogenous and exogenous compounds. It is a principal carrier of fatty acids and it functions as a transport protein for variety of drugs. Due to its availability and biodegradable nature, albumin nanoparticles were prepared to check for its drug transportation property. Albumin nanoparticle is widely prepared as a drug carrier for various compounds like aspirin, apolipoprotein A1 and B100, ciprofloxacin, loperamide (Das et al., 2005; Kreuter et al., 2007; Kumar and Jain, 2007; Michaelis et al., 2006).

The HSA nanoparticles were prepared by desolvation and cross linked using glutaraldehyde. Curcumin was added after dispersing HSA nanoparticles in water and allowed to equilibrate. The morphological analysis was made using SEM and size of the particles were measured using DLS (Figure 3.23A, 3.23B & 3.23C). The particle size was around 239 ± 10 nm, with the shape being spherical. Langer et al., (2003) reported similar results for the preparation of HSA nanoparticles. HSA nanoparticles encapsulated about 56% of curcumin and released ~66% curcumin in 24 h, at pH 7.0 (Figure 3.24).

To conclude the properties of the above explained nanoparticles, the surface charge on β LG was more -ve and therefore, β LG NPs were smaller in size and exhibited slower release of curcumin, when compared with α_{S1} -casein and HSA system. In HSA, initial curcumin release was rapid and burst type, followed by diffusion. In β LG, initial release of curcumin was slow. At acidic pH, there was no release of curcumin from β LG NP, whereas α_{S1} -casein and HSA NPs released curcumin. At higher pH, release of curcumin

from β LG NP was good α_{S1} -casein and HSA NPs are easily digestible and is expected to release the bound substrate in the stomach. β LG may offer a choice of carrier system in intestine.

Concentration of protein and ligand affects the encapsulation efficiency as reported by Somchue et al. (2009). To prolong the release of α -tocopherol in simulated intestinal conditions, coating with alginate was carried out as there was immediate release of α -tocopherol in simulated gastric condition (Somchue et al., 2009). Nano-curcumin formulation synthesized by Maitra group (Bisht et al., 2007) has shown about > 90% entrapment efficiency and ~40% release of curcumin from the copolymer (NIPAAM/VP/PEG-A: NIPAAM = N-isopropylacrylamide; VP = N-vinyl-2-pyrrolidone (VP); PEG-A = poly (ethyleneglycol)monoacrylate) in 24 h at physiological pH. Nearly 51% of curcumin is released from the alginate-chitosan-pluronic acid composite particles under neutral pH conditions. The release kinetics in this case obeys the power law with the 'anomalous transport' being the release mechanism (Das et al., 2010). The solubility of curcumin encapsulated in HSA, α_{S1} -casein and β LG nanoparticles and *in vitro* release of curcumin from these nanoparticles have been studied. The comparative parameters like physical, morphological properties, solubility and release kinetics of curcumin encapsulated in different protein nanoparticles are tabulated in Table 3.5.

A major advantage of using nanoparticle for the delivery of nutraceuticals is their ability to control the release of the incorporated material and deliver them to the required site. This can be achieved by formulating the desired structure and controlling the particle size. Larger particles generally release encapsulated compounds more slowly and over

longer period of time. Reduction in particle size results in increased adhesive force and prolonged transit time, leading to higher bioavailability of bioactives.

Carrier systems allow hydrophobic compounds to be thermodynamically stable in aqueous solution for oral drug delivery applications. Carriers prolong the residence time of the compound in the gut & therefore increase the time during which absorption occurs. These carrier systems may serve as effective oral delivery nanovehicles for solubilization and stabilization of curcumin.

In addition to being a vital nutrient in food, protein possesses many functional properties like emulsification, gelation, foaming, and water binding capacity which makes it a good coating material for the encapsulation of bioactive compounds.

β LG is resistant to pepsin but is completely degraded by pancreatin, leading to the complete release of bioactive compounds. Thus β LG form good matrices to carry and protect fat soluble compounds *in vivo* at intestinal sites.

Food proteins show great promise for developing and engineering a range of new GRAS matrices with the potential to incorporate nutraceutical compounds and provide controlled release *via* the oral route. Advantages of food protein matrices include their high nutritional value, abundant renewable sources, and acceptability as naturally occurring food components degradable by digestive enzymes.

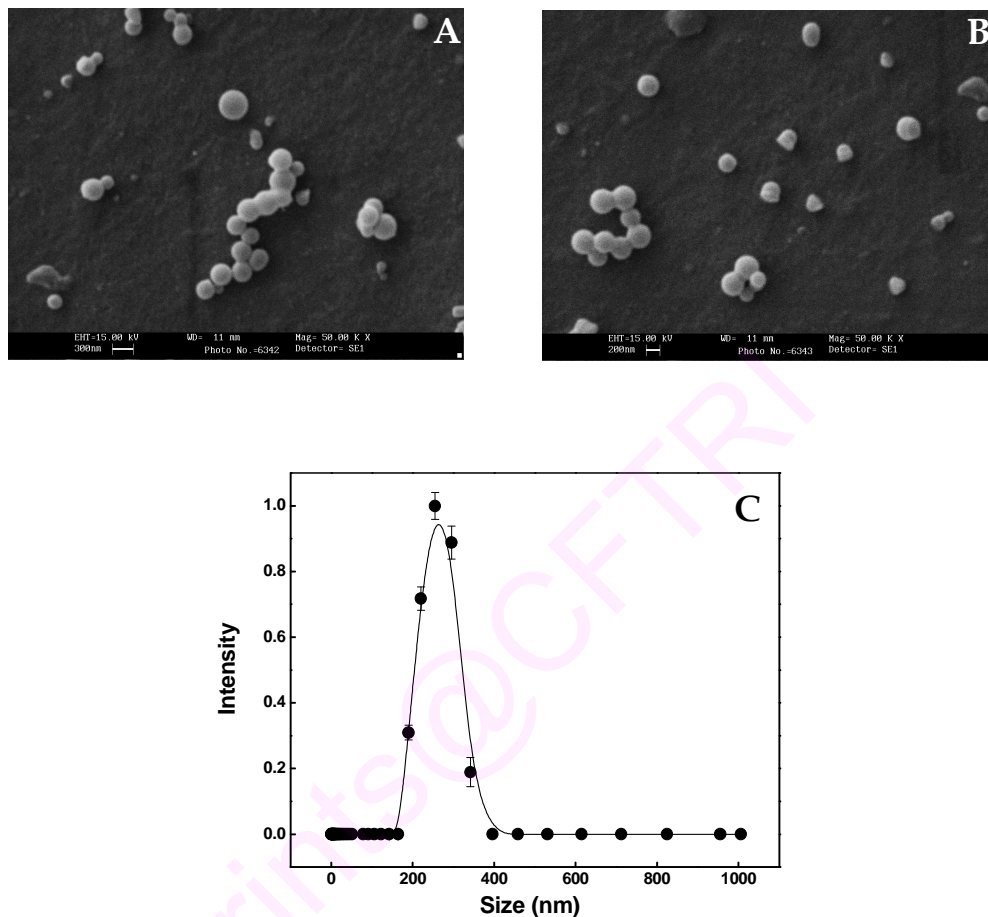


Figure 3.23. Scanning electron microscopic photograph of (A) HSA nanoparticle and (B) HSA nanoparticle loaded with curcumin. The sample was vacuum dried, coated with gold before viewing under microscope. (C) Graphical representation of particle size distribution of curcumin encapsulated in HSA nanoparticle at pH 7.0. Average size of particles was 239 ± 10 nm. Similar results were obtained with HSA nanoparticle. The error bars represents the mean and standard deviation of experiments in duplicate.

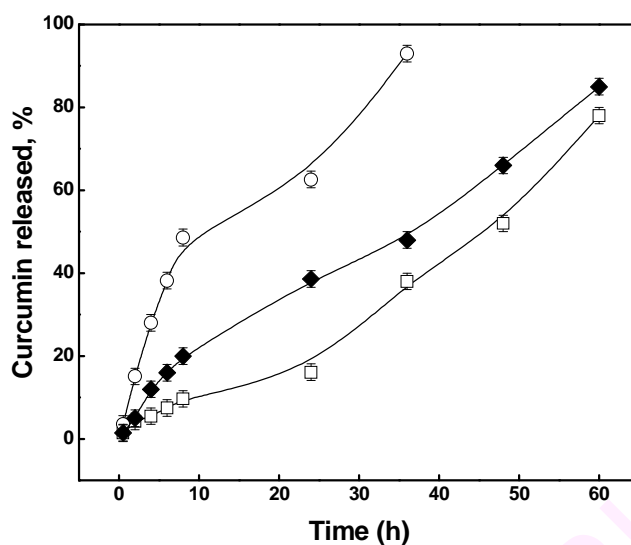


Figure 3.24. *In vitro* release kinetics of curcumin from (—○—) HSA, (—◆—) α_{S1} -casein and (—□—) β LG at pH 7.0.

Table 3.5. Comparative physical, morphological properties, solubility and release kinetics of curcumin encapsulated in different protein nanoparticles.

	HSA	α_{S1} -Casein	β LG
Average size, nm	$\sim 239 \pm 10$	$\sim 166 \pm 5$	$\sim 141 \pm 5$
Zeta potential, ζ (mV)	-25.7	-20	-31.3
Encapsulation efficiency, E	> 56%	> 94%	> 96%
Solubility/10 mg mL ⁻¹ nanoparticle, mM	~ 0.2	~ 0.62	~ 0.625
<i>In vitro</i> release of curcumin at pH 7.0 (24 h)	66 %	38 %	16 %
<i>In vitro</i> release of curcumin at pH 2.0 (48 h)	89%	68%	No release
Kinetics	Zero order	Zero order	Zero order
Release constant, <i>k</i>	2.15	1.43	1.17
Correlation coefficient, R	0.94	0.99	0.97

Apparent Solubility of Curcumin in Mixed PC Micelles, HSA, β LG and α_{S1} -Casein

Apparent solubility of curcumin in the presence of PC micelles, HSA, α_{S1} -casein and β LG proteins as a function of temperature was determined and is plotted in Figure 3.25. The Y- intercept on the plot of log mole fraction solubility versus the temperature gives the apparent solubility and the results are tabulated in Table 3.6. The solubility of curcumin in these different conditions are PC micelles > HSA > α_{S1} -casein > β LG. The results infer that the solubility of curcumin depends on the hydrophobicity of the environment and the solubility of curcumin increases with the hydrophobicity.

ePrints@CFTRI

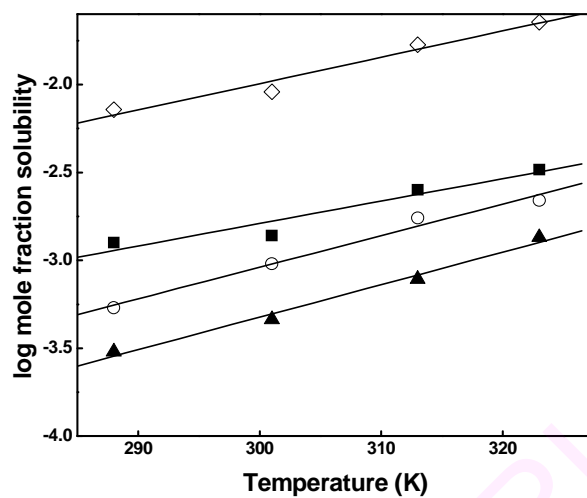


Figure 3.25. Plot to calculate the apparent solubility of curcumin as a function of temperature in the presence of mixed PC micelles ($-\diamond-$), HSA ($-\blacksquare-$), α_{S1} -casein ($-\circ-$) and β LG ($-\blacktriangle-$). The Y-intercept gives the apparent solubility of curcumin.

Table 3.6. Apparent solubility of curcumin (mM) in different media

Curcumin medium	Apparent solubility (mM)
Mixed PC micelles	6.03
HSA	1.05
α_{S1} -Casein	0.5
β LG	0.23

3.1.3. Curcumin as a Tool to Assess the Surface Hydrophobicity of Proteins

Proteins contain both hydrophilic and hydrophobic side chain residues. Because of the specific folding pattern of each protein, some hydrophobic residues may be buried in the interior, while others may be exposed at the surface. Hydrophobic interactions in proteins play an important role in dictating the conformation, solubility, ligand binding, aggregating properties and so on. Hydrophobic interactions in proteins have a major role in mediating protein-protein interactions. Among various methods to quantify surface hydrophobicity of proteins, one approach is the fluorescent probe method. The quantum yields and wavelength of maximum fluorescence emission of probes depend on the polarity of their environment (Li-Chan, 1999). Several fluorescent probes such as 1-anilinonaphthalene-8-sulfonic acid and *cis*-parinaric acid have been widely used to measure the protein surface hydrophobicity. These probes have low quantum yield of fluorescence in aqueous solution. Upon binding to accessible hydrophobic regions on proteins, an increase in fluorescence is observed, which is used as a measure of protein surface hydrophobicity. Due to high sensitivity, noninvasiveness and availability of imaging techniques, fluorescence technique has been considered to be one of the most promising and widely used technique. Fluorescence property of curcumin gets enhanced, when it comes in contact with hydrophobic surface. This has been confirmed by its interaction with lipids and proteins (Began et al., 1999; Kunwar et al., 2006). Based on these observations, the possible use of curcumin as a fluorescent probe to assess the surface hydrophobicity of proteins was evaluated. This was achieved by determining the surface hydrophobicity with different proteins by two methods. They are, (i) by calculating the initial slope (S_0) of fluorescence intensity vs. protein concentration - a plot

used as an index of the protein hydrophobicity (Kato and Nakai, 1980) (ii) by analyzing the association constant for curcumin with different proteins (Cardamone and Puri, 1992). Cardamone and Puri (1992) measured the binding constant with ANS and has reported that the binding constant of proteins decreases with the S_0 .

Change in Curcumin Fluorescence after Binding of Curcumin to BSA, β LG, α_{S1} - Casein, Soy LOX-1, Ovalbumin and Lysozyme

The binding of apolar compound curcumin to protein is associated with an enhanced fluorescence and a blue shift in the wavelength of peak emission as illustrated in the Figure 3.26. The change in curcumin fluorescence was of sufficient magnitude to evaluate the association constant for each protein-curcumin interaction. The changes in the emission maximum, association constant and the effective surface hydrophobicity are tabulated in Table 3.7.

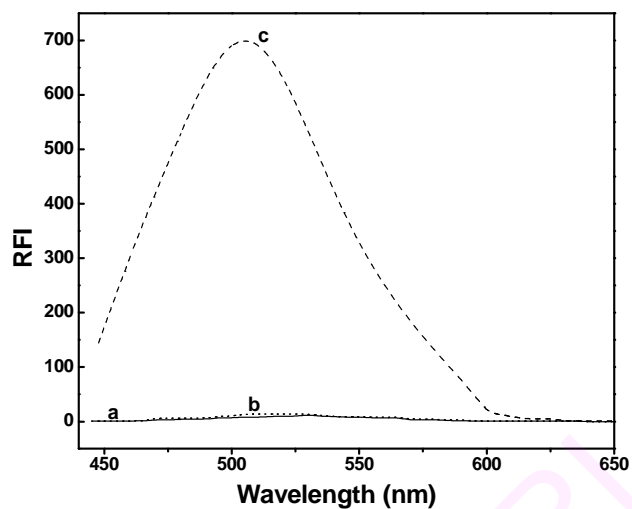


Figure 3.26. Enhancement of curcumin fluorescence, (a) The fluorescence emission spectra of 5 μM curcumin in 50 mM Tris-HCl, pH 7.4 (b) 5 μM curcumin added to lysozyme (0.1 mg/mL) (c) 5 μM curcumin added to BSA (0.1 mg/mL). Excitation wavelength was 430 nm and the slit widths were 5 and 10 nm. Curcumin in aqueous solution has an emission maximum around ~ 530 nm. After binding to BSA there is a great enhancement in the fluorescence intensity with blue shift in the emission maximum from ~ 530 to 500 nm. By contrast, the change in the fluorescence of curcumin after binding to lysozyme was not observed. Spectra were recorded at 25 $^{\circ}\text{C}$.

Table 3.7. Comparison of the curcumin emission maximum, association constant (25 °C) and surface hydrophobicity with different proteins.

Protein	Emission maxima (nm)	K_a (M^{-1})[†]	S_0	n
BSA	500	2.6×10^6	843	2
α_{S1}-Casein	510	2×10^6	680	2
βLG	505	1.0×10^5	558	1
Soy LOX-1	505	5.8×10^4	456	1
Ovalbumin	510	4.2×10^3	149	1
Lysozyme	~530	-	-	-

[†] Association constant derived from Scatchard plot

^{||} Surface hydrophobicity (S_0) as defined by Kato and Nakai (1980)

n - Binding sites

The association constant and surface hydrophobicity could not be determined with lysozyme since there was no perceptible enhancement in the fluorescence of curcumin.

Therefore, it is taken as negative control.

Table 3.8. Comparison of the ANS emission maximum, association constant and average hydrophobicity with different proteins

Protein	Emission maximum (nm)	Association constant (M ⁻¹)	Average hydrophobicity
Bacteriorhodopsin	466	9.21×10 ⁵	1120
BSA	471	8.2×10 ⁵	1000
PST	480	1.78×10 ⁵	994
Ovalbumin	485	7.57×10 ⁵	980
Lysozyme	480	7.69×10 ⁴	890
RNAase	519	1.25×10 ⁴	780
BLG*		4.7×10 ⁵	
Soy LOX-1†	475	2.3×10 ⁴	1149
α _{S1} -Casein‡	500	1.8×10 ⁴	1170

Values taken from Cardamone and Puri (1992)

* Sawyer and Kontopidis (2000)

† Sudharshan and Rao (1997)

‡ K_a value is taken from present study, Average hydrophobicity as measured by Bigelow (1967).

Table 3.9. Surface hydrophobicity of different proteins determined using *cis*-parinaric acid

Protein	S ₀
BSA	1400
βLG	750
k-Casein	1300
Trypsin	90
Ovalbumin	60
Conalbumin	70
Lysozyme	100
α-Chymotrypsin	40

Kato and Nakai (1980)

Two different fluorimetric approaches to determine the surface hydrophobicity parameter, namely the slope method and determination of binding constant were used to determine the S_0 . The S_0 and K_a followed relatively, the same order. The K_a at 25 °C of curcumin-protein complexes were calculated for the various proteins using Scatchard plot. BSA appears to be the most hydrophobic among the selected proteins with higher value of K_a and S_0 followed by α_{S1} -casein, β LG, soy LOX-1 and ovalbumin with median and lower K_a and S_0 . Lysozyme was least hydrophobic and on addition of curcumin, fluorescence enhancement in the curcumin emission region was not found. For comparison, surface hydrophobicity values for different proteins published by different groups are tabulated in Table 3.8 and 3.9.

Effect of Urea

Surface hydrophobicity of proteins undergoes changes with unfolding. Therefore, surface hydrophobicity for proteins using the fluorescent probe-curcumin, as a function of increasing concentration of urea was calculated. BSA was chosen as a representative example and is depicted in Figure 3.27. In the presence of urea, surface hydrophobicity increased up to 3 M of urea concentration and then decreased. The initial increase in surface hydrophobicity with increase in urea concentration can be ascribed to the availability of newly exposed sites on the surface of BSA. The subsequent decrease in surface hydrophobicity could be due the disruption of binding site for curcumin, due to extensive unfolding of the protein molecule. The disruption of the curcumin binding hydrophobic cleft results in change in the polarity of bound curcumin, which was accompanied by red shift in the emission maximum. Fluorescence quantum yield of

ANS is known to be reduced as its environment polarity is increased (Stryer, 1965). Similar trend was observed for all other proteins.

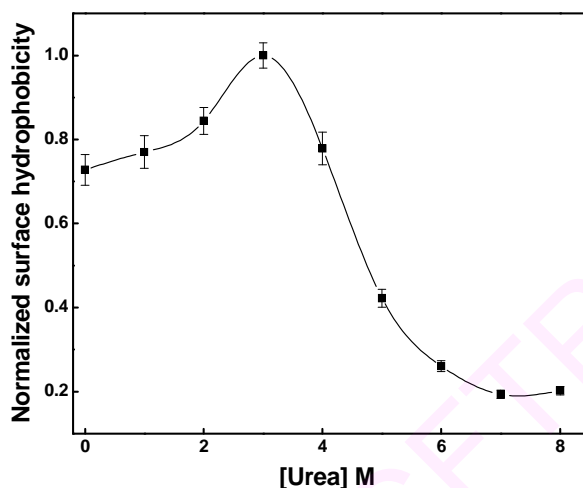


Figure 3.27. Effect of urea on the surface hydrophobicity of BSA. The plot of normalized surface hydrophobicity versus the concentration of urea. Excitation wavelength was 430 nm and emission readings were recorded at 500 nm with the slit width of 5 and 10 nm. Readings were corrected for blank contributions from urea and curcumin.

Attempts have been made to analyze the fluorescence property of curcumin for its use as a surface hydrophobic probe. Curcumin is a non-fluorescent molecule in aqueous solutions and becomes fluorescent in apolar/hydrophobic environment. A marked enhancement in the curcumin fluorescence property after binding to BSA was observed: however, there was no significant increase in curcumin fluorescence after interaction with lysozyme as suggested from the K_a and S_0 . The difference in behavior of curcumin presumably reflects the differences in surface hydrophobicity of these proteins, particularly the lack of suitable hydrophobic 'clefts' for curcumin binding.

In summary, the results presented here demonstrate that curcumin binding and the resultant K_a and S_0 may be used to get the preliminary idea on relative surface hydrophobicity of proteins. Because of low quantum yield of curcumin compared to ANS and CPA, curcumin may not be an appropriate fluorescent probe to use for measuring the S_0 of proteins. Along with the other well established procedures/probes for determining the surface hydrophobicity, curcumin can also be used to measure the surface hydrophobicity as a supplementary method.

ePrints@CFTRI

Inhibition and Interaction of CPA with Soy LOX-1

Fatty acids with conjugated double bonds occur naturally (Solodovnik, 1967) and recently there has been great interest in exploring the biological properties. Conjugated fatty acids are proposed to possess anti-atherosclerotic effect, induce immune response and modulate energy metabolism (Banni and Martin, 1998; Pariza et al., 2000; Scimeca et al., 1994; Solodovnik, 1967; Yurawecz et al., 1999). The other facet of conjugated fatty acids is its use as fluorescent probe for studying the membrane structure (Sklar et al., 1975). CPA is a C₁₈ fluorescent fatty acid and its fluorescent property is attributed to the presence of 4 conjugated π -electron bonds. Sklar et al. (1975, 1976, 1977a and 1977b) demonstrated that parinaric acid (9Z, 11E, 13E, 15Z-octadecatetraenoic acid) can be used to detect phase transitions in bilayers and to study the interactions among lipids and proteins (Comfort and Howell, 2002). This is due to the hydrophobic nature of CPA, which is similar to the other lipid membrane components and the similarity in the physical characteristics with other fatty acids. CPA is used for detecting the initial stages in the lipid peroxidation of membranes as its fluorescence property is lost upon oxidation (Kuypers et al., 1987). CPA can be incorporated into phospholipids by lipid biosynthetic pathways and spectroscopic investigations can be performed resulting with its wide use as a membrane probe.

Due to the structural similarity with the fatty acid, ability of CPA to inhibit LOX-1 was investigated. This was carried out by investigating the *in vitro* inhibition of LOX-1 with CPA. With increasing concentration of CPA, LOX-1 activity decreased as shown in Figure 3.28A. The residual activity of LOX-1 was checked in the presence of CPA. The concentration at which 50% inhibition (IC_{50}) occurred was 15.8 μ M (Figure 3.28B).

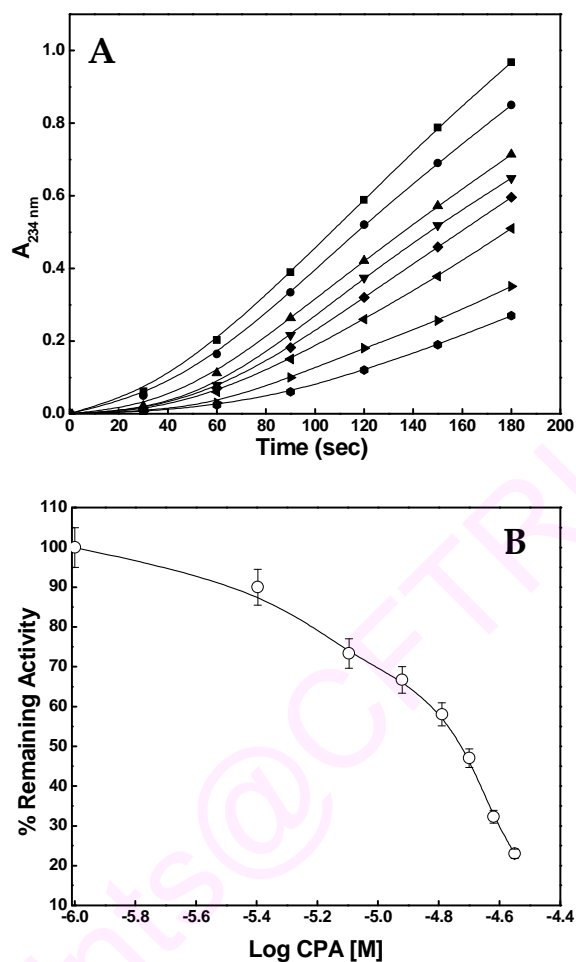


Figure 3.28. (A) Time course of LOX-1 catalyzed reaction in the presence of CPA. Aliquots of CPA were added from CPA stock solution (6 mM in ethanol) to buffer containing LOX-1, (—■—) 0, (—●—) 2, (—▲—) 5, (—▼—) 7.2, (—◆—) 10.3, (—◀—) 14, (—▶—) 21 and (—●—) 25 μM . The linoleic acid substrate was added and the assay at 234 nm was carried out for 3 min. The reference cuvette contained all the components except the substrate. The total volume of the reaction mixture is 3 mL. (B) Determination of IC_{50} value of CPA for inhibition of LOX-1. Values are average of three different sets of experiment.

Kinetics of Inhibition of LOX-1 by CPA

The kinetics for inhibition of LOX-1 by CPA has been evaluated. The type of inhibition was competitive as deduced from Lineweaver-Burk plot and is represented in Figure 3.29A. The K_i value of CPA for inhibition of LOX-1 was 9.8 μM obtained from replot of Lineweaver-Burk plot and the Dixon plot (Figure 3.29B and 3.29C). There was no decrease in the fluorescence under the experimental conditions, when excited at 320 nm indicating that CPA was not getting oxidized.

Molecular docking studies provided insight for the nature and mode of binding of CPA to LOX. Figure 3.30A shows the docking of CPA to the ribbon model of LOX-3 (PDB ID: 1JNQ). CPA binds close to iron cofactor with the distance of carboxylate group of CPA to the iron being 3.3 Å. Figure 3.30B shows the amino acids closer to the CPA and the amino acids within 2.5 Å distance from the CPA are His518, His523, Ala524, Ala561, Ser564, Ser281, Leu277, Leu560, Leu520, Leu515, Gln514, Val566 and Ile572.

Oleate (9Z-octadecenoic acid), a C_{18} fatty acid lacks 1, 4 pentadiene system of linoleate and is reported to be a competitive inhibitor of lipoxygenase. Due to the similarity in the structure with linoleic acid, oleate binds to the linoleate binding site. The K_i value for oleate inhibited reaction was $22 \pm 2 \mu\text{M}$ (van der Heijdt et al., 1995). Since 1965, there are many reports exploring the possibility of the triple bond analogues of polyunsaturated fatty acids as the inhibitors and inactivators of lipoxygenase (Blain & Shearer, 1965; Shieh et al., 1985; Nieuwenhuizen et al., 1995). Shieh et al. (1985) found that lipoxygenase converted 11Z-eicosa-11-en-14-ynoic acid (EEYA) into 11-hydroperoxy-12E-eicosa-12-en-14-ynoic acid (11-HP-EEYA) and 11-oxo-12E-eicosa-12-en-14-ynoic acid (11-oxo-EEYA). The product 11-HP-EEYA decomposed nonenzymatically into 11-oxo-

EEYA. Octadeca- 9,12-diyynoic acid (ODYA) inhibits active lipoxygenase by itself getting oxidized to 11- oxooctadeca-9,12-diyynoic acid (11-oxo-ODYA) (Nieuwenhuizen et al., 1995).

Effect of two synthetic fatty acids - 9Z-octadecenyl sulfate (OS) and 9Z-palmitoleyl sulfate (PS) were studied on the soy LOX-1 by Ruddat et al., (2003). OS inhibited LOX-1 and 15-human lipoxygenase by allosteric mechanism (Ruddat et al., 2003; Mogul et al., 2000). OS is similar in size to linoleic acid, the natural substrate of soy LOX-1, however linoleic acid binds to catalytic site, while, OS binds to allosteric site. PS acts as competitive inhibitor versus the product 13-hydroperoxy-9,11-(Z,E)-octadecadienoic acid, with a K_i of $17.5 \pm 3.8 \mu\text{M}$. The authors concluded that the presence of an allosteric site was significant with regard to the design of lipoxygenase inhibitors, since it may open the possibility of a new class of inhibitors (Ruddat et al., 2003). Anacardic acid (C15:1; 6[8'(Z)-Pentadecenyl]salicylic acid), is a competitive inhibitor soy LOX-1 with an IC_{50} value of $6.8 \mu\text{M}$ and K_i value of $2.8 \mu\text{M}$. The inhibition was due to the presence of alkenyl side chain (Ha and Isao, 2005). Therefore, CPA with low IC_{50} value may be included under the class of analogues of LOX inhibitors.

The emission spectra of CPA in the presence of different concentration of LOX are shown in Figure 3.31A. The concentration of CPA is fixed to $1.1 \mu\text{M}$. There is increase in the fluorescence intensity with the addition of LOX-1 when excited at 325 nm, representing the binding of CPA to LOX. Figure 3.31B is the primary plot of fluorescence intensity against the concentration of LOX-1. The binding constant was calculated using the mass action plot which is shown in Figure 3.31C. The association constant calculated

by following the enhancement in fluorescence of CPA on binding to LOX-1 is $2.1 \pm 0.5 \times 10^4 \text{ M}^{-1}$.

Energy transfer was detected from the overlap of the tryptophan fluorescence emission spectrum of LOX-1 with the incremental addition of CPA. The emission spectra of LOX-1 and the LOX-1–CPA complex when excited at 295 nm are shown in Figure 3.32A. In the absence of CPA, the emission maximum was at 333 nm due to the excitation of tryptophan residues in LOX-1. Titration of LOX-1 with CPA resulted in quenching of tryptophan fluorescence at 333 nm, with concurrent increase and shift in emission maximum towards the longer wavelength (373 nm). This shift in wavelength from 333 nm to 373 nm is depicted in Figure 3.32B. Since free CPA does not fluoresce when excited at 295 nm, the longer wavelength band is due to the resonance energy transfer from the tryptophan residues of LOX-1 to the bound CPA. There are about 14 Trp residues in LOX-1. Figure 3.33A and 3.33B shows the plots to calculate the association constant for the binding of CPA to LOX-1 by quenching and K_a is $6.0 \pm 0.5 \times 10^4 \text{ M}^{-1}$. Sklar et al. (1977b) reported that BSA has 5 binding sites with the binding constant in the range 10^6 to 10^8 M^{-1} for CPA. The association constant for the binding of CPA to PPAR γ ligand binding domain is $1.5 \times 10^6 \text{ M}^{-1}$ (Palmer and Wolf, 1998).

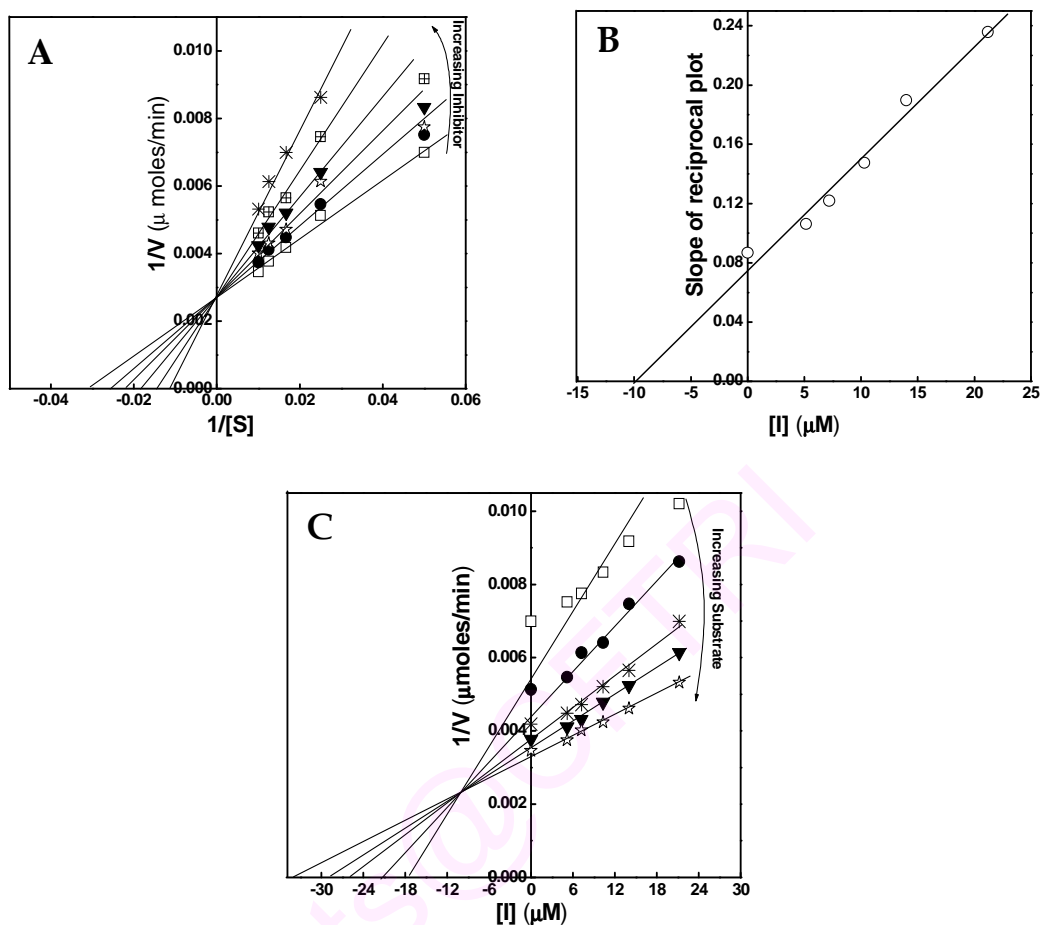


Figure 3.29. (A) Lineweaver-Burk plot to determine the kinetics of inhibition of LOX-1 by CPA. The concentration of CPA were 0 ($-\square-$), 5.15 ($-\bullet-$), 7.2 ($-\star-$), 10.3 ($-\blacktriangledown-$), 14 ($-\boxplus-$), and 21.2 μ M ($-\ast-$). The substrate concentration varied from 20-100 μ M. (B) The slope (K_m/V_{max}) of the lines obtained from the L-B plot is plotted against the CPA concentration in order to determine the K_i value of CPA. All values are average of three experiments. (C) Dixon plot: The value corresponding to the intersect point on the X-axis gives the K_i . The concentration of CPA and linoleic acid are similar used in the L-B plot. The concentration of linoleic acid were 20 ($-\square-$), 40 ($-\bullet-$), 60 ($-\ast-$), 80 ($-\blacktriangledown-$) and 100 μ M ($-\star-$). Values are average of three different sets of experiment.

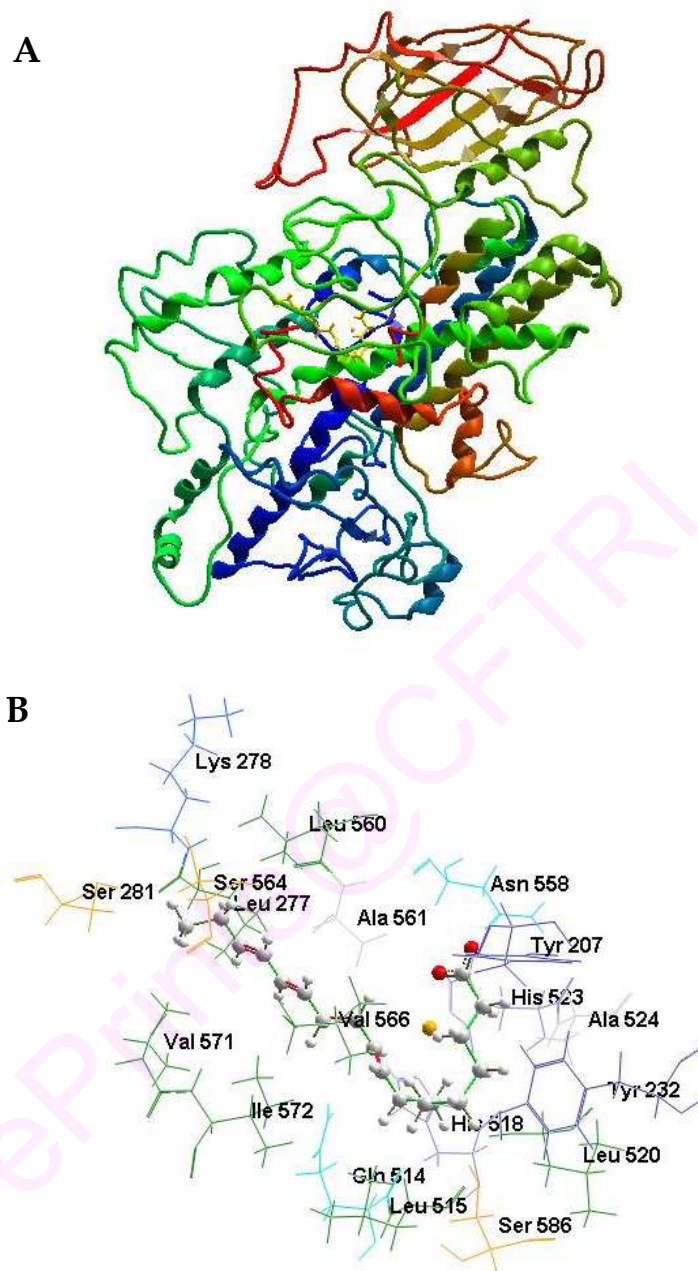


Figure 3.30. (A) Cartoon ribbon model showing the binding of CPA to soy LOX-3 (PDB ID: 1JNQ). (B) A closer look of the amino acid residues present at the binding site of CPA. The ligand (ball and stick model) is occupying the site closer to the cofactor iron.

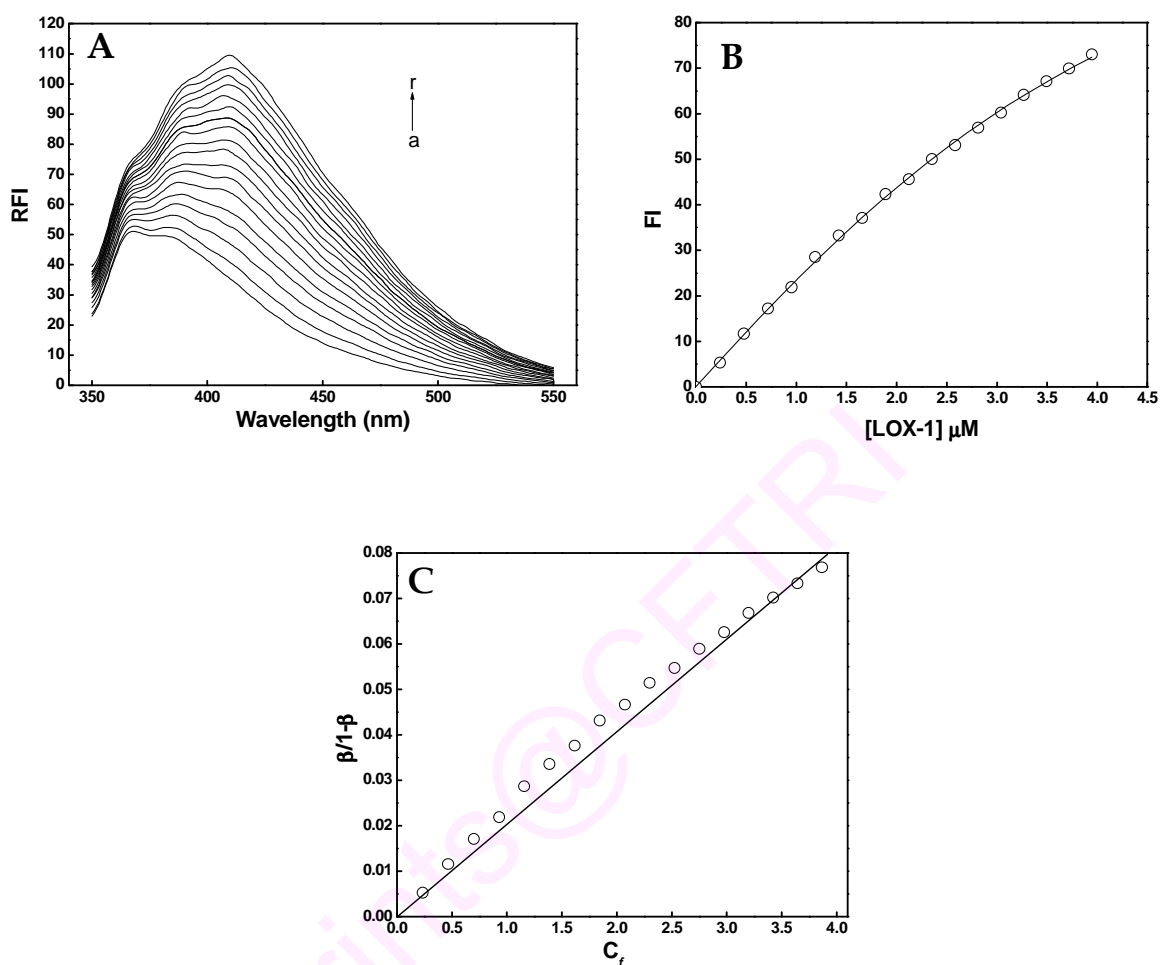


Figure 3.31. (A) Emission spectra of CPA on titration with LOX-1. Excitation wavelength is 325 nm, Slit widths were 5 and 10 nm and the temperature is 25 °C. CPA concentration is fixed to 1.1 μM , 5 μL of LOX-1 added from 0.12 mM stock in the concentration range 0 - 4.0 μM (a-r) and the buffer is 0.1 M borate, pH 9.0. (B) Primary plot of fluorescence intensity versus the concentration of LOX-1. The data are taken from the above spectra, from wavelength 410 nm. (C) Mass action plot to calculate the association constant for the binding of CPA to LOX-1.

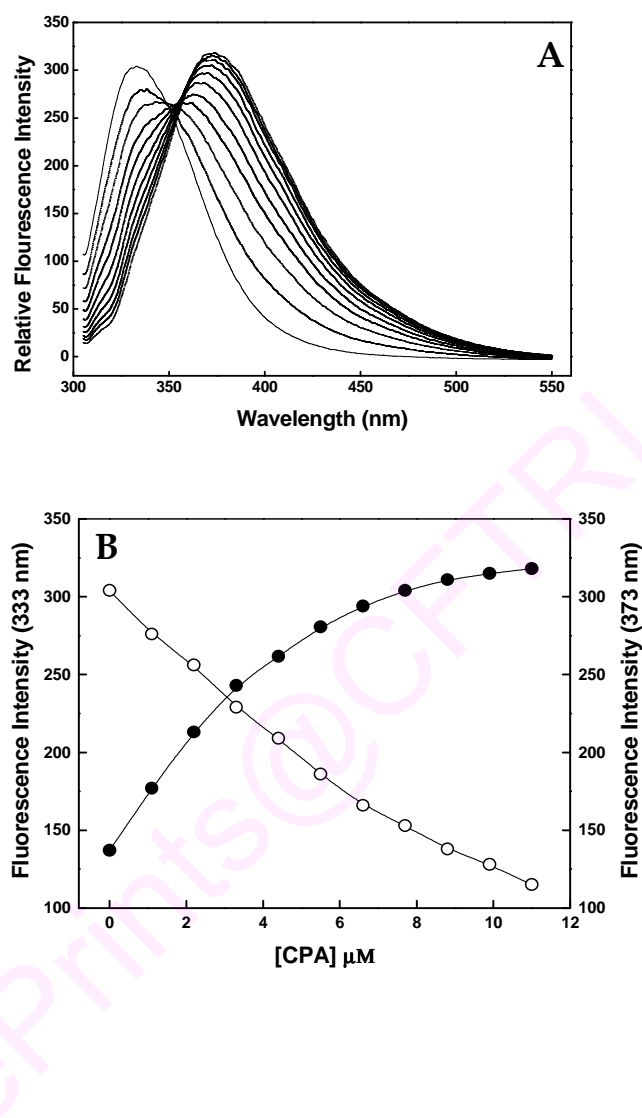


Figure 3.32. (A) Quenching of intrinsic fluorescence of LOX-1 on titration with CPA. Excitation wavelength is 295 nm, 5, 10, 25 °C, concentration of LOX-1 is 0.37 μM : 2.75 mM stock CPA in ethanol, 1 μL of CPA added and concentration of CPA ranges from 0-11 μM . (B) Concentration dependence of energy transfer between tryptophan and bound CPA. LOX-1 is excited at 295 nm and emission was measured at 333 (—○—) and 373 nm (—●—).

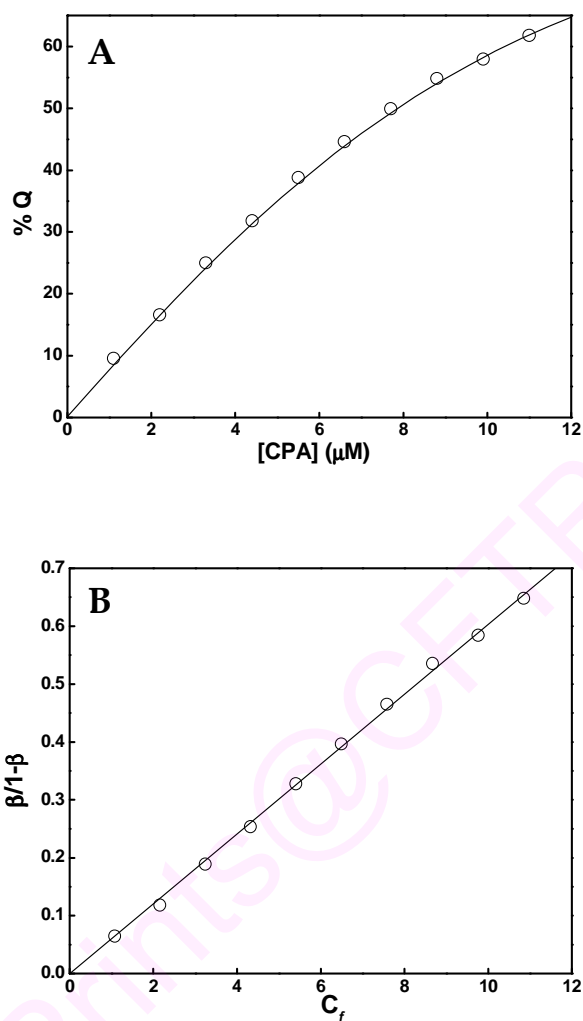


Figure 3.33. (A) Primary plot of quenching (%) of fluorescence at 333 nm vs. the concentration of CPA. (B) Mass action plot to calculate the association constant for the binding of CPA to LOX-1.

***3.2. Molecular Basis of Interaction of Curcumin
with Proteins – Inhibition of Soy LOX-1 by
Tetrahydrocurcumin***

3.2. Inhibition Studies of LOX-1 by Tetrahydrocurcumin

THC was prepared to 97% purity. The purity was ascertained by observing a single peak on RP-HPLC and from the NMR data. Mass of the compound was determined to be 373.6 (THC+H⁺). Soy LOX-1 was purified to homogeneity with the specific activity of 185 $\mu\text{moles}/\text{min}/\text{mg}$ of protein.

Stability Measurements

THC has maximum absorption at 282 nm. At pH 5.8 and 7.0, THC was stable for 48 h. At pH 9.0, ~90% was retained for 3 h, while ~68% was retained at the end of 48 h. These measurements were carried out by following the decrease in absorbance at 282 nm.

Kinetics

Inhibition of LOX-1 by THC was found to be concentration dependent. Time course for the inhibition of LOX-1 by THC in the concentration range 0 - 120 μM is shown in Figure 3.34A. The IC_{50} value was determined to be 59.4 μM (Figure 3.34B). The IC_{50} value for the PC micelles encapsulated THC was 44.6 μM . As there was no significant decrease in the IC_{50} value with bound form of THC, further experiments were conducted using free THC. The L-B plot, at fixed concentration of THC, revealed changes in both K_m and V_{max} (Figure 3.35A) indicating mixed type inhibition. Mixed inhibitory mechanism implies that the inhibitor binds to both free enzyme (to give enzyme-inhibitor complex [EI]) and also to the enzyme-substrate complex [ES], thus changing the affinity for the substrate. K_i was calculated from the replot of L-B plot (Figure 3.35B). Steady state kinetics was analyzed from Dixon plot (Figure 3.35C) and the K_i was determined to be 39 μM .

Lipoxygenase and cyclooxygenase catalyzed reaction products are implicated as the initiators of many pathological conditions. LOX expression and activity is upregulated during tumor growth and progression. Hence, inhibitors of LOX enzyme are useful in preventing many pathological conditions. Soy LOX-1 is inhibited in competitive manner by curcumin when presented in bound form with PC micelles at pH 7.4, whereas, no inhibition was observed with curcumin in free form, at pH 9.0 (Figure 3.34B) (Began et al., 1998). Human PMNL 5-LOX was inhibited by curcumin with IC_{50} value of 30 μ M (Prasad et al., 2004). In studies carried out with human recombinant 5-LOX, potent inhibition was seen with curcumin and THC with the IC_{50} value of 0.7 and 3 μ M, respectively (Hong et al., 2004). Curcumin in its free form is reported to inhibit soy LOX-3 in noncompetitive manner with the IC_{50} value of 1.2 μ M (Skrzypezak-Jankun et al., 2002). However, curcumin degrades rapidly at the pH of the assay carried out (Wang et al., 1998). The stability of THC was checked at different pH and appreciable stability was found at all the pH measured. At pH 9.0, ~ 32% was degraded in 48 h. Thus, THC is a stable molecule at neutral and acidic pH, while at basic pH, it is more stable compared to curcumin. This is due to the structural difference with the curcumin, where THC is more saturated and hydrophilic. THC inhibits soy LOX-1 in a mixed linear type of inhibition. Thus, THC is complexing with both free enzyme and the enzyme substrate complex.

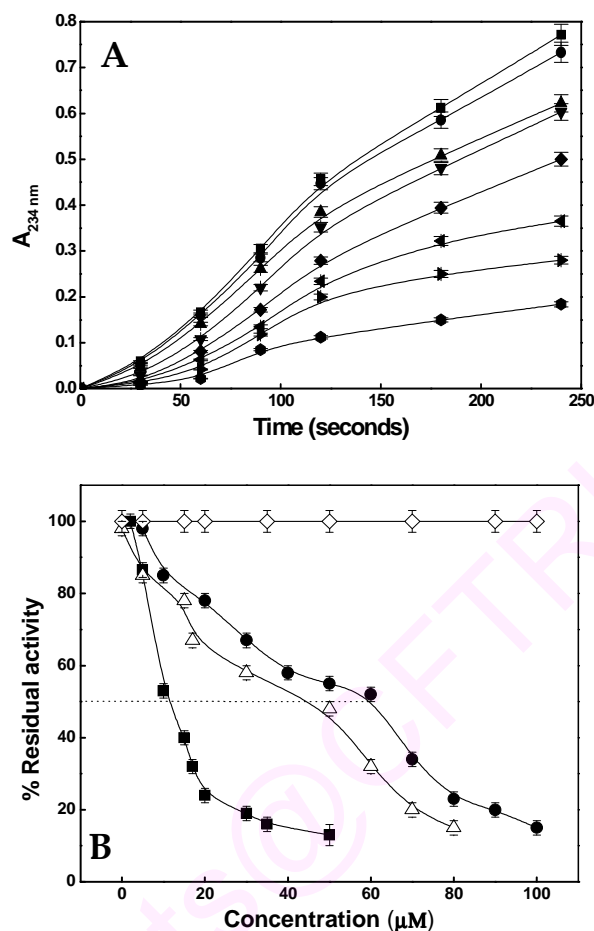


Figure 3.34. (A) Time course of lipoxxygenase catalyzed reaction. Formation of the hydroperoxide products of LOX assay was followed at 234 nm in the presence of different concentration of THC: 0 (—■—), 15 (—●—), 30 (—▲—), 45 (—▼—), 60 (—◆—), 75 (—◄—), 90 (—►—) and 120 μM (—●—). (B) IC_{50} value was determined by following the inhibition of lipoxxygenase with free curcumin (—◇—), PC micelle encapsulated curcumin (—■—), free THC (—●—) and PC micelle encapsulated THC (—△—). Free or encapsulated inhibitors were added to LOX-1 in 0.2M borate buffer, pH 9.0. The reaction was started by the addition of 100 μM linoleic acid and enzyme activity was followed spectrophotometrically at 234 nm.

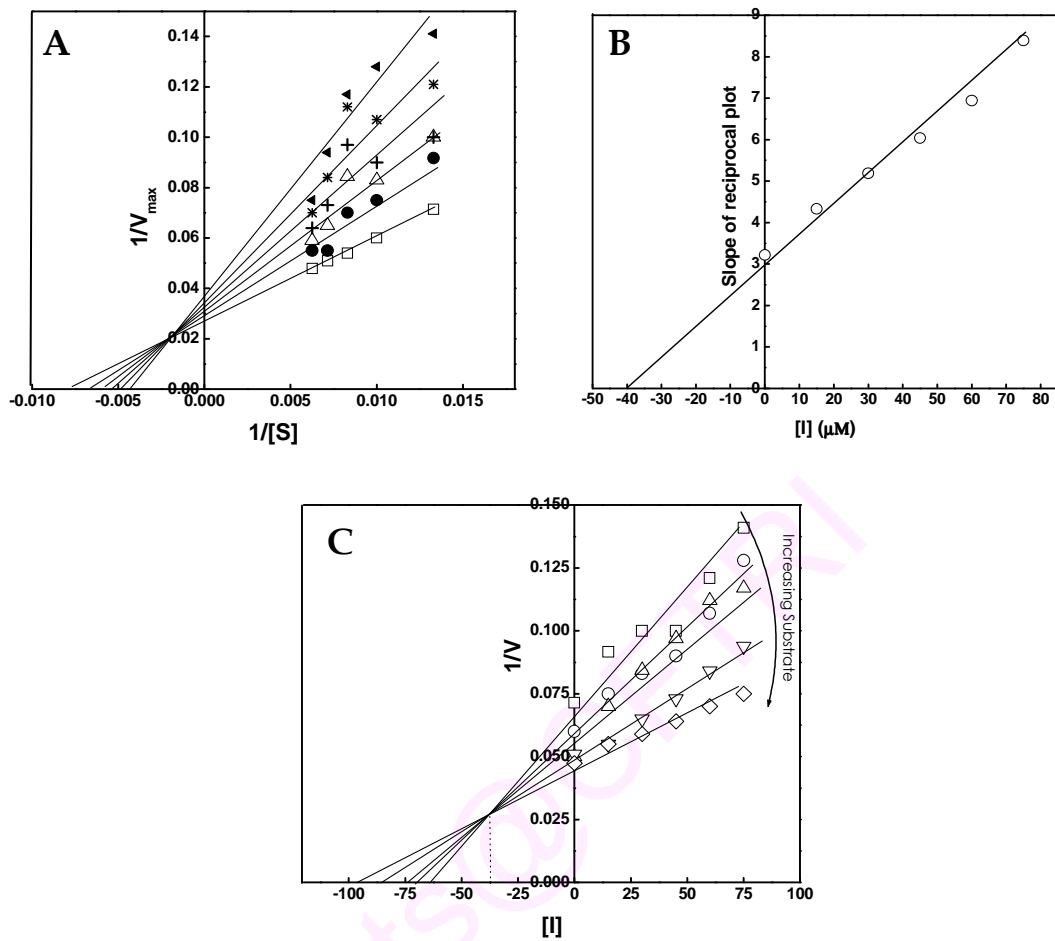


Figure 3.35. (A) Double reciprocal plot (Lineweaver-Burk plot) for inhibition of lipoygenase by THC, to determine the kinetics of inhibition. The concentration of THC were 0 ($-\square-$), 15 ($-\bullet-$), 30 ($-\triangle-$), 45 ($-\text{+}-$), 60 ($-\ast-$) and 75 μM ($-\blacktriangleleft-$). The substrate concentration varied from 75-160 μM . All values are average of three experiments. (B) Replot of L-B plot: The slope (K_m/V_{\max}) of the lines obtained from the above plot is plotted against the THC concentration in order to determine the K_i value of THC. All values are average of three experiments. (C) Dixon plot: The value corresponding to the intersect point on the X-axis gives the K_i . The concentration of THC and linoleic acid are similar used in the L-B plot. The concentration of linoleic acid were 75 ($-\square-$), 100 ($-\circ-$), 120 ($-\triangle-$), 140 ($-\nabla-$) and 160 μM ($-\diamond-$).

Absorption Measurements and Circular Dichroism Measurements

LOX-1 in its inactive state shows maximum absorption at 280 nm. In the presence of hydroperoxides, the ferrous form of the enzyme is converted to ferric form (active enzyme), resulting in the appearance of a shoulder at 350 nm as shown in Figure 3.36A. Addition of THC resulted in the conversion of ferric form of enzyme back to its inactive ferrous form, with the disappearance of the band at 350 nm. Spectrophotometric measurements of the yellow form of enzyme shows a band at 350 nm, which disappears on conversion to ferrous inactive form. On addition of THC to the ferric form of enzyme, the band at 350 nm disappears, indicating that the enzyme is reverting back to its inactive state. This is further confirmed by circular dichroic measurements. LOX-1, in its active yellow form, exhibits a positive circular dichroic band at 425 nm attributed to the ferric form of enzyme (Figure 3.36B). In the presence of THC, ferric is converted to ferrous state, as revealed from the disappearance of the band at 425 nm, thus reverts the enzyme to the inactive form. The positive induced band at 425 nm is due to the chelation of ferric iron to the amino acid residues of the protein (Spaapen et al., 1979). Disappearance of the induced band at 425 nm indicates the reversion back to inactive ferrous form. THC inhibits the enzyme by converting the active ferric form of enzyme to its inactive ferrous form. It may be competing with the hydroperoxides, thus, preventing the conversion of ferrous to the ferric state. Many inhibitors preventing the conversion of ferrous to ferric form are well known. 4-Nitrocatechol, N-alkylhydroxylamine, naphthols, disulfiram and soy isoflavones are the reductive inhibitors, inhibiting LOX-1 by converting the active ferric enzyme to the inactive ferrous form (Galpini et al., 1976; Clapp et al., 1985; Hausknecht and Funk, 1984; Mahesha et al., 2007). Catechol, *p*-Aminophenol, hydroquinone are inhibitors of LOX-1 which are oxidized to free radical

metabolites or one-electron oxidation products. They reduce the catalytically active ferric lipoxygenase to its resting ferrous form. It has been reported these inhibitors undergo base-catalyzed auto-oxidation in the pH range 6.5 - 9.0 (van der Zee et al., 1989).

HPLC Measurement and Mass Spectrometry

To check the state of THC during the enzyme catalyzed reaction, HPLC measurements were carried out. LOX-1 was assayed in the presence of THC and at the end of the reaction; THC was extracted with diethyl ether, and estimated using RP-HPLC. There was no change in the retention time of THC, which eluted at 5.8 min as shown in Figure 3.37. This indicated that there was no change in the state of THC during the reaction process.

To negate the possibility of THC being oxidized which may show the same retention time, mass of THC was checked. The peak sample from the RP-HPLC was collected and analyzed using the mass spectra. Mass spectra revealed the molecular weight of THC as 373.6 Da (Inset of Figure 3.37). This confirms the native state of THC.

Docking Studies

Based on experimental evidence, molecular docking studies were carried out to get an insight on the binding site and the mode of binding. The best candidature pose with the lowest minimal energy was selected from the pose clustering. Figure 3.38A shows the ribbon model representing the binding of THC to protein. A closer inspection of the binding site of THC reveals the predominance of hydrophobic amino acid residues as shown in Figure 3.38B. THC binds close to the cofactor-iron. Amino acid residues-Trp519 and Tyr719, are in the same plane with each of the aromatic rings of THC, in

orientation suitable to form π - π interaction. Phe576 is perpendicular and closer to the aromatic ring of THC. His518 and Gln716 are closer to the oxygen atom involved in the keto group formation. The methoxy group of THC at one end is closer to the amino acid Ile857 at the C-terminus of the enzyme. Docking studies revealed the binding site of THC being closer to the cofactor iron. The vicinity of THC to iron lends strength to the experimental evidence that enzyme inhibition is through the prevention the conversion of resting ferrous to active ferric form. THC is surrounded mainly by hydrophobic amino acids like isoleucine, valine, and leucine. Polyunsaturated fatty acids, the substrates for lipoxygenases bind to the enzyme with their olefinic part placed between the Trp519 and one of the iron ligand - His518 (Faridi et al., 2004). Aromatic ring of THC is parallel and closer to Trp519 and the keto group is nearer to His518. Therefore THC may be inhibiting the LOX-1 by blocking access to the substrate. Epigallocatechin (EGC) binds and inhibits soy LOX-3. EGC binds to soy LOX-3 with A ring near the iron and the hydroxyl group of the B ring interacts with the surrounding amino acids through hydrogen bonds (Skrzypczak-Jankun et al., 2003b). X-ray analysis reveals the binding of protocatechuic acid, the degradative product of quercetin to soy LOX-3 near the iron cofactor. C4-hydroxyl group forms hydrogen bond with the C-terminus of the enzyme and the carboxyl group of the protocatechuic acid is hydrogen bonded to the Gln514 present in the active site of the enzyme (Borbulevych et al., 2004). X-ray analysis of the complex of 4-nitrocatechol with soy LOX-3 reveals the formation of a trigonal bipyramid with the involvement of residues like His518, His709, His523 and Ile857. 4-Nitrocatechol binds very close to the iron cofactor, thus blocking the access to the iron (Skrzypczak-Jankun et al., 2004).

Apart from being a competitor for the hydroperoxides, THC may be scavenging the hydroperoxides. THC has been demonstrated to be more potent than curcumin towards protection against ferric nitrilotriacetate induced oxidative renal damage in mice (Okada et al., 2001). THC produces this protective effect to cells against oxidative stress by scavenging free radicals (Khopde et al., 2000b). THC inhibits lipid peroxidation and formation of hydroperoxides (Pari and Murugan, 2001). It is a potent antioxidant under the conditions where the radical initiators are produced in the polar water medium (Khopde et al., 2000a). It is also effective in inhibiting the cyclooxygenase-2 and phospholipase A₂ (Hong et al., 2004). Venkatesan and Rao (2000) reported that THC has higher activity than curcumin in protecting the nitrite induced oxidation of hemoglobin and lysis of erythrocytes. Lipoxygenase inhibitors like nordihydroguaiaretic acid (NDGA), n-propylgallate and butyl hydroxytoulene which are antioxidants, function by reacting with free radical intermediates and thereby acting as free radical scavengers (Tappel et al., 1952).

In conclusion, THC may be preventing the conversion of inactive form of enzyme to active form by scavenging the hydroperoxides (which activate the enzyme) and at the same time converting the ferric (active state of LOX-1) to the inactive ferrous form. Thus, THC can be included under the class of redox inhibitors of LOX-1. However, THC is less powerful in inhibiting the LOX-1, but higher stability of THC compared to curcumin provides valuable leads for the use of this compound as an alternative to curcumin. These observations indicate the importance of methylene bridge at carbon seven in curcumin, in inhibiting the soy LOX-1 enzyme.

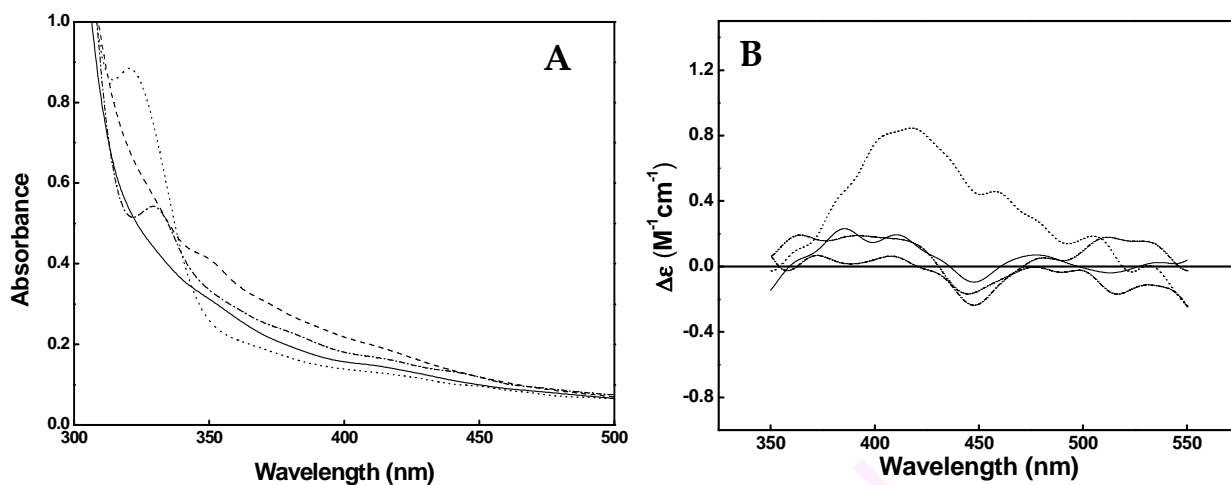


Figure 3.36 (A) Effect of THC on the absorption spectra of ferric lipoxigenase. Absorption experiments were carried out in the region of 300 – 500 nm in 0.1M borate buffer, pH 9.0. Resting LOX-1 (160 μM) was treated with linoleic acid (160 μM) to convert it to active ferric form. To this THC (160 and 320 μM) was added. *Solid line*, native LOX-1 (Fe^{2+}); *dashed line*, ferric LOX-1 (Fe^{3+}); *dash & dotted line*, THC (160 μM); *dotted*, THC (320 μM). The cell path length was 1 cm and spectra were recorded in a double beam spectrophotometer. (B) Effect of THC on the CD spectrum ferric lipoxigenase. CD measurement was carried out in the visible region of 350–550 nm in 0.1M borate buffer, pH 9.0. Equimolar concentration of LOX-1 was added to linoleic acid (160 μM , each) to convert it to optically active ferric form. To this THC was added. *Solid line*, native LOX-1 (Fe^{2+}); *dashed line*, ferric LOX-1 (Fe^{3+}); *dash & dotted line*, THC (160 μM); *dotted*, THC (320 μM)., CD spectrum of LOX-1 treated with THC showing the disappearance of positive dichroic band at 425 nm. The cell path length was 1 cm and spectra were recorded at a speed of 10 nm/min. All scans are an average of three runs. A mean residue weight of 115 was used for calculating the molar ellipticity values.

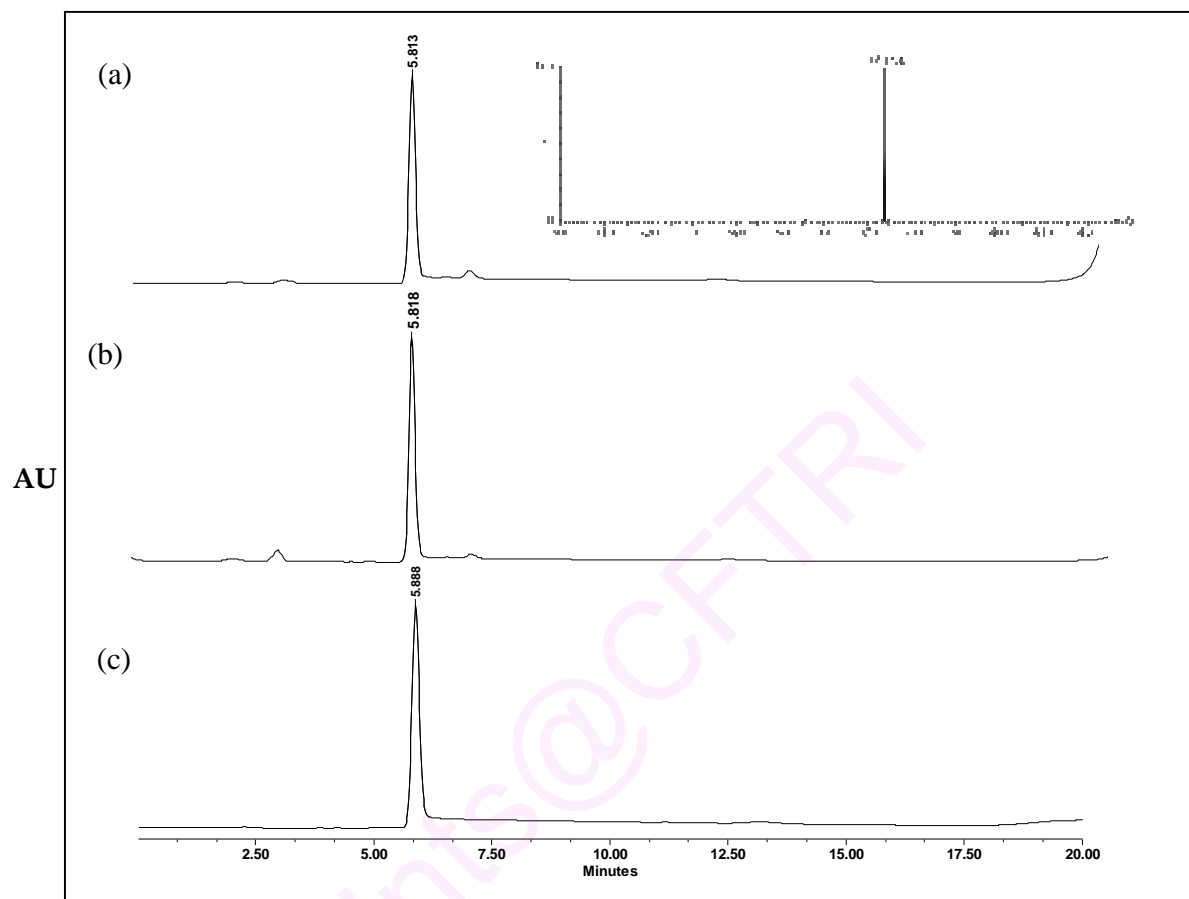


Figure 3.37. HPLC profile of THC in the presence of LOX-1 and linoleic acid. (a) THC in 0.2 M borate buffer, pH 9.0. (b) THC in presence of LOX-1 (c) THC in presence of LOX-1 and 100 μ M linoleic acid (**Inset:** Mass spectra of THC, extracted from LOX-1 and linoleic acid mixture).

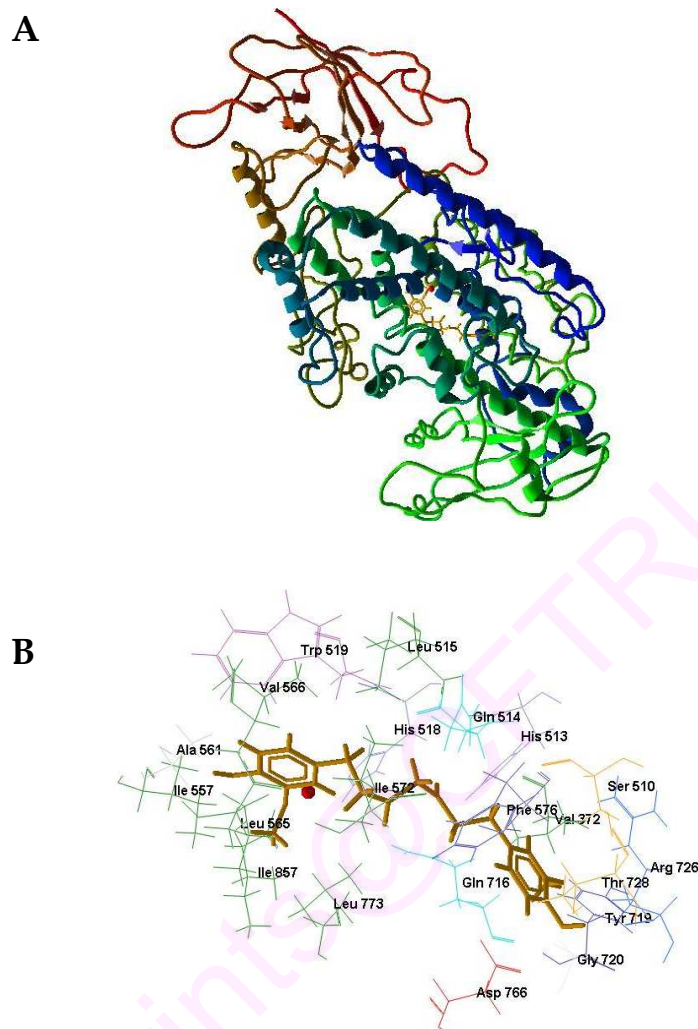


Figure 3.38. Molecular docking of THC with soy LOX-1. The coordinates of the LOX-1 structure are taken from the protein data bank and the ID is 1JNQ. Best candidate posture with lowest minimal energy is selected. **(A)** Cartoon ribbon structure of the LOX1 with the THC (yellow capped stick structure) at the binding site closer to iron (red ball). **(B)** THC in contact with the amino acid residues at the binding site within 3 Å distance.

***3.3. Activity Modulation of Carbonic Anhydrase
by Curcumin***

ePrints@CETRI

3.3. Activity Modulation of Carbonic Anhydrase by Curcumin

The ability of curcumin to affect physiological and biological activity is due to the non specific interaction with different proteins and metal ions. Curcumin is known to be a chelator of metal ions. Curcumin reduces the amyloid aggregation and oxidative neurotoxicity by chelating metal ions. These metal ions induce A β aggregation and toxicity and are concentrated in Alzheimer's brain. Two molecules of curcumin is chelated by iron and copper, whereas zinc showed little binding (Baum and Ng, 2004).

Carbonic anhydrase was selected to check the modulation on the activity of zinc containing enzyme. The assay was carried out by continuous spectrophotometric rate determination. The activity profile of carbonic anhydrase in various concentration of curcumin is shown in Figure 3.39. Curcumin did not induce any change in the activity of carbonic anhydrase. Previous study (Began et al., 1998) showed that curcumin encapsulated in PC micelles exhibited competitive inhibition against soy LOX-1, an iron containing enzyme. Curcumin was binding near and chelating the iron thus inhibiting the enzyme. In the present study curcumin did not affect the activity of carbonic anhydrase. It is reported that curcumin binds more readily to redox-active metal ions like iron or copper, but not to redox inactive ions like zinc (Baum and Ng, 2004). As curcumin does not bind to redox inactive metal ions, there was no effect on the activity of carbonic anhydrase. Such studies provide examples and may help in understanding the specificity of binding of curcumin and its modulation on molecular targets.

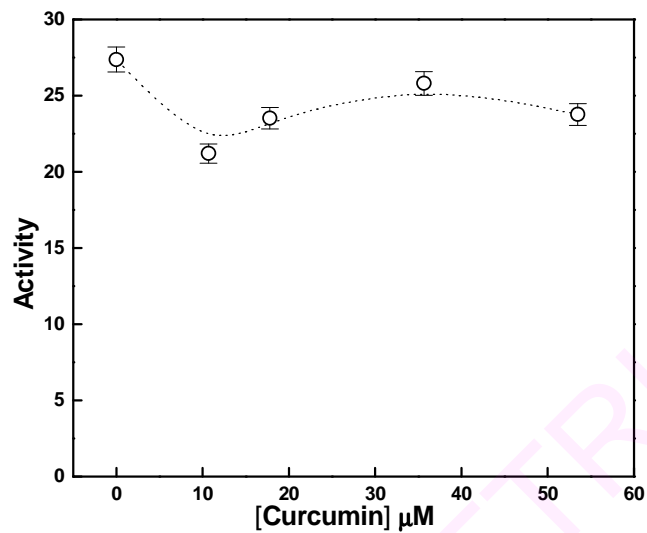


Figure. 3.39. Activity of carbonic anhydrase followed in the presence of different concentrations of curcumin. Activity of carbonic anhydrase was monitored by continuous spectrophotometric rate determination.

4. Summary and Conclusions

ePrints@CFTRI

Summary and Conclusions

Curcumin (diferuloylmethane; 1,7-bis[4-hydroxy-3-methoxy-phenyl]-1,6-heptadiene-3,5-dione), a natural lipid-soluble yellow compound from the plant *Curcuma longa* L., is a potent antioxidant, antitumorigenic and anti-inflammatory molecule. Researchers have evinced a great interest in this molecule, because of its potential health benefits. Biological activities of curcumin depend on its bioavailability and metabolism. Very limited solubility and stability in aqueous medium and poor bioavailability limits the use of curcumin as an efficient therapeutic agent. Efforts are on to enhance the solubility of curcumin by making complexes with natural biodegradable carriers, such as serum albumin, casein micelles, phospholipid complexes. The present study was directed primarily, towards exploring possible medium/carrier to increase the solubility and stability of curcumin. This was approached by selecting biocompatible and easily available major milk proteins. The binding site has been investigated by spectroscopic methods and molecular docking. These binding studies prompted the preparation and encapsulation of curcumin in milk protein nanoparticles.

Encapsulation of small bioactive molecules in nanoparticles improves biodistribution and solubility of these molecules. Food based nanocomplexes improve the bioavailability and stability of small molecules, providing protection against degradation by heat, light, oxygen or pH sensitivity. Protein nanoparticles, being biodegradable and metabolizable serve over other carriers, as they can incorporate a wide variety of small molecules in a nonspecific fashion. Nanocomplexes, based on proteins such as serum albumin or bovine β -lactoglobulin (β LG) or α_{s1} -casein, capable of binding hydrophobic molecules serve as base materials for the encapsulation and

controlled release of bioactive compounds. In an approach to enhance the solubility of curcumin, encapsulation of curcumin has been evaluated using easily available and biodegradable proteins - β -lactoglobulin, α_{S1} -casein and human serum albumin.

Interaction Studies of Curcumin with β -Lactoglobulin and its Nanoparticle Preparation

β -Lactoglobulin is a low molecular weight whey protein, abundant in cow's milk (3 g/L). It is a small, globular extracellular protein, belongs to lipocalins superfamily; as it binds and transports small hydrophobic molecules within the central cavity known as calyx. Bovine β -lactoglobulin occurs as a dimer at neutral pH, and monomerises at $\text{pH} \leq 2$, with a molecular weight of ~ 18000 Da. β -Lactoglobulin contains 162 amino acids, with a predominant β sheet consisting of nine β strands (A-I) of which, strand A to H form an up and down β barrel and a major α -helix, at the C-terminal end of the molecule. The proposal of β LG as an oral drug carrier is supported by its ability to bind many biochemically important hydrophobic compounds. The potential of β LG to be a carrier molecule for curcumin was investigated, by following the interaction between curcumin and β LG, using spectroscopic techniques. Major findings were,

- The stability of curcumin in the presence of β LG was enhanced by ~ 6.7 folds at pH 7.0, in comparison of the stability of curcumin in aqueous medium.
- β LG interacts with curcumin at pH 7.0, with an association constant of $1.04 \pm 0.1 \times 10^5 \text{ M}^{-1}$, to form a 1:1 complex, at 25 °C.
- Entropy and free energy changes for the interaction derived from van't Hoff plot were $18.7 \text{ cal mol}^{-1}$ and $-6.8 \text{ kcal mol}^{-1}$, respectively

- Effect of pH on the binding of curcumin to β LG was analyzed by determining its association constant. There was a precipitous decrease in association constant when the pH was decreased from 7.0 to 5.5 from 1.1×10^5 to $1.1 \times 10^3 \text{ M}^{-1}$.
- The binding constant of curcumin with denatured β LG was found to be $7.0 \pm 0.2 \times 10^2 \text{ M}^{-1}$, which is very low compared to that of native β LG.
- Fluorescence resonance energy transfer through Förster mechanism revealed the binding of curcumin located near Trp19, situated at the base of calyx.
- The near UV CD spectrum of native β LG showed two sharp negative bands centered at ~ 292 and ~ 284 nm with two smaller bands located at ~ 277 and ~ 266 nm.
- The CD spectrum of curcumin in presence of β LG induces negative and positive extrinsic bands at ~ 389 and ~ 450 nm, respectively.
- Interaction of β LG with curcumin does not affect either the conformation or the state of association of β LG.
- Molecular docking studies together with the above mentioned experimental evidence revealed the calyx of β LG as the binding site for curcumin, with the main interacting force being hydrophobic.
- Nanoparticles of β LG prepared by desolvation were found to encapsulate curcumin with $> 96\%$ efficiency.
- The solubility of curcumin in β LG nanoparticle was significantly enhanced to $\sim 625 \mu\text{M}$ in comparison with its aqueous solubility (30 nM).

Interaction Studies of Curcumin with α_{S1} -Casein and its Nanoparticle Preparation

Casein constitutes nearly 80% of total milk proteins and is a mixture of 4 phosphoprotein fractions namely, α_{S1} -, α_{S2} -, β - and κ -casein. Casein is amphiphilic in nature. The presence of hydrophobic clusters and negatively charged regions along the peptide chain helps to form large colloidal aggregate leading to the formation of casein micelle complexes. Caseins have aperiodic structure, characterized by lack of folded structure. Due to lack of folded structure, they have high intramolecular flexibility. Although caseins function is largely nutritional, recent studies provide insight about the functional properties of caseins exhibiting chaperone-like activity and its ability to solubilize hydrophobically aggregated proteins.

The most abundant fraction of casein is α_{S1} -casein, constituting 40% of total casein. α_{S1} -casein is a single polypeptide chain with 199 amino acid residues including 8-9 serine monophosphates, as a molecular weight of 23619 Da. The structure of α_{S1} -casein consists of a short hydrophilic amino-terminal portion, a segment of hydrophobic β -sheet, phosphopeptide region and a short portion of α -helix, which connects the N-terminal portion to the highly hydrophobic carboxy-terminal domain (residues 100-199) containing extended β -strands (residues 134-160 and 163-178). The binding characteristics of curcumin with α_{S1} -casein and the stability of the bound curcumin were evaluated.

- The stability of curcumin in the presence of α_{S1} -casein was enhanced by ~39 folds at pH 7.2, in comparison of the stability of curcumin in aqueous medium.

- Curcumin binds to α_{S1} -casein at two different binding sites, one with high affinity and one with low affinity characterized by association constants of $2.01 \pm 0.6 \times 10^6$ and $6.3 \pm 0.4 \times 10^4 \text{ M}^{-1}$.
- The carboxyl-terminal of α_{S1} -casein (100-199 residues) and the residues 14-24 in α_{S1} -casein are hydrophobic in nature. Curcumin may probably binding at these two sites, with two different ranges of affinity through hydrophobic interaction
- The free energy change for the binding of curcumin to α_{S1} -casein, ΔG° at 27 °C, was $-8.65 \text{ kcal mol}^{-1}$. The ΔH° and ΔS° for the binding reaction were estimated to be $-1.28 \text{ kcal mol}^{-1}$ and $24.7 \text{ cal mol}^{-1}$, respectively.
- Hydrophobic force was the main contributing factor for the interaction of curcumin to α_{S1} -casein.
- Chaperone activity of α_{S1} -casein was enhanced when bound to curcumin.
- The biological activity of curcumin like, its protective action against hemolysis was unchanged on interaction with α_{S1} -casein.
- Average size of curcumin encapsulated α_{S1} -casein protein nanoparticles was $\sim 166 \pm 5 \text{ nm}$. Encapsulation efficiency of curcumin was $> 94\%$, and 38% curcumin release was observed from nanoparticles in 24 h.
- The solubility of curcumin in α_{S1} -casein nanoparticle was enhanced to $\sim 620 \mu\text{M}$ in comparison with its aqueous solubility (30 nM).

Curcumin was encapsulated in HSA nanoparticles and the results are as follows:

- The particle size was around $239 \pm 10 \text{ nm}$, with the shape being spherical.
- HSA nanoparticles encapsulated about 56% of curcumin and released $\sim 66\%$ curcumin in 24 h, at pH 7.0.

- The solubility of curcumin in HSA nanoparticle was $\sim 0.2 \mu\text{M}$, which was very less compared to the solubility of curcumin in βLG and α_{S1} -casein.

Apparent solubility of curcumin in the presence of PC micelles and other proteins in aqueous solution were studied.

- The solubility was in the order PC micelles > HSA > α_{S1} -casein > βLG , as a function of temperature.

Curcumin as a Fluorescent Probe to Measure the Surface Hydrophobicity of Proteins

To understand the molecular basis of interaction of curcumin with proteins, the ability of curcumin to measure the surface hydrophobicity of proteins with a standard fluorescent probe, *cis*-parinaric acid was compared.

- Surface hydrophobicity of BSA, βLG , soy LOX-1, ovalbumin and lysozyme are in the order BSA > α_{S1} -casein > βLG > soy LOX-1 > ovalbumin > lysozyme. The binding affinities of curcumin decreased with the decrease in the surface hydrophobicity of proteins.
- Surface hydrophobicity index (S_0) value determined using curcumin correlated with the values calculated using CPA, a known fluorescent probe. The order of S_0 values for different proteins were same as above.
- The S_0 value of proteins determined using curcumin decreased in the presence of urea, suggesting the possible use of curcumin as a probe to determine the surface hydrophobicity of proteins.

The structural similarities between CPA and linoleic acid, the substrate for soy LOX-1, prompted to study the inhibition of soy LOX-1 with CPA, and the following conclusions were drawn.

- CPA, a C₁₈ fatty acid inhibits soy LOX-1 activity with the IC₅₀ value of 18.8 μM.
- The mechanism of inhibition of soy LOX-1 by CPA was competitive with the K_i value of 9.8 μM.
- CPA binds close to iron cofactor with the distance of carboxylate group of CPA to the iron being 3.3 Å.
- The binding constant for the binding of CPA to soy LOX-1 is $2.1 \pm 0.5 \times 10^4 \text{ M}^{-1}$.

Inhibition Studies of Soy LOX-1 by Tetrahydrocurcumin

Tetrahydrocurcumin (THC), the reduced derivative of curcumin, is the major metabolite *in vivo*. It is known to possess potent antioxidant activity in comparison to curcumin. Curcumin is a strong anti-inflammatory agent. Inflammation is mediated by the products released by the metabolism of unsaturated fatty acids. This occurs enzymatically either by lipoxygenase or cyclooxygenase pathway. Curcumin is a well known inhibitor of lipoxygenase enzyme. It is requisite to understand the structural requirements for the exertion of such physiological activity by analogues. Therefore to understand the structural relationship, curcumin and THC were selected and the potency to inhibit the soy LOX-1 was compared and evaluated. As a transformed product of curcumin, THC appears to be involved in physiological and pharmacological activity. Inhibition of soy LOX-1 by tetrahydrocurcumin was studied and the kinetics and mechanism of inhibition was evaluated.

- THC inhibited soy LOX-1 activity with an IC₅₀ value of 59.4 μM for THC (in aqueous solution) and 44.6 μM for PC micelles encapsulated THC, a higher IC₅₀ value compared to its parent compound - curcumin. The lag phase for enzyme activation from its resting state increased with increasing concentrations of THC.

- A mixed linear type of inhibition of LOX-1 was observed with a K_i value of ~ 39 μM .
- Molecular docking simulations suggested the binding of THC near the iron cofactor.
- Spectroscopic and CD studies revealed that, THC could prevent the conversion of the resting inactive ferrous form of the enzyme to its active ferric form thus inhibiting the enzyme
- The higher solubility and stability of THC, compared to curcumin, provides valuable leads for the use of this compound as an alternative to curcumin in anti-inflammatory drugs
- These observations indicate the importance of methylene bridge at carbon seven in curcumin, in inhibiting the soy LOX-1 enzyme.

Activity Modulation of Carbonic Anhydrase by Curcumin

The effect of curcumin on the activity of carbonic anhydrase was studied. No change in the activity of carbonic anhydrase, *in vitro* in the presence of curcumin was observed. Though, curcumin is a known chelator of metal ions, it had no effect on redox inactive metal-zinc containing enzyme.

The application of curcumin as a potent bioactive molecule is dependent on its bioavailability, stability and solubility in aqueous medium. This study has helped to improve the solubility and stability of curcumin by complexing with protein particles. This in turn may help in developing protein based carrier system for the delivery of curcumin. It is expected that these studies will lead to a better understanding of the protein-ligand interaction.

Bibliography

ePrints@CFTRI

Bibliography

- Aggarwal BB and Shishodia S. Molecular targets of dietary agents for prevention and therapy of cancer. *Biochem Pharmacol* **2006**, 71, 1397-1421.
- Aggarwal BB, Bhatt ID, Ichikawa H, Ahn KS, Sethi G, Sandur SK, Sundaram C, Seeram N and Shishodia S. In *Turmeric - The Genus Curcuma*; Ravindran P, Nirmalbabu K and Sivaraman K. eds. Taylor and Francis Press: London, UK, **2007**, pp 298-348.
- Alaimo MH, Farrell HM Jr and Germann MW. Conformational analysis of the hydrophobic peptide α_{s1} -casein (136-196). *Biochim Biophys Acta* **1999**, 1431, 410-420.
- Ammon HP and Wahl MA. Pharmacology of *Curcuma longa*. *Planta Med* **1991**, 57, 1-7.
- Anand P, Kunnumakkara AB, Newman RA and Aggarwal BB. Bioavailability of curcumin: Problems and promises. *Mol Pharm* **2007**, 4, 807-818.
- Anand P, Nair HB, Bokyung S, Kunnumakkara AB, Yadav VR, Tekmal RR and Aggarwal BB. Design of curcumin-loaded PLGA nanoparticles formulation with enhanced cellular uptake, and increased bioactivity *in vitro* and superior bioavailability *in vivo*. *Biochem Pharmacol* **2010**, 79, 330-338.
- Andrade SM and Costa SMB. Spectroscopic studies on the interaction of water soluble porphyrin and two drug carrier proteins. *Biophys J* **2002**, 82, 1607-1619.
- Ankola DD, Viswanad B, Bhardwaj V, Ramarao P and Kumar MN. Development of potent oral nanoparticulate formulation of coenzyme Q10 for treatment of hypertension: Can the simple nutritional supplements be used as first line therapeutic agents for prophylaxis/therapy? *European J Pharm Biopharm* **2007**, 67, 361-369.

- Arbos P, Arangoa MA, Campanero MA and Irache JM. Quantification of the bioadhesive properties of protein-coated PVM/MA nanoparticles. *Int J Pharm* **2002**, *242*, 129-136.
- Aschaffenburg R and Drewry J. Occurrence of different beta-lactoglobulins in cow's milk. *Nature* **1955**, *176*, 218-219.
- Atkins and de Paula. Physical chemistry for life sciences. *W. H. Freeman; 1st ed.* **2005**.
- Atsumi T, Fujisawa S and Tonosaki K. Relationship between intracellular ROS production and membrane mobility in curcumin and tetrahydrocurcumin treated human gingival fibroblasts and human submandibular gland carcinoma cells. *Oral Dis* **2005**, *11*, 236-242.
- Awasthi S, Pandya U, Singhal SS, Lin JT, Thiviyanathan V, Seifert WE, Awasthi Jr YC and Ansari GA. Curcumin-glutathione interactions and the role of human glutathione S-transferase P1-1. *Chem Biol Interact* **2000**, *128*, 19-38.
- Axelrod B, Cheesbrough TM and Laakso S. Lipoxygenase from soybeans. *Meth Enzymol* **1981**, *71*, 441-451.
- Babu PS and Srinivasan K. Influence of dietary curcumin and cholesterol on the progression of experimentally induced diabetes in albino rat. *Mol Cell Biochem* **1995**, *152*, 13-21.
- Babu SP and Srinivasan K. Amelioration of renal lesions associated with diabetes by dietary curcumin in streptozotocin diabetic rats. *Mol Cell Biochem* **1998**, *181*, 87-96.
- Bala I, Bhardwaj V, Hariharan S, Kharade SV, Roy N and Ravi Kumar MN. Sustained release nanoparticulate formulation containing antioxidant-ellagic acid as potential prophylaxis system for oral administration. *J Drug Targeting* **2006**, *14*, 27-34.

- Banni S and Martin JC. Conjugated linoleic acid and metabolites. In: Trans fatty acids in human nutrition. *Sebedio JL, Christie WW (Eds.), Oily Press, Dundee, Scotland, 1998, pp. 261-302.*
- Basile V, Ferrari E, Lazzari S, Belluti S, Pignedoli F and Imbriano C. Curcumin derivatives: Molecular basis of their anti-cancer activity. *Biochem Pharmacol* **2009**, 78, 1305-1315.
- Baum L and Ng A. Curcumin interaction with copper and iron suggests one possible mechanism of action in alzheimer's disease animal models. *J Alzheimers Dis* **2004**, 6, 367-77.
- Began G, Sudharshan E and Rao AGA. Inhibition of lipoygenase-1 by phosphatidylcholine micelles-bound curcumin. *Lipids* **1998**, 33, 1223-1228.
- Began G, Sudharshan E, Udaya Sankar K, Rao AGA. Interaction of curcumin with phosphatidylcholine: A spectrofluorometric study. *J Agri Food Chem* **1999**, 47, 4992-4997.
- Belloque J and Smith G M. Thermal denaturation of β -lactoglobulin. A ^1H NMR study. *J Agric Food Chem* **1998**, 46, 1805-1813.
- Benesi HA and Hildebrand JH. A spectrophotometric investigation of the interaction of iodine with aromatic hydrocarbons. *J Am Chem Soc* **1949**, 71, 2703-2707.
- Berova N, Gargiulo D, Derguini F, Nakanishi K and Harada N. Unique UV-Vis absorption and circular dichroic exciton-split spectra of a chiral biscyanine dye. Origin and nature. *J Am Chem Soc* **1993**, 115, 4769-4775.
- Bhattacharyya J and Das KP. Molecular chaperone-like property of an unfolded protein, α_s -casein. *J Biol Chem* **1999**, 274, 15505-15509.
- Bigelow CC. On the average hydrophobicity of proteins and the relation between it and protein structure. *J Theor Biol* **1967**, 16, 187-211.

- Bisht S, Feldmann G, Soni S, Ravi R, Karikar C, Maitra A and Maitra A. Polymeric nanoparticle-encapsulated curcumin (“nanocurcumin”): A novel strategy for human cancer therapy. *J Nanobiotechnology* **2007**, 5:3.
- Blain JA and Shearer G. Inhibition of soya lipoxidase. *J Sci Food Agric* **1965**, 16, 373- 378.
- Bohm HJ and Scheinder G. Protein-ligand interaction from molecular recognition to drug design. *19, Wiley-VCH Verlag GmbH & Co, KGaA, Weinheim, 2003.*
- Bongrand P. Physical basis of cell-cell adhesion, *CRC press, Boca Raton, FL, 1988.*
- Borbulevych OY, Jankun J, Selman SH, Skrzypczak-Jankun E. Lipoxygenase interactions with natural flavonoid, quercetin, reveal a complex with protocatechuic acid in its x-ray structure at 2.1 Å resolution. *Proteins* **2004**, 54, 13-19.
- Borgeat P, Picard S, Drapeau J and Vallerand P. Metabolism of arachidonic acid in leukocytes: Isolation of a 5,15-dihydroxy-eicosatetraenoic acid. *Lipids* **1982**, 17, 676-681.
- Brash AR. Lipoxygenases: occurrence, functions, catalysis and acquisition of substrate. *J Biol Chem* **1999**, 8, 373-380.
- Brodbeck U and Ebner KE. The subcellular distribution of the A and B proteins of lactose synthetase in bovine and rat mammary tissue. *J Biol Chem* **1966**, 241, 5526-5532.
- Brouet I and Ohshima H. Curcumin, an anti-tumour promoter and anti-inflammatory agent, inhibit induction of nitric oxide synthase in activated macrophages. *Biochem Biophys Res Commun* **1995**, 206, 533–540.
- Brownlow S, Cabral JHM, Cooper R, Flower DR, Yewdall SJ, Polikarpov I, North ACT and Sawyer L. Bovine β LG at 1.8 Å resolutions—still an enigmatic lipocalin. *Structure* **1997**, 5, 481–495.

- Bruylants G, Wouters J and Michaux C. Differential scanning calorimetry in life science: Thermodynamics, stability, molecular recognition and application in drug design. *Curr Med Chem* **2005**, *12*, 2011-2020.
- Bulheller BM, Miles AJ, Wallace BA and Hirst JD. Charge-transfer transitions in the vacuum-ultraviolet of protein circular dichroism spectra. *J Phy Chem B* **2008**, *112*, 1866-1874.
- Busti P, Scarpeci S, Gatti CA and Delorenzi, NJ. Interaction of alkylsulfonate ligands with β -lactoglobulin AB from bovine. *J Agric Food Chem* **1999**, *47*, 3628-3631.
- Calabrese V, Scapagnini G, Colombrita C, Ravagna A, Pennisi G, Stella GAM, Galli F and Butterfield DA. Redox regulation of heat shock protein expression in aging and neurodegenerative disorders associated with oxidative stress: A nutritional approach. *Amino acids* **2003**, *25*, 437-444.
- Cann JR, Rao AGA and Winzor DJ. Numerical and experimental demonstrations of the need for caution in the use of zonal gel chromatography for characterizing ligand interactions with small acceptors. *Arch Biochem Biophys* **1989**, *270*, 173-183.
- Cao Y, Balamurali MM, Sharma D and Hongbin L. A functional single- molecule binding assay via force spectroscopy. *Proc Natl Acad Sci* **2007**, *104*, 15677-15681.
- Cardamone M and Puri NK. Spectrofluorimetric assessment of the surface hydrophobicity of proteins. *Biochem J* **1992**, *282*, 589-593.
- Castellan A, Ruggiero R, de Silva LG, Portes E, Grelier S and Gardrat C. Photophysics and photochemistry of tetrahydrocurcuminoids. *J Photochem Photobiol* **2007**, *190*, 110-120.
- Chearwae W, Anuchapreeda S, Nandigama K, Ambudkar SV and Limtrakul P. Biochemical mechanism of modulation of human P-glycoprotein (ABCB1) by curcumin I, II, and III purified from turmeric powder. *Biochem Pharmacol* **2004**, *68*, 2043-2052.

- Chen L, Remondetto GE and Subirade M. Food protein-based materials as nutraceutical delivery systems. *Trends Food Sci Technol* **2006**, *17*, 272-283.
- Chignell CF, Bilski P, Reszka KJ, Motten AG, Sik RH and Dahl TA. Spectral and photochemical properties of curcumin. *Photochem Photobiol* **1994**, *59*, 295-302.
- Chipman DM, Grisaro V and Sharon N. The binding of oligosaccharides containing N-acetylglucosamine and N-acetylmuramic acid to lysozyme. *J Biol Chem* **1967**, *242*, 4388-4394.
- Cho K, Wang X, Nie S, Chen ZG and Shin DM. Therapeutic nanoparticles for drug delivery in cancer. *Clin Cancer Res* **2008**, *14*, 1310-1316.
- Clapp CH, Banerjee A and Rotenberg SA. Inhibition of soybean lipoxygenase-1 by N-alkylhydroxylamines *Biochemistry* **1985**, *24*, 1826-1830.
- Clapp CH, McKown J, Xu H, Grandizio AM, Yang G and Fayer J. The action of soybean lipoxygenase-1 on 12-iodo-cis-9-octadecaenoic acid: The importance of C11-H bond breaking. *Biochemistry* **2000**, *39*, 2603-2611.
- Comfort S and Howell NK. Gelation properties of soya and whey protein isolate mixtures. *Food Hydrocolloids* **2002**, *16*, 661- 672.
- Cooke RM and Campbell ID. Protein structure determination by nuclear magnetic resonance. *Bioessays* **1988**, *8*, 52-56.
- Cooper DJ, Husband FA, Mills EN and Wilde PJ. Role of beer lipid-binding proteins in preventing lipid destabilization of foam. *J Agri Food Chem* **2002**, *50*, 7645-7650.
- Cornelius AS, Yerram NR, Kratz DA and Spector AA. Cytotoxic effect of *cis*-parinaric acid in cultured malignant cells. *Cancer Res* **1991**, *51*, 6025-6030.
- Corson TW and Crews CM. Molecular understanding and modern application of traditional medicines: Triumphs and trials. *Cell* **2007**, *130*, 769-774.

- Creamer LK and Harris DP. In: Milk protein polymorphism, Hill JP, Creamer LK and Boland MJ. eds., *International Dairy Federation, Amsterdam*, **1997**, 110-123.
- Creamer LK, Bienvenue A, Nilsson H, Paulsson M, van Wanroij M, Lowe EK, Anema SG, Boland MJ and Nez-flores RJ. Heat-induced redistribution of disulfide bonds in milk proteins. 1. Bovine β -lactoglobulin. *J Agric Food Chem* **2004**, *52*, 7660-7668.
- Creamer LK, Zoerb HF, Olson NF and Richardson T. Surface hydrophobicity of α_{S1} -I, α_{S1} -Casein A and B and its implications in cheese structure. *J Dairy Sci* **1982**, *65*, 902-906.
- Das S, Banerjee R and Bellare J. Aspirin loaded albumin nanoparticles by coacervation: implications in drug delivery. *Trends Biomater Artif Organs* **2005**, *18*, 203-212.
- Das RK, Kasoju N and Bora U. Encapsulation of curcumin in alginate-chitosan-pluronic composite nanoparticles for delivery to cancer cells. *Nanomed: Nanotech Biol Med* **2010**, *6*, 153-160.
- Davis BD. Binding of sulphonamide drugs by plasma proteins. A factor in determining the distribution of drugs in the body. *J Clin Invest* **1943**, *22*, 753-762.
- de Jongh HH, Groneveld T and de Groot J. Mild isolation procedure discloses new protein structural details of β -lactoglobulin. *J Dairy Sci* **2001**, *84*, 562-571.
- de Kruif CG and Holt C. Casein micelle structure, functions, and interactions. In *Advanced Dairy Chemistry – 1. Proteins. Part A*. Fox PF and Mc Sweeney PLH, ed. *Kluwer Academic/Plenum Publishers, NY*, **2003**, 233–270.
- Deng SL, Chen W F, Zhou B, Yang L and Liu ZL. Protective effects of curcumin and its analogues against free radical-induced oxidative haemolysis of human red blood cells. *Food Chem* **2006**, *98*, 112-119.
- Deodhar SD, Sethi R and Srimal RC. Preliminary study on antirheumatic activity of curcumin (diferuloyl methane). *Indian J Med Res* **1980**, *71*, 632–634.

- Drummen GP, Op den Kamp JA and Post JA. Validation of the peroxidative indicators, cis-parinaric acid and parinaroyl-phospholipids, in a model system and cultured cardiac myocytes. *Biochim Biophys Acta* **1999**, 1436, 370– 382.
- Dufour E, Roger P and Haertle T. Binding of benzo(α)pyrene, ellipticine, and cis-parinaric acid to β -lactoglobulin: Influence of protein modifications. *J Protein Chem* **1992**, 11, 645-652.
- Eisen HN. Immunology, 3rd ed. *Harper & Row Publishers, New York*, **1990**.
- Ekins S, Mestres J and Testa B. *In silico* pharmacology for drug discovery: methods for virtual ligand screening and profiling. *Br J Pharmacol* **2007**, 152, 9–20.
- Falgueyret JP, Hutchinson JH and Riendeau D. Criteria for the identification of non-redox inhibitors of 5-lipoxygenase. *Biochem Pharmacol* **1993**, 45, 978-981.
- Fang J, Lu J and Holmgren A. Thioredoxin reductase is irreversibly modified by curcumin: A novel molecular mechanism for its anticancer activity. *J Biol Chem* **2005**, 280, 25284–25290.
- Faridi AV, Brault PA, Shah P, Kim YW, Dunham WR and Funk MO Jr. Interaction between non-heme iron of lipoxygenases and cumene hydroperoxide: Basis for enzyme activation, inactivation, and inhibition. *J Am Chem Soc* **2004**, 126, 2006–2015.
- Farrell HM, Bede M J and Enyeart JA. Binding of p-nitrophenyl phosphate and other aromatic compounds by β -lactoglobulin. *J Dairy Sci* **1987**, 70, 252-258.
- Farrell HM Jr, Brown EM, Hoagland PD and Malin EL. Higher order structures of caseins: A paradox. *Advanced Dairy Chemistry – 1. Proteins Part A. 3rd ed.* Fox PF and McSweeney P, ed. *Kluwer Academic, London, UK*, 203– 232, **2003**.
- Farrell HM Jr, Jimenez-Flores R, Bleck GT, Brown EM, Butler JE, Creamer LK, Hicks CL, Hollar CM, Ng- Kwai-Hang KF and Swaisgood HE. Nomenclature of the proteins of cows' milk – Sixth revision. *J Dairy Sci* **2004**, 87, 1641–1674.

- Farrell HM Jr, Qi PX and Uversky VN. New views of protein structure: Applications to the caseins: Protein structure and functionality. *Advances in Biopolymers: Molecules, Clusters, Networks, and Interactions*. Fishman ML, Qi PX and Wisker L, ed. *Am Chem Soc, Washington, DC*, 52-70, **2006**.
- Fink AL and Uversky VN eds. Protein misfolding, aggregation and conformational diseases: I, Protein aggregation and conformational disorders. *Springer, New York, USA*, **2006**.
- Ford-Hutchinson AW, Gresser M and Young RN. 5-Lipoxygenase. *Annu Rev Biochem* **1994**, *63*, 383-417.
- Forrest SA, Yada RY and Rousseau DR. Interaction of vitamin D3 with β -lactoglobulin A and β casein. *J Agric Food Chem* **2005**, *53*, 8003-8009.
- Galpini JR, Tielens LGM, Veldink GA, Vliegthart JFG and Bolding J. On the interaction of some catechol derivatives with the iron atom of soybean lipoxygenase. *FEBS Lett* **1976**, *69*, 178-182.
- Garcea G, Jones DJ, Singh R, Dennison AR, Farmer PB, Sharma RA, Steward WP, Gescher AJ and Berry DP. Detection of curcumin and its metabolites in hepatic tissue and portal blood of patients following oral administration. *Br J Cancer* **2004**, *90*, 1011-1015.
- Gardner HW. Recent investigations into the lipoxygenase pathway of plants. *Biochim Biophys Acta* **1991**, *1084*, 221-239.
- Gatti CA, Risso PH and Pires MS. Spectrofluorometric study on surface hydrophobicity of bovine casein micelles in suspension and during enzymic coagulation. *J Agri Food Chem* **1995**, *43*, 2339-2344.
- Ghatak N and Basu N. Sodium curcumin as an effective anti-inflammatory agent. *Indian J Exp Biol* **1972**, *10*, 235-236.

- Goel A, Ajaikumar B, Kunnumakkara and Aggarwal BB. Curcumin as "Curecumin": From kitchen to clinic. *Biochem Pharmacol* **2008**, *75*, 787– 809.
- Gosh J and Myers CE. Inhibition of arachidonate 5-lipoxygenase triggers massive apoptosis in human prostate cancer cells. *Proc Natl Acad Sci USA* **1998**, *95*, 13182-13187.
- Gradishar WJ, Tjulandin S, Davidson N, Shaw H, Desai N, Bhar P, Hawkins M and O'Shaughnessy J. Phase III trial of nanoparticle albumin-bound paclitaxel compared with polyethylated castor oil-based paclitaxel in women with breast cancer. *J Clinical Oncol* **2005**, *23*, 7794–7803.
- Grechkin A. Recent developments in the biochemistry of plant lipoxygenase pathway. *Prog Lipid Res* **1998**, *37*, 317-352.
- Gunasekaran S, Ko S and Xiao L. Use of whey proteins for encapsulation and controlled delivery applications. *J Food Eng* **2007**, *83*, 31–40.
- Gupta KK, Bharne SS, Rathinasamy K, Naik NR and Panda D. Dietary antioxidant curcumin inhibits microtubule assembly through tubulin binding. *FEBS J* **2006**, *273*, 5320–5332.
- Gupta PK and Hung CT. Albumin microspheres II: Applications in drug delivery. *J Microencapsul* **1989**, *6*, 463-472.
- Gupta V, Aseh A, Rios CN, Aggarwal BB and Mathur AB. Fabrication and characterization of silk fibroin-derived curcumin nanoparticles for cancer therapy. *Int J Nanomed* **2009**, *4*, 115–122.
- Ha TJ and Isao K. Lipoxygenase inhibitory activity of anacardic acids. *J Agric Food Chem* **2005**, *53*, 4350-4354.
- Hambling SG, MacAlpine AS and Sawyer L. Beta-lactoglobulin. In: Fox PF, ed. *Advanced dairy chemistry II*. Amsterdam Elsevier 141–190, **1992**.

- Hariharan S, Bhardwaj V, Bala I, Sitterberg J, Bakowsky U and Ravi Kumar MN. Design of estradiol loaded PLGA nanoparticulate formulations: A potential oral delivery system for hormone therapy. *Pharm Res* **2006**, 23, 184-95.
- Harris BL. Selection to increase β -lactoglobulin B variant in New Zealand dairy cattle. In Milk Protein Polymorphism. J. P. Hill and M. Boland, eds. *International Dairy Federation, Brussels, Belgium* 467-473, **1997**.
- Hattori M, Watabe A and Takahashi K. β -Lactoglobulin protects β -ionone related compounds from degradation by heating, oxidation and irradiation. *Biosci Biotechnol Biochem* **1995**, 59, 2295-2297.
- Hausknecht EC and Funk MO. The differential effect of disulfiram on lipoxygenase from *Glycine max*. *Phytochemistry* **1984**, 23, 1535-1539.
- Havea P, Singh H and Creamer LK. Characterization of heat-induced aggregates of β -lactoglobulin, α -lactalbumin and bovine serum albumin in a whey protein concentrate environment. *J Dairy Res* **2001**, 68, 483-497.
- Heath DD, Khwaja F and Rock CL. Curcumin content of turmeric and curry powders. *FASEB J* **2004**, 18, A125.
- Hegde ML, Bharathi P, Suram A, Venugopal V, Jagannathan R, Poddar P, Srinivas P, Sambamurti K, Rao KSJ, Scancar J, Messori L, Zecca L, Zatta P. Challenges associated with metal chelation therapy in Alzheimer's disease. *J Alzheimers Dis* **2009**, 17, 457-468.
- Henderson R. Realizing the potential of electron cryo-microscopy. *Q Rev Biophys* **2004**, 37, 3-13.
- Hill JP, Boland M and Smith AF. The effect of β -lactoglobulin variants on milk powder manufacture and properties. In Milk Protein Polymorphism. J. P. Hill and M. Boland, eds. *International Dairy Federation, Brussels, Belgium* **1997**, 372-394.

- Hoehle SI, Pfeiffer E, Solyom AM and Metzler M. Metabolism of curcuminoids in tissue slices and subcellular fractions from rat liver. *J Agric Food Chem* **2006**, *54*, 756-764.
- Hoffmann MAM and van Mil PJJM. Heat induced aggregation of β -lactoglobulin: Role of the free thiol group and disulfide bonds. *J Agric Food Chem* **1997**, *45*, 2942-2948.
- Holt C. Structure and stability of bovine casein micelles. *Adv Protein Chem* **1992**, *43*, 63-133.
- Holt C and Sawyer L. Caseins as rheomorphic proteins: Interpretation of the primary and secondary structures of the α_{s1} -, β -, and κ -caseins. *J Chem Soc Faraday Trans* **1993**, *89*, 2683-2692.
- Hong J, Bose M, Ju J, Ryu J, Chen X, Sang S, Lee M and Yang CS. Modulation of arachidonic metabolism by curcumin and related β -diketone derivatives: effects on cytosolic phospholipase A_2 , cyclooxygenases and 5-lipoxygenase. *Carcinogenesis* **2004**, *25*, 1671-1679.
- Horne DS. Casein structure, self assembly and gelation. *Curr Opin Colloid Interface Sci* **2002**, *7*, 456-461.
- Hummel JP and Dreyer WJ. Measurement of protein binding phenomenon by gel filtration. *Biochim Biophys Acta* **1962**, *63*, 530-534.
- Hussain MS and Chandrasekhara N. Influence of curcumin on cholesterol gallstone induction in mice. *Indian J Med Res* **1992**, *96*, 288-291.
- Hussain MS and Chandrasekhara N. Influence of curcumin and capsaicin on cholesterol gallstone induction in hamsters and mice. *Nutr Res* **1993**, *13*, 349-357.
- Iametti S, Cairoli S, de Gregori B and Bonomi F. Modifications of high order structures upon heating of β -lactoglobulin: Dependence on the protein concentration. *J Agric Food Chem* **1995**, *43*, 53-58.
- Iersel ML, Ploemen JP, Struik I, van Amersfoort C, Keyzer AE, Schefferlie JG and van Bladeren P J. Inhibition of glutathione-S transferase activity in human melanoma

- cells by alpha,beta-unsaturated carbonyl derivatives. Effects of acrolein, cinnamaldehyde, citral, crotonaldehyde, curcumin, ethacrynic acid and trans-2-hexenal. *Chem Biol Interact* **1996**, *102*, 117-132.
- Ireson CR, Jones DJ, Orr S, Coughtrie MW, Boocock DJ, Williams ML, Farmer PB, Steward WP and Gescher AJ. Metabolism of the cancer chemopreventive agent curcumin in human and rat intestine. *Cancer Epidemiol Biomarkers Prev* **2002**, *11*, 105-111.
- Jagetia GC and Aggarwal BB. "Spicing Up" of the immune system by curcumin. *J Clin Immunol* **2007**, *27*, 19-35.
- Jain RK. Delivery of novel therapeutic agents in tumor; Physiological barriers and strategies. *J Nat Cancer Inst* **1989**, *81*, 570-576.
- Jain SK and de Filippis RA. Medicinal plants of India. *Algonac, Michigan*, **1991**.
- Jayprakasha GK, Rao LJ and Sakariah KK. Improved HPLC method for the detection of curcumin, demethoxycurcumin and bisdemethoxycurcumin. *J Agri Food Chem* **2002**, *50*, 3668-3672.
- Jayaprakasha GK, Rao LJ and Sakariah KK, **2004**. A process for the recovery of curcuminoid mixture from spent turmeric oleoresin. *Indian Patent 194592 dated, 2004-11-20*.
- Jayaprakasha GK, Rao LJ and Sakariah KK. Antioxidant activities of curcumin, demethoxycurcumin and bisdemethoxycurcumin. *Food Chem* **2006**, *98*, 720-724.
- Jelesarov I and Bosshard HR. Isothermal titration calorimetry and differential scanning calorimetry as complementary tools to investigate the energetics of biomolecular recognition. *J Mol Recognit* **1999**, *12*, 3-18.
- Joe B and Lokesh BR. Role of capsaicin, curcumin and dietary *n* - 3 fatty acids in lowering the generation of reactive oxygen species in rat peritoneal macrophages. *Biochim Biophys Acta* **1994**, *1224*, 255-263.

- Joe B and Lokesh BR. Prophylactic and therapeutic effects of *n* - 3 polyunsaturated fatty acids, capsaicin, and curcumin on adjuvant induced arthritis in rats. *J Nutr Biochem* **1997**, *8*, 397-407.
- Joe B and Lokesh BR. Biological properties of curcumin-cellular and molecular mechanisms of action. *Crit Rev Food Sci Nutr* **2004**, *44*, 97-111.
- Jovanovic SV, Steenken S, Boone CW and Simic MG. H-Atom transfer is a preferred antioxidant mechanism of curcumin. *J Am Chem Soc* **1999**, *121*, 9677-9681.
- Jovanovic SV, Boone CW, Steenken S, Trinoga M and Kaskey RB. "How curcumin works preferentially with water soluble antioxidants." *J Am Chem Soc* **2001**, *123*, 3064-3068.
- Kato A and Nakai S. Hydrophobicity determined by a fluorescence probe method and its correlation with surface properties of proteins. *Biochim Biophys Acta* **1980**, *624*, 13-20.
- Kawashim Y. Nanoparticulate systems for improved drug delivery. *Adv Drug Delivery Rev*, **2001**, *47*, 1-2.
- Kemal C, Flamberg PL, Olsen RK and Shorter AL. Reductive inactivation of soybean lipoxygenase 1 by catechols: a possible mechanism for regulation of lipoxygenase activity. *Biochemistry* **1987**, *26*, 7064-7072.
- Kempaiah RK and Srinivasan K. Beneficial influence of dietary curcumin, capsaicin and garlic on erythrocyte integrity in high-fat fed rats. *J Nutr Biochem* **2006**, *17*, 471-478.
- Khopde SM, Priyadarsini KI, Palit DK and Mukherjee T. Effect of solvent on the excited-state photophysical properties of curcumin. *Photochem Photobiol* **2000a**, *72*, 625-631.
- Khopde SM, Priyadarshini KI, Guha SN, Satav JG, Venkatesan P and Rao MNA. Inhibition of radiation-induced lipid peroxidation by tetrahydrocurcumin:

- Possible mechanism by pulse radiolysis. *Biosci Biotechnol Biochem* **2000b**, *64*, 503-509.
- Kim JM, Araki S, Kim DJ, Park CB, Takasuka N, Baba-Toriyama H, Ota T, Nir Z, Khachika F, Shimidzu N, Tanaka Y, Ozawa T, Uraji T, Murakoshi M, Nishino H and Tsuda H. Chemopreventive effects of carotenoids and curcumins on mouse colon carcinogenesis after 1,2-dimethylhydrazine initiation. *Carcinogenesis* **1998**, *19*, 81- 85.
- Kiso Y, Suzuki Y, Watanabe N, Oshima Y and Hikino H. Antihepatotoxic principles of *Curcuma longa* rhizomes. *Planta Med* **1983**, *49*, 185-187.
- Kiuchi, F, Goto Y, Sugimoto N, Akao N, Kondo K and Tsuda Y. Nematocidal activity of turmeric: Synergistic action of curcuminoids. *Chem Pharm Bull* **1993**, *41*, 1640-1643.
- Klotz IM. The application of the law of mass action to binding by proteins. Interactions with calcium. *Arch Biochem* **1946**, *9*, 109-117.
- Klotz IM. Physicochemical aspects of drug protein interactions: A general perspective *Ann N Y Acad Sci* **1973**, *226*, 18-35.
- Knepp WA, Jayakrishna A, Quigg JM, Sitren HS, Bagnall JJ and Goldberg EP. Synthesis, properties and intratumoural evaluation of mitoxantrone loaded casein microspheres in Lewis lung carcinoma. *J Pharm Pharmacol* **1993**, *45*, 887-891.
- Kontopidis G, Holt C and Sawyer L. β -Lactoglobulin: Binding properties, structure, and function. *J Dairy Sci* **2004**, *87*, 785-796.
- Kramer PK. Albumin microspheres as vehicles for achieving specificity in drug delivery. *J Pharm. Sci* **1974**, *63*, 1646-1647.
- Kreuter J, Hekmatara T, Dreis S, Vogel T, Gelperina S and Langer K. Covalent attachment of apolipoprotein A-I and apolipoprotein B-100 to albumin

- nanoparticles enables drug transport into the brain. *J Controlled Rel* **2007**, *118*, 54-58.
- Kuang ZH, Wang PF, Zheng RL, Liu ZL and Liu YC. Making vitamin C liposoluble enhances its protective effect against radical induced hemolysis of erythrocytes. *Chem Phys Lipids* **1994**, *71*, 95-97.
- Kuhn H and Borngaber S. Mammalian 15-lipoxygenases, enzymatic properties and biological implications. *Adv Exp Med Biol* **1999**, *447*, 5-28.
- Kumar PA, Suryanarayana P, Reddy YP, Reddy BG. Modulation of α -crystallin chaperone activity in diabetic rat lens by curcumin. *Mol Vis* **2005**, *11*, 561-568.
- Kumar PV and Jain NK. Suppression of agglomeration of ciprofloxacin-loaded human serum albumin nanoparticles. *AAPS Pharm Sci Tech* **2007**, *8*, E1-E6.
- Kumar V, Lewis SA, Mutalik S, Shenoy DB, Venkatesh and Udupa N. Biodegradable microspheres of curcumin for treatment of inflammation. *Indian J Physiol Pharmacol* **2002**, *46*, 209-217.
- Kumosinski TF, Brown EM and Farrell HM Jr. Three-dimensional molecular modeling of bovine caseins: α_{S1} casein. *J Dairy Sci* **1991**, *74*, 2889-2828.
- Kunwar A, Barik A, Pandey R and Priyadarsini KI. Transport of liposomal and albumin loaded curcumin to living cells: an absorption and fluorescence spectroscopic study. *Biochem Biophys Acta* **2006**, *1760*, 1513-1520.
- Kunwar A, Barik A, Mishra B, Rathinasamy K, Pandey R and Priyadarsini KI. Quantitative cellular uptake, localization and cytotoxicity of curcumin in normal and tumor cells. *Biochim Biophys Acta* **2008**, *1780*, 673-679.
- Kuypers FA, van den Berg JJ, Schalkwijk C, Roelofsen B and Op den Kamp JA. Parinaric acid as a sensitive fluorescent probe for the determination of lipid peroxidation. *Biochim Biophys Acta* **1987**, *921*, 266- 274.

- Lakowicz JR. Principles of Fluorescence Spectroscopy, 2nd ed. Kluwer Academic/Plenum Publishers, New York, **1999**.
- Laemmli UK. Cleavage of structural proteins during the assembly of the head of bacteriophage T4. *Nature* **1970**, 277, 680-685.
- Lampe V and Milobedzka J. *Ve Dtsch Chem Ges* **1913**, 46, 2235.
- Langer K, Balthasar S, Vogel V, Dinauer N, von Briesen H and Schubert D. Optimization of the preparation process for human serum albumin nanoparticles. *Int J Pharm* **2003**, 257, 169-180.
- Lao CD, Ruffin MT, Normolle D, Heath DD, Murray SI, Bailey JM, Boggs ME, Crowell J, Rock CL and Brenner DE. Dose escalation of a curcuminoid formulation. *BMC Complement Altern Med* **2006**, 6, 10-13.
- Larson BL, Heary IR and Devery JE. Immunoglobulin production and transport by the mammary gland. *J Dairy Sci* **1980**, 63, 665-671.
- Lee GU, Kidwell DA and Colton RJ. Sensing discrete streptavidin-biotin interactions with atomic force microscopy. *Langmuir* **1994**, 10, 354-357.
- Lehrer SS and Fasman GD. Fluorescence of lysozyme and lysozyme substrate complexes; Separation of tryptophan contributions by fluorescence difference methods. *J Biol Chem* **1967**, 242, 4644-4651.
- Lehrer SS. Solute perturbation of protein fluorescence. Quenching of the tryptophyl fluorescence of model compounds and of lysozyme by iodide ion. *Biochemistry* **1971**, 10, 3254-3263.
- Lenhart JA, Ling X, Gandhi R, Guo TL, Gerk PM, Brunzell DH and Zhang S. "Clicked" bivalent ligands containing curcumin and cholesterol as multifunctional A β oligomerization inhibitors: design, synthesis, and biological characterization. *J Med Chem* **2010**, 53, 6198-6209.

- Letchford K, Liggins R and Burt H. Solubilization of hydrophobic drugs by methoxy poly(ethylene glycol)-block-polycaprolactone diblock copolymer micelles: Theoretical and experimental data and correlations. *J Pharm Sci* **2008**, *97*, 1179-1190.
- Leu TH, Su SL, Chuang YC and Maa MC. Direct inhibitory effect of curcumin on Src and focal adhesion kinase activity. *Biochem Pharmacol* **2003**, *66*, 2323-2331.
- Leung MHM and Kee TW. Effective stabilization of curcumin by association to plasma proteins: human serum albumin and fibrinogen. *Langmuir*, **2009**, *25*, 5773 – 5777.
- Li L, Braiteh FS, Kurzrock R. Liposome-encapsulated curcumin: *in vitro* and *in vivo* effects on proliferation, apoptosis, signaling, and angiogenesis. *Cancer* **2005**, *104*, 1322-1331.
- Liang G, Yang S, Zhou H, Shao L, Huang K, Xiao J, Huang Z and Li X. Synthesis, crystal structure and anti-inflammatory properties of curcumin analogues. *Eur J Med Chem* **2009**, *44*, 915-919.
- Li-Chan ECY. Hydrophobicity in food protein systems. *Encyclopedia of Food Science and Technology* 2nd ed. Francis FJ, Wiley, New York, **1999**, Chapter 144.
- Linderstorm-Lang, K and Kodama S. Studies on casein 1. On the solubility of casein in hydrochloric acid. *Compt Rend Trav Lab Carlsberg* **1925**, *xvi*, No. 1.
- Liu F and Ng TB. Antioxidative and free radical scavenging activities of selected medicinal herbs. *Life Sciences* **2000**, *66*, 725-735.
- Livney YD. Milk proteins as vehicles for bioactives. *Curr Opin Colloid Interface Sci* **2010**, *15*, 73-83.
- Logan-Smith MJ, Lockyer PJ, East JM and Lee AG. Curcumin, a molecule that inhibits the Ca²⁺-ATPase of sarcoplasmic reticulum but increases the rate of accumulation of Ca²⁺. *J Biol Chem* **2001**, *276*, 46905-46911.

- MacArthur MW and Thornton JM. Influence of proline residues on protein conformation. *J Mol Biol* **1991**, 218, 397-412.
- Mahesha HG, Singh SA, Srinivasan N and Rao AGA. A spectroscopic study of the interaction of isoflavones with human serum albumin. *FEBS J* **2006**, 273, 451-467.
- Mahesha HG, Singh SA and Rao AGA. Inhibition of lipoxygenase by soy isoflavones: Evidence of isoflavones as redox inhibitors. *Arch Biochem Biophys* **2007**, 461, 176-185.
- Maiti K, Mukherjee K, Gantait A, Saha BP, Mukherjee PK. Curcumin- phospholipid complex: preparation, therapeutic evaluation and pharmacokinetic study in rats. *Int J Pharm* **2007**, 330, 155- 63.
- Majeed M, Badmaev V, Shivakumar U and Rajendran R. Curcuminoids: Antioxidant Phytonutrients. *Nutriscience Publishers Inc., Piscataway*, **1990**.
- Malin EL, Brown EM, Wickham ED and Farrell HM Jr. Contributions of terminal peptides to the associative behavior of α s1-casein. *J Dairy Sci* **2005**, 88, 2318-2328.
- Maliwal BP, Rao AGA and Rao MSN. Spectroscopic study of the interaction of gossypol with bovine serum albumin. *Int J Pep Protein Res* **1985**, 25, 382-388.
- Manjunatha H and Srinivasan K. Protective effect of dietary curcumin and capsaicin on induced oxidation of low-density lipoprotein, iron-induced hepatotoxicity and carrageenan-induced inflammation in experimental rats. *FEBS J* **2006**, 273, 4528-4537.
- Manjunatha H and Srinivasan K. Hypolipidemic and antioxidant effects of dietary curcumin and capsaicin in induced hypercholesterolemic rats. *Lipids* **2007**, 42, 1133-1142.
- Marczylo TH, Verschoyle RD, Cooke DN, Morazzoni P, Steward WP and Gescher AJ. Comparison of systemic availability of curcumin with that of curcumin

- formulated with phosphatidylcholine. *Cancer Chemother Pharmacol* **2007**, *60*, 171–177.
- Marshall K. Therapeutic applications of whey protein. *Altern Med Rev* **2004**, *9*, 136–156.
- Martin-Cordero C, Lopez-Lazaro M, Galvez M and Ayuso MJ. Curcumin as a DNA topoisomerase II poison. *J Enzyme Inhib Med Chem* **2003**, *18*, 505–509.
- Mazumdar A, Raghavan K, Weinstein J, Kohn KW and Pommer Y. Inhibition of human immunodeficiency virus type-1 integrase by curcumin. *Biochem Pharmacol* **1995**, *49*, 1165–1170.
- Mercier JC, Grosclaude F and Ribadeau-Dumas B. Primary structure of α_{S1} -casein bovine. Complete sequence. *Eur J Biochem* **1971**, *23*, 41–51.
- Michaelis K, Hoffmann MM, Dreis S, Herbert E, Alyautdin RN, Michaelis M, Kreuter J and Langer K. Covalent linkage of apolipoprotein E to albumin nanoparticles strongly enhances drug transport into the brain. *J Pharmacol Exp Ther* **2006**, *317*, 1246–1253.
- Minor W, Steczko J, Stec B, Otwinowski Z, Bolin JT, Walter R and Axelrod B. Crystal structure of soybean lipoxygenase L-1 at 1.4 Å resolution. *Biochemistry*, **1996**, *35*, 10687–10701.
- Mishra S, Karmodiya K, Surolia N and Surolia A. Synthesis and exploration of novel curcumin analogues as anti-malarial agents. *Bioorg Med Chem* **2008**, *16*, 2894–2902.
- Mogul R, Johansen E and Holman TR. Oleyl sulfate reveals allosteric inhibition of soybean lipoxygenase-1 and human 15-lipoxygenase. *Biochemistry* **2000**, *39*, 4801–4807
- Mohammadi F, Bordbar AK, Divsalar A, Mohammadi K and Saboury AA. Interaction of curcumin and diacetylcurcumin with the lipocalin member β -lactoglobulin. *Protein J* **2009**, *28*, 117–123.

- Mohammadzadeh KA, Smith LM and Feeney RE. Hydrophobic binding of hydrocarbons by proteins. II. Relationship of protein structure. *Biochim Biophys Acta* **1969**, 194, 256-264.
- Molegro Virtual Docker, Molegro ApS, Denmark. <http://www.molegro.com>.
- Monaco HL, Zanotti G, Spadon P, Bolognesi M, Sawyer L and Eliopoulos EE. Crystal structure of the trigonal form of bovine β -lactoglobulin and its complex with retinol at 2.5 Å resolution. *J Mol Biol* **1987**, 197, 695-706.
- Morgan PE, Treweek TM, Lindner RA, Price WE and Carver JA. Casein proteins as molecular chaperones. *J Agri Food Chem* **2005**, 53, 2670-2683.
- Mu L and Feng SS. A novel controlled release formulation for the anticancer drug paclitaxel (Taxol): PLGA nanoparticles containing vitamin E TPGS. *J Controlled Rel* **2003**, 86, 33-48.
- Mullally JE and Fitzpatrick FA. Pharmacophore model for novel inhibitors of ubiquitin isopeptidases that induce p53-independent cell death. *Mol Pharmacol* **2002**, 62, 351-358.
- Nagaoka S, Futamura Y, Miwa K, Awano T, Yamauchi K, Kanamaru Y, Tadashi K and Kuwata T. Identification of novel hypocholesterolemic peptides derived from bovine milk β -lactoglobulin. *Biochem Biophys Res Commun* **2001**, 281, 11-17.
- Naguib YMA. A fluorometric method for measurement of peroxy radical scavenging activities of lipophilic antioxidants. *Anal Biochem* **1998**, 265, 290-298.
- Nakamura Y, Ohto Y, Murakami A, Osawa T and Ohigashi H. Inhibitory effects of curcumin and tetrahydrocurcuminoids on the tumor promoter-induced reactive oxygen species generation in leukocytes *in vitro* and *in vivo*. *Jpn J Cancer Res* **1998**, 89, 361-370.
- Natarajan R and Nadler JM. Role of lipoxygenases in breast cancer. *Front Biosci* **1998**, 3, E81-E88.

- Nieuwenhuizen WF, Schilstra MJ, van der Kerk-van Hoof A, Brandsma L, Veldink GA and Vliegthart JFG. Fe(III)-Lipoxygenase converts its suicide-type inhibitor octadeca-9,12-dienoic acid into 11-oxooctadeca-9,12-dienoic acid. *Biochemistry* **1995**, *34*, 10538-10545.
- Nirmala C and Puvanakrishnan R. Protective role of curcumin against isoproterenol induced myocardial infarction in rats. *Mol Cell Biochem* **1996**, *159*, 85-93.
- Nuhn P, Buge A, Kohler T, Lettau H and Schneider R. Trends in development of lipoxygenase inhibitors. *Die Pharmazie* **1991**, *46*, 81-88.
- Ohtsuka K, Kawashima D, Gu Y and Saito K. Inducers and co-inducers of molecular chaperones. *Int J Hyperthermia* **2005**, *21*, 703-711.
- Okada K, Wangpoengtrskul C, Tanaka T, Toyokuni S, Uchida K and Osawa T. Curcumin and especially tetrahydrocurcumin ameliorate oxidative stress-induced hepatotoxicity. *J Nutr* **2001**, *131*, 2090-2095.
- Oracova J, Sojkova D and Lindner W. Comparison of the Hummel–Dreyer method in high-performance liquid chromatography and capillary electrophoresis conditions for study of the interaction of (RS)-, (R)- and (S)-carvedilol with isolated plasma proteins. *J Chromatogr B* **1996**, *682*, 349-357.
- Osawa T, Sugiyama Y, Inayoshi M and Kawakishi S. Antioxidative activity of tetrahydrocurcuminoids. *Biosci Biotechnol Biochem* **1995**, *59*, 1609-1612.
- O'Shannessy DJ. Determination of kinetic rate and equilibrium binding constants for macromolecular interactions: a critique of the surface plasmon resonance literature. *Curr Opin Biotechnol* **1994**, *5*, 65-71.
- Palazolo G, Rodríguez F, Farruggia B, Picó G and Delorenzi N. Heat treatment of beta-lactoglobulin: Structural changes studied by partitioning and fluorescence. *J Agric Food Chem* **2000**, *48*, 3817-3822.

- Palmer CNA and Wolf CR. cis-Parinaric acid is a ligand for the human peroxisome proliferator activated receptor γ : development of a novel spectrophotometric assay for the discovery of PPAR γ ligands. *FEBS Lett* **1998**, 431, 476-480.
- Pan MH, Huang TM and Lin JK. Biotransformation of curcumin through reduction and glucuronidation in mice. *Drug Metab Dispos* **1999**, 27, 486-494.
- Pari L and Murugan P. Protective role of tetrahydrocurcumin against erythromycin estolate-induced hepatotoxicity. *Pharm Res* **2004**, 49, 481-486.
- Pariza MW, Park Y and Cook ME. Mechanisms of action of conjugated linoleic acid: evidence and speculation. *Proc Soc Exp Biol Med* **2000**, 223, 8-13.
- Parvathy KS, Negi PS and Srinivas P. Antioxidant, antimutagenic and antibacterial activities of curcumin β -diglucoside. *Food Chem* **2009**, 115, 265-271.
- Patil B S, Jayaprakasha GK, Murthy KNC and Vikram A. Bioactive Compounds: Historical perspectives, opportunities and challenges. *J Agri Food Chem* **2009**, 57, 8142-8160.
- Peppas LB. Recent advances on the use of biodegradable microparticles and nanoparticles in controlled drug delivery. *Int J Pharm* **1992**, 116, 1- 9.
- Perez MD, Sbnchez L, Aranda P, Ena JM and Calvo M. Synthesis and evaluation of concentration of β -lactoglobulin and α -lactalbumin from cow and sheep colostrum and milk throughout early lactation. *Cell Mol Biol* **1990**, 36, 205-212.
- Pierce MM, Raman CS and Nall BT. Isothermal titration calorimetry of protein-protein interactions. *Methods* **1999**, 19, 213-221.
- Pistoriuss EK and Axelrod B. Evidence for participation of iron in lipoxygenase: Reaction from optical and electron spin resonance studies. *J Biol Chem* **1976**, 251, 1144-1148.
- Pothakamury UR and Cánovas GVB. Fundamental aspects of controlled release in foods. *Trends Food Sci Tech* **1995**, 6, 397-406.

- Prabhakaran S and Damodaran S. Thermal unfolding of β -lactoglobulin: Characterization of initial unfolding events responsible for heat-induced aggregation. *J Agri Food Chem* **1997**, *45*, 4303-4308.
- Prasad NS, Raghavendra R, Lokesh BR and Naidu KA. Spice phenolics inhibit human PMNL 5-lipoxygenase. *Prostaglandins Leukot Essent Fatty Acids* **2004**, *70*, 521-528.
- Prasad NS. Spectrophotometric estimation of curcumin. *Indian Drugs* **1997**, *34*, 227-228.
- Qin BY, Bewley MC, Creamer LK, Baker HM, Baker EN and Jameson G B. Structural basis of the Tanford transition of bovine β -lactoglobulin. *Biochemistry* **1998a**, *37*, 14014-14023.
- Qin BY, Creamer LK, Baker EN and Jameson G B. 12-Bromododecanoic acid binds inside the calyx of bovine β -lactoglobulin. *FEBS Lett* **1998b**, *438*, 272-278.
- Rao AGA and Cann JR. A comparative study of the interaction of chlorpromazine, trifluoperazine, and promethazine with mouse brain tubulin. *Mol Pharmacol* **1981**, *19*, 295-301.
- Rao RR, Platel K and Srinivasan K. *In vitro* influence of spices and spice-active principles on digestive enzymes of rat pancreas and small intestine. *Nahrung* **2003**, *47*, 408-12.
- Rasmussen LK, Hojrup P and Petersen T E. Disulphide arrangement in bovine caseins: Localization of intrachain disulphide bridges in monomers of κ - and α_{s2} -casein from bovine milk. *J Dairy Res* **1992**, *61*, 485-493.
- Ravindran J, Subbaraju JV, Ramani MV, Sung B and Aggarwal BB. Bisdemethylcurcumin and structurally related hispolon analogues of curcumin exhibit enhanced prooxidant, anti-proliferative and anti-inflammatory activities *in vitro*. *Biochem Pharmacol* **2010**, *79*, 1658-1666.
- Ravindranath V and Chandrashekar N. Absorption and tissue distribution of curcumin in rats. *Toxicology*, **1980**, *16*, 259-265.

- Ravindranath V and Chandrashekar N. *In vitro* studies on the intestinal absorption of curcumin in rats. *Toxicology*, **1981**, 20, 251-257.
- Ravindranath V and Chandrashekar N. Metabolism of curcumin: Studies with 3H-curcumin. *Toxicology* **1982**, 22, 337-344.
- Reddy ACP and Lokesh BR. Effect of dietary turmeric (*Curcuma longa*) on iron induced lipid peroxidation in the liver. *Food Chem Toxicol* **1994a**, 32, 279-283.
- Reddy ACP and Lokesh BR. Studies on the anti-inflammatory activity of spice principles and dietary *n* - 3 fatty acids on carrageenan-induced inflammation in rat. *Ann Nutr Metab* **1994b**, 38, 349-358.
- Reddy ACP and Lokesh BR. Alterations in lipid peroxidation in rat liver by dietary *n* - 3 fatty acids: Modulation of antioxidant enzymes by curcumin, eugenol and vitamin E. *Eur J Nutr Biochem* **1994c**, 229, 181-188.
- Reddy ACP, Sudharshan E, Rao AGA and Lokesh BR. Interaction of curcumin with human serum albumin – A spectroscopic study. *Lipids* **1999**, 34, 1025-1029.
- Reddy RC, Vatsala PG, Keshamouni VG, Padmanaban G and Rangarajan PN. Curcumin for malaria therapy. *Biochem Biophys Res Comm* **2005**, 326,472-474.
- Reddy S and Aggarwal BB. Curcumin is a non-competitive and selective inhibitor of phosphorylase kinase. *FEBS Lett* **1994**, 341, 19-22.
- Romiti N, Tongiani R, Cervelli F and Chieli E. Effects of curcumin on P-glycoprotein in primary cultures of rat hepatocytes. *Life Sci* **1998**, 62, 2349-2358.
- Ross PD and Subramanian S. Thermodynamics of protein association reactions: Forces contributing to stability. *Biochemistry* **1981**, 20, 3096-3102.
- Ruddat VC, Whitman S, Holman TR and Bernasconi CF. Stopped-flow kinetic investigations of the activation of soybean lipoxygenase-1 and the influence of inhibitors on the allosteric site. *Biochemistry* **2003**, 42, 4172-4178.

- Sahu A, Kasoju N and Bora U. Fluorescence study of the curcumin - casein micelle complexation and its application as a drug nanocarrier to cancer cells. *Biomacromolecules* **2008**, *9*, 2905-2912.
- Salimath BP, Sunderesh CS and Srinivas L. Dietary components inhibit lipid peroxidation in erythrocyte membrane. *Nutr Res* **1986**, *6*, 1171-1178.
- Salmaso S, Bersani S, Semenzato A and Caliceti P. New cyclodextrin bioconjugates for active tumour targeting. *J Drug Targeting* **2007**, *15*, 379-390.
- Samuelsson B, Dahlen SE, Lindgren JA, Rouzer CA and Serhan CN. Leukotrienes and lipoxins: Structures, biosynthesis, and biological effects. *Science* **1983**, *237*, 1171-1176.
- Sandur SK, Pandey MK, Sung B, Ahn KS, Murakami A, Sethi G, Limtrakul P, Badmaev V and Aggarwal BB. Curcumin, demethoxycurcumin, bisdemethoxycurcumin, tetrahydrocurcumin and turmerones differentially regulate anti-inflammatory and anti-proliferative responses through a ROS-independent mechanism. *Carcinogenesis* **2007**, *28*, 1765-1773.
- Sawyer L and Kontopidis G. The core lipocalin, bovine beta-lactoglobulin. *Biochim Biophys Acta* **2000**, *1482*, 136-148.
- Scatchard G. The attractions of proteins for small molecules and ions. *Ann N Y Acad Sci* **1949**, *51*, 660-672.
- Schermann SM, Simmons DA and Konermann L. Mass spectrometry-based approaches to protein-ligand interactions. **2005**, *2*, 475-485.
- Schroeder F, Holland JF and Vagelos PR. Use of beta-parinaric acid, a novel fluorimetric probe, to determine characteristic temperatures of membranes and membrane lipids from cultured animal cells. *J Biol Chem* **1976**, *251*, 6739-6746.

- Schuettelkopf AW and van Aalten DMF. PRODRG: A tool for high-throughput crystallography of protein-ligand complexes. *Acta Crystallogr* **2004**, D60, 1355-1363.
- Scimeca JA, Thompson HJ and Ip C. Effect of conjugated linoleic acid on carcinogenesis. *Adv Exp Med Biol* **1994**, 364, 59-65.
- Sebille B, Thuaud N and Tillement JP. Equilibrium saturation chromatographic method for studying the binding of ligands to human serum albumin by high-performance liquid chromatography. Influence of fatty acids and sodium dodecyl sulphate on warfarin-human serum albumin binding. *J Chromatogr* **1979**, 180, 103-110.
- Sha RS, Kane CD, Xu Z, Banaszak LJ and Bernlohr DA. Modulation of ligand binding affinity of the adipocyte lipid-binding protein by selective mutation. *J Biol Chem* **1993**, 268, 7885-7892.
- Shankar BTN and Murthy SV. Effect of turmeric (*Curcuma longa*) fractions on the growth of some intestinal and pathogenic bacteria *in vitro*. *Indian J Exp Biol* **1979**, 17, 1363-1366.
- Shchez L, Calvo M and Brock J. Biological role of lactoferrin. *Arch Dis Child* **1992**, 67, 657-661.
- Shieh WR, Cacioli P and Sih CJ. Mechanisms of inactivation of soybean lipoxygenase by acetylenic fatty acids. *Adv Prostaglandin Thromboxane Leukotriene Res* **1985**, 15, 303-306.
- Shim JS, Kim JH, Cho HY, Yum YN, Kim SH, Park HJ, Shim BS, Choi SH and Kwon HJ. Irreversible inhibition of CD13/aminopeptidase N by the antiangiogenic agent curcumin. *Chem Biol* **2003**, 10, 695-704.
- Shoba G, Joy D, Joseph T, Majeed M, Rajendran R and Srinivas PS. Influence of piperine on the pharmacokinetics of curcumin in animals and human volunteers. *Planta Med* **1998**, 64, 353-356.

- Sklar LA, Hudson BS and Simoni RD. Conjugated polyene fatty acids as membrane probes: Preliminary characterization. *Proc Natl Acad Sci* **1975**, 72, 1649-1653.
- Sklar LA, Hudson BS and Simoni RD. Conjugated polyene fatty acids as fluorescent membrane probes: Model system studies. *J Supramol Struct* **1976**, 4, 449-465.
- Sklar LA, Hudson BS, Petersen M and Diamond J. Conjugated polyene fatty acids as fluorescent probes: Spectroscopic characterization. *Biochemistry* **1977a**, 16, 813-819
- Sklar LA, Hudson BS and Simoni RD. Conjugated polyene fatty acids as fluorescent probes: Binding to bovine serum albumin. *Biochemistry* **1977b**, 16, 5100-5108.
- Skrzypczak-Jankun E, Zhou K and McCabe NP. Natural polyphenols in complexes with lipoxygenase – Structural studies and their relevance to cancer. *Proceedings 93rd Annual Meeting AACR*, p205, **2002**.
- Skrzypczak-Jankun E, Zhou K, McCabe NP, Selman SH and Jankun J. Structure of curcumin in complex with lipoxygenase and its significance in cancer. *Int J Mol Med* **2003a**, 12, 17-24.
- Skrzypczak-Jankun E, Zhou K and Jankun J. Inhibition of lipoxygenase by (-)-epigallocatechin gallate: X-ray analysis at 2.1 Å reveals degradation of EGCG and shows soybean LOX-3 complex with EGC instead. *Int J Mol Med* **2003b**, 12, 415-420.
- Skrzypczak-Jankun E, Borbulevych OY, Jankun J. Soybean lipoxygenase-3 in complex with 4-nitrocatechol. *Acta Crystallogr D Biol Crystallogr* **2004**, 60, 613-615.
- Slappendel S, Veldink GA, Vliegthart JFG, Aasa R and Malmström BG. EPR Spectroscopy of soybean lipoxygenase-1 : Description and quantification of the high-spin Fe(III) signals. *Biochim Biophys Acta* **1981**, 667, 77-86.
- Smith E, Clegg R and Holt C. A biological perspective on the structure and function of caseins and casein micelles. *Int J Dairy Technol* **2004**, 57, 121-126.

- Solodovnik VD. Chemistry of natural aliphatic acids containing a conjugated system of double bonds. *Russ Chem Rev* **1967**, *36*, 272-283.
- Somchue W, Sermsri W, Shiowatana J and Siripinyanond, A. Encapsulation of α -tocopherol in protein-based delivery particles. *Food Res Int* **2009**, *42*, 909-914.
- Somparn P, Phisalaphong C, Nakornchai S, Unchern S and Morales NP. Comparative antioxidant activities of curcumin and its demethoxy and hydrogenated derivatives. *Biol Pharm Bull* **2007**, *30*, 74-78.
- Sou K, Inenaga S, Takeoka S and Tsuchida E. Loading of curcumin into macrophages using lipid-based nanoparticles. *Int J Pharm* **2008**, *352*, 287-293.
- Spaapen LJM, Veldink GA, Liefkens TJ, Vliegthart JFG and Kay CM, Circular dichroism of lipoxygenase-1 from soybeans. *Biochim Biophys Acta* **1979**, *574*, 301-311.
- Sreejayan MNR. Nitric oxide scavenging by curcuminoids. *J Pharm Pharmacol* **1997**, *49*, 105-107.
- Srimal RC, Dhawan BN. Pharmacology of diferuloyl methane (curcumin), a non-steroidal anti-inflammatory agent. *J Pharm Pharmacol* **1973**, *25*, 447-452.
- Srinivasan KR. The coloring matter in Turmeric. *Current Science* **1952**, *21*, 311-312.
- Srivastava R, Dikshit M, Srimal RC and Dhawan BN. Antithrombotic effect of curcumin. *Thromb Res* **1985**, *40*, 413-417.
- St. Angelo AJ and Ory RL. Lipoxygenase inhibition by naturally occurring monoenoic fatty acids. *Lipids* **1984**, *19*, 34-37.
- Stryer L. The interaction of a naphthalene dye with apomyoglobin and apohemoglobin: A fluorescent probe of non-polar binding sites. *J Mol Biol* **1965**, *13*, 482-495.

- Sudharshan E and Rao AGA. Rapid method to separate the domains of soybean lipoxygenase-1: Identification of the interdomain interactions. *FEBS Lett* **1997**, *406*, 184-188
- Sudharshan E and Rao AGA. Involvement of cysteine residues and domain interactions in the reversible unfolding of lipoxygenase-1. *J Biol Chem* **1999**, *274*, 35351-35358.
- Sugiyama Y, Kawakishi S and Osawa T. Involvement of the β -diketone moiety in the antioxidative mechanism of tetrahydrocurcumin. *Biochem Pharmacol* **1996**, *52*, 519-525.
- Sun A, Shoji M, Lu YJ, Liotta DC and Snyder JP. Synthesis of EF24-tripeptide chloromethyl ketone: a novel curcumin related anticancer drug delivery system. *J Med Chem* **2006**, *49*, 3153-3158.
- Suresh D, Gurudutt KN and Srinivasan K. Degradation of bioactive spice compound: Curcumin during domestic cooking. *Eur Food Res Technol* **2009**, *228*, 807-812.
- Sykes BD and Hull WE. Recent advances in methodology: Nuclear magnetic resonance. *Ann N Y Acad Sci* **1973**, *226*, 60-68.
- Takahashi M, Kitamoto D, Imura T, Oku H, Takara K and Wada K. Characterization and bioavailability of liposomes containing a ukon extract. *Biosci Biotechnol Biochem* **2008**, *72*, 1199-1205.
- Takeuchi T, Ishidoh T, Iijima H, Kuriyama I, Shimazaki N, Koiwai O, Kuramochi K, Kobayashi S, Sugawara F, Sakaguchi K, Yoshida H and Mizushima Y. Structural relationship of curcumin derivatives binding to the BRCT domain of human DNA polymerase lambda. *Genes Cells* **2006**, *11*, 223-35.
- Tanford C, Bunville LG and Nozaki Y. The reversible transformation of β LG at pH 7.5. *J Am Chem Soc* **1959**, *81*, 4032-4036.
- Tappel AL, Boyer PD and Lundberg WO. The reaction mechanism of soybean lipoxidase. *J Biol Chem* **1952**, *199*, 267-281.

- Thies C and Bissery M. Biodegradable microspheres for parenteral administration in biomedical applications of microencapsulation. *CRC Press, Boca Raton, FL*. 53-74, **1984**.
- Thorn DC, Meehan S, Sundae M, Rekas A, Gras SL, MacPhee CE, Dobson CM, Wilson MR and Carver JA. Amyloid fibril formation by bovine milk κ -casein and its inhibition by the molecular chaperones α - and β -casein. *Biochemistry* **2005**, *44*, 17027-17036.
- Tijssen P. Practice and theory of enzyme immunoassays. *Elsevier, Amsterdam*, **1985**.
- Tonnesen HH, Karlsen J and van Henegouwen GB. Studies on curcumin and curcuminoids. VIII. Photochemical stability of curcumin. *Z Lebensm Unters Forsch* **1986**, *183* 116-22.
- Tonnesen HH, de Vries H, Karlsen J and van Henegouwen GB. Studies on curcumin and curcuminoids. IX: Investigation of the photobiological activity of curcumin using bacterial indicator systems. *J Pharm Sci* **1987**, *76*, 371-733.
- Tonnesen HH, Masson M and Loftsson T. Studies of curcumin and curcuminoids. XXVII. Cyclodextrin complexation: Solubility, chemical and photochemical stability. *Int J Pharm* **2002a**, *244*, 127-135.
- Tonnesen HH. Solubility, chemical and photochemical stability of curcumin in surfactant solutions. Studies of curcumin and curcuminoids, XXVIII. *Die Pharmazie* **2002b**, *57*, 820-824.
- Townsend AA and Nakai S. Relationships between hydrophobicity and foaming characteristics of food proteins. *J Food Sci* **1983**, *48*, 588-594.
- Traynelis VC, Ryken TC and Cornelius AS. Cytotoxicity of *cis*-parinaric acid in cultured malignant gliomas. *Neurosurgery* **1995**, *37*, 484-489.
- van der Heijdt LM, Schilstra MJ, Feiters MC, Nolting HF, Hermes C, Veldink GA and Vliegthart JFG. Changes in the iron coordination sphere of Fe(II) lipoxygenase-

- 1 from soybeans upon binding of linoleate or oleate. *Eur J Biochem* **1995**, 231, 186-191.
- van der Zee J, Eling TE and Mason RP. Formation of free-radical metabolites in the reaction between soybean lipoxygenase and its inhibitors. An ESR study. *Biochemistry* **1989**, 28, 8363-8367.
- van Oss CJ, Absolom DR and Neumann AW. Repulsive van der Waals forces. II. Mechanism of hydrophobic chromatography. *Separ Sci Tech* **1979**, 14, 305 - 317.
- Vasey PA, Kaye SB, Morrison R, Twelves C, Wilson P, Duncan R, Thomson AH, Murray LS, Hilditch TE, Murray T, Burtles S, Fraier D, Frigerio E and Jim Cassidy. Phase I clinical and pharmacokinetic study of PK1 [N-(2-hydroxypropyl) methacrylamide copolymer doxorubicin]: First member of a new class of chemotherapeutic agents–drug–polymer conjugates. On behalf of Cancer Research Campaign Phase I/ II Committee. *Clinical Cancer Research* **1999**, 5, 83-94.
- Veldink GA, Vliegenthart JFG and Boldingh J. Plant lipoxygenases. *Prog Chem Fats Other Lipids* **1977**, 15, 131-166.
- Venkatesan N. Curcumin attenuation of acute adriamycin myocardial toxicity in rats. *Br J Pharmacol* **1998**, 124, 425-427.
- Venkatesan P and Rao MNA. Structure-activity relationship for the inhibition of lipid peroxidation and scavenging of free radicals by synthetic symmetrical curcumin analogues. *J Pharm Pharmacol* **2000**, 52, 1123-1128.
- Vogel and Pelletier. *J Pharm* **1818**, 2, 50.
- Wahlstrom B and Blennow G. A study on the fate of curcumin in the rat. *Acta Pharmacol Toxicol (Copenh)* **1978**, 43, 86-92.

- Wallace BA and Janes RW. Circular dichroism and synchrotron radiation circular dichroism spectroscopy: Tools for drug discovery. *Biochem Soc Trans* **2003**, *31*, 631-633.
- Wang YJ, Pan MH, Cheng AL, Lin LL, Ho YS, Hsieh CY and Lin JK. Stability of curcumin in buffer solutions and characterization of its degradation products. *J Pharm Biomed Anal* **1997**, *15*, 1867-1876.
- Warne PK, Mommy FA, Rumball SV, Tuttle RW and Scheraga HA. Computation of structures of homologous proteins. Alpha-lactalbumin from lysozyme. *Biochemistry* **1974**, *13*, 768-782.
- Weber C, Coester C, Kreuter J and Langer K. Desolvation process and surface characterisation of protein nanoparticles. *Int J Pharm* **2000**, *194*, 91-102.
- Willmott N, Magee GA, Cummings J, Halbert GW and Smyth JM. Doxorubicin-loaded casein microspheres: Protein nature of drug incorporation. *J Pharm Pharmacol* **1992**, *44*, 472-475.
- Wright PE and Dyson HJ. Intrinsically unstructured proteins: Re-assessing the protein structure-function paradigm. *J Mol Biol* **1999**, *293*, 321-331.
- Wu SY, Perez MD, Puyol P and Sawyer L. β -Lactoglobulin binds palmitate within its central cavity. *J Biol Chem* **1999**, *274*, 170-174.
- Xiao J, Suzuki M, Jiang Z, Chen X, Yamamoto K, Ren F and Xu M. Influence of B-ring hydroxylation on interactions of flavonols with bovine serum albumin. *J Agric Food Chem* **2008**, *56*, 2350-2356.
- Yanagisawa D, Shirai N, Amatsubo T, Taguchi H, Hirao K, Urushitani M, Morikawa S, Inubushi T, Kato M, Kato F, Morino K, Kimura H, Nakano I, Yoshida C, Okada T, Sano M, Wada Y, Wada KN, Yamamoto A and Tooyama I. Relationship between the tautomeric structures of curcumin derivatives and their Abeta-binding activities in the context of therapies for Alzheimer's disease. *Biomaterials* **2010**, *31*, 4179-4185.

- Yang TJ, Wu CSC and Martinez HM. Calculation of protein conformation from circular dichroism. *Methods Enzymol* **1986**, 130, 208-269.
- Yang F, Lim GP, Begum AN, Ubeda OJ, Simmons MR, Ambegaokar SS, Chen PP, Kaye R, Glabe CG, Frautschy SA and Cole GM. Curcumin inhibits formation of amyloid beta oligomers and fibrils, binds plaques, and reduces amyloid *in vivo*. *J Biol Chem* **2005**, 280, 5892-5901.
- Yang MC, Chen NC, Chen CJ, Wu CY and Mao SJ. Evidence for β -lactoglobulin involvement in vitamin D transport *in vivo*-role of the γ -turn (Leu-Pro-Met) of β -lactoglobulin in vitamin D binding. *FEBS J* **2009**, 276, 2251-2265.
- Yang MC, Guan HH, Liu MY, Lin YH, Yang JM, Chen WL, Chen CJ and Mao SJT. Crystal structure of a secondary vitamin D₃ binding site of milk β -lactoglobulin. *Proteins* **2008**, 71, 1197-1210.
- Yurawecz MP, Mossoba MM, Kramer JKG, Pariza MW and Nelson GJ. Advances in conjugated linoleic acid research. *AOCS Press, Champaign* **1999**.
- Zaheer A, Sahu SK, Ryken TC and Traynelis VC. *cis*-Parinaric acid effects, cytotoxicity, c-Jun N-terminal protein kinase, forkhead transcription factor and Mn-SOD differentially in malignant and normal astrocytes. *Neurochem Res* **2007**, 32, 115-124.
- Zeder-Lutz G, Benito A and van Regenmortel MHV. Active concentration measurements of recombinant biomolecules using biosensor technology. *J Mol Recogn* **1999**, 12, 300-309.
- Zhu H and Damodaran S. Heat-induced conformational changes in whey protein isolate and its relation to foaming properties. *J Agri Food Chem* **1994**, 42, 846-855.
- Zimmerman KD, Barlow GH and Klotz IM. Dissociation of β -lactoglobulin near neutral pH. *Arch Biochem Biophys* **1970**, 138, 101-109.

- Zimmermann JG, Krause I, Baranyi M, Fruhholz SF, Juszczak J, Erhardt G, Buchberger J and Klostermeyer H. Isolation and rapid sequence characterization of two novel bovine β -lactoglobulins I and J. *J Protein Chem* **1996**, *15*, 743-750.
- Zsila F, Bikadi Z and Simonyi M. Unique, pH-dependent biphasic band shape of the visible circular dichroism of curcumin-serum albumin complex. *Biochem Biophys Res Commun* **2003**, *301*, 776-782.
- Zsila F, Bikadi Z and Simonyi M. Induced circular dichroism spectra reveal binding of the antiinflammatory curcumin to human alpha1-acid glycoprotein. *Bioorg Med Chem* **2004a**, *12*, 3239-3245.
- Zsila F, Bikadi Z and Simonyi M. Circular dichroism spectroscopic studies reveal pH dependent binding of curcumin in the minor groove of natural and synthetic nucleic acids. *Org Biomol Chem* **2004b**, *2*, 2902-2910.